

02: Techniques for characterizing nanostructures

January 13, 2010

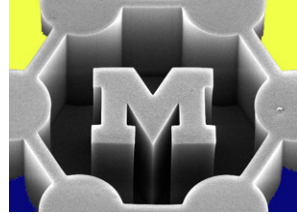
John Hart

ajohnh@umich.edu

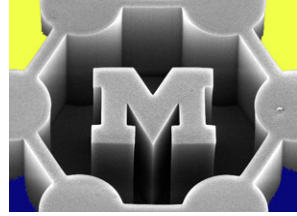
<http://www.umich.edu/~ajohnh>

Announcements

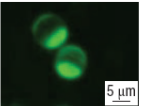
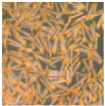
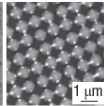
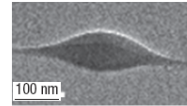
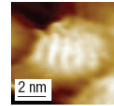
- Please fill out the info sheet if you are new
- How many plan to take the GCC?
- No class next M (Jan/18)



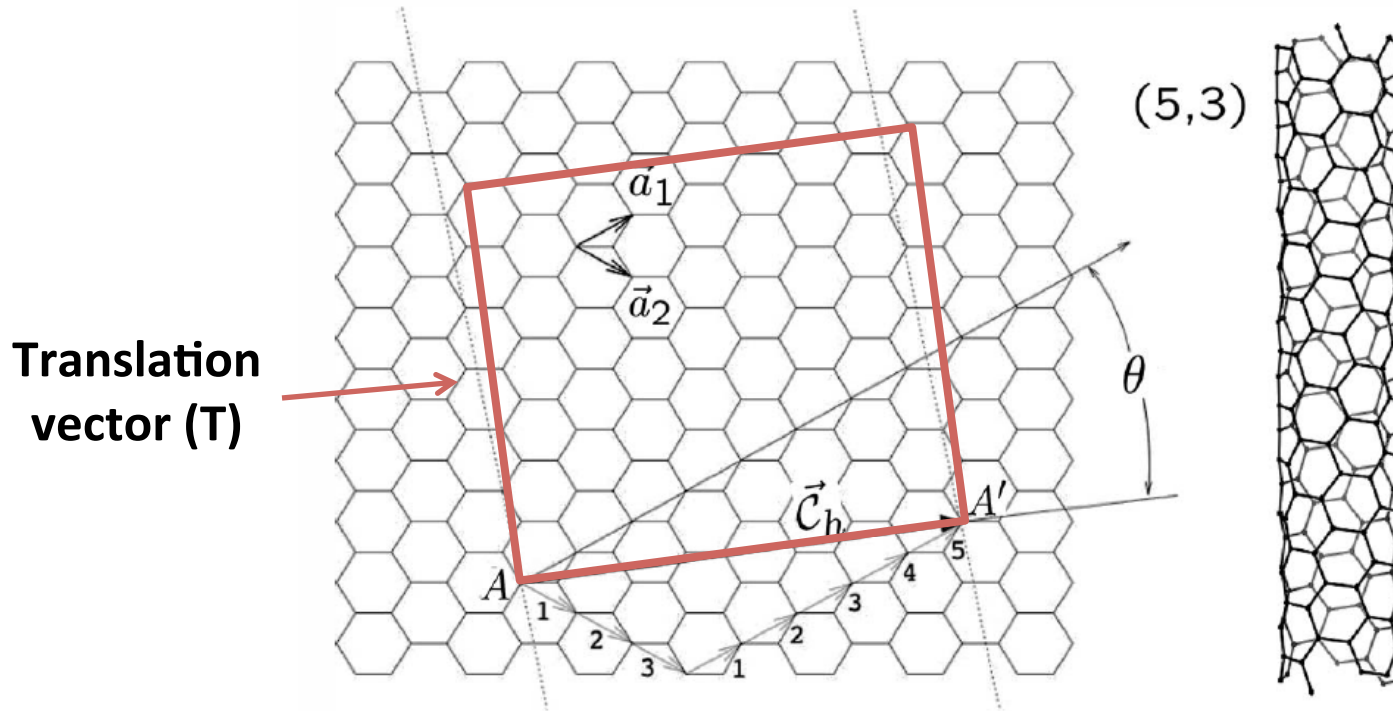
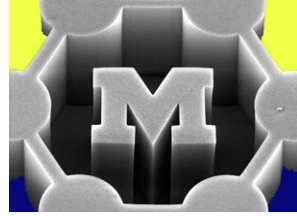
Recap: nanoscale structures



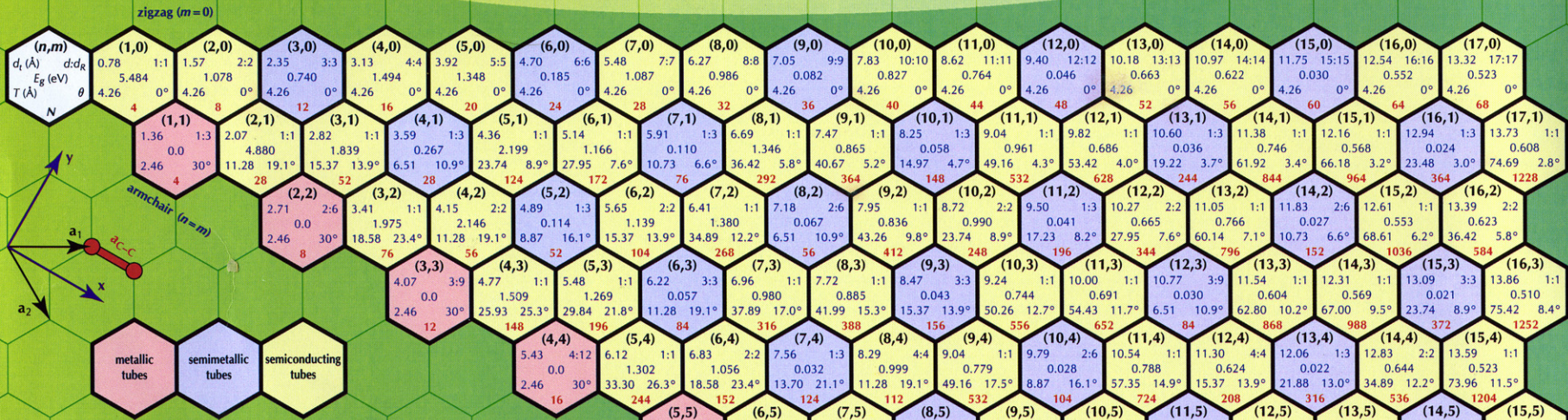
- **Taxonomy:** nano-clusters, -wires, -tubes, sheets, heterostructures
 - 0D, 1D, 2D – how many degrees of freedom would you have if you were inside the structure?
 - Emphasis on structural diversity
 - We will see effects of size and shape on properties



CNT unit cell

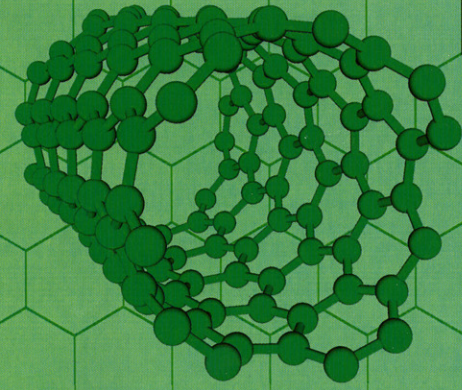


Periodic Table of Carbon Nanotubes



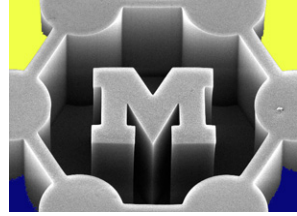
The semi-empirical bandgap E_g is calculated according to H. Yorikawa and S. Muramatsu, Phys. Rev. B 52, 2723 (1995) for the semiconducting tubes (no curvature effects) and A. Kleiner and S. Eggert, Phys. Rev. B 63, 073408 (2001) for the metallic and semi-metallic tubes (includes curvature). All other values are evaluated from the expressions below.

a_{C-C}	carbon-carbon distance	1.421 Å (graphite)
a	length of unit vector	$\sqrt{3} a_{C-C}$ 2.461 Å
a_1, a_2	unit vectors	$\frac{a}{2}(\sqrt{3}, 1), \frac{a}{2}(\sqrt{3}, -1)$ in (x, y) coordinates
b_1, b_2	reciprocal unit vectors	$\frac{2\pi}{a}(\frac{1}{\sqrt{3}}, 1), \frac{2\pi}{a}(\frac{1}{\sqrt{3}}, -1)$ in (x, y) coordinates
C_h	chiral vector	$n\mathbf{a}_1 + m\mathbf{a}_2$ n, m integer
L	circumference of tube	$L = C_h = a\sqrt{n^2 + m^2 + nm}$ $0 \leq m \leq n$
d_t	diameter of tube	$d_t = L/\pi$
θ	chiral angle	$\tan \theta = \frac{\sqrt{3}m}{2n+m}$ $0^\circ \leq \theta \leq 30^\circ$
d	highest common divisor of (n, m)	
d_R	highest common divisor of $(2n + m, 2m + n)$	$d_R = \begin{cases} d & \text{if } n - m \text{ is not a multiple of } 3d \\ 3d & \text{if } n - m \text{ is a multiple of } 3d \end{cases}$
T	translational vector of 1D unit cell	$T = t_1\mathbf{a}_1 + t_2\mathbf{a}_2$ t_1, t_2 integer $t_1 = (2m + n)/d_R$ $t_2 = -(2n + m)/d_R$
T	length of T	$T = \sqrt{3}L/d_R$
N	number of atoms per 1D unit cell	$N = 4(n^2 + m^2 + nm)/d_R$ $N/2 = \text{hexagons/unit cell}$

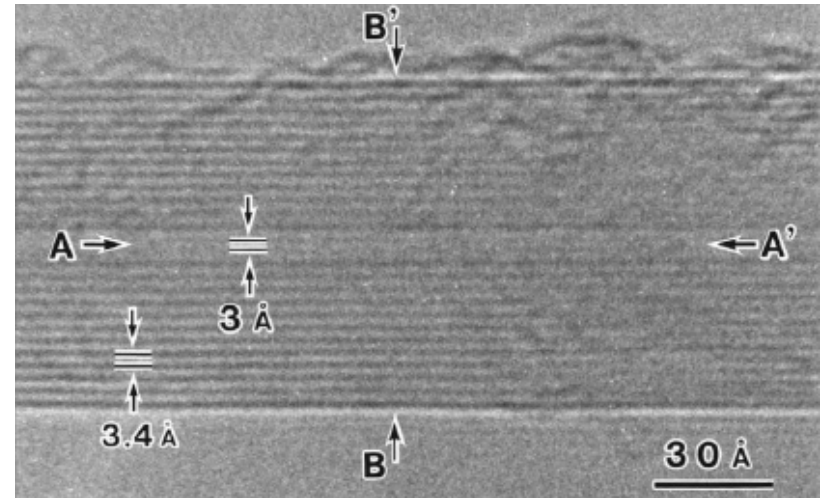
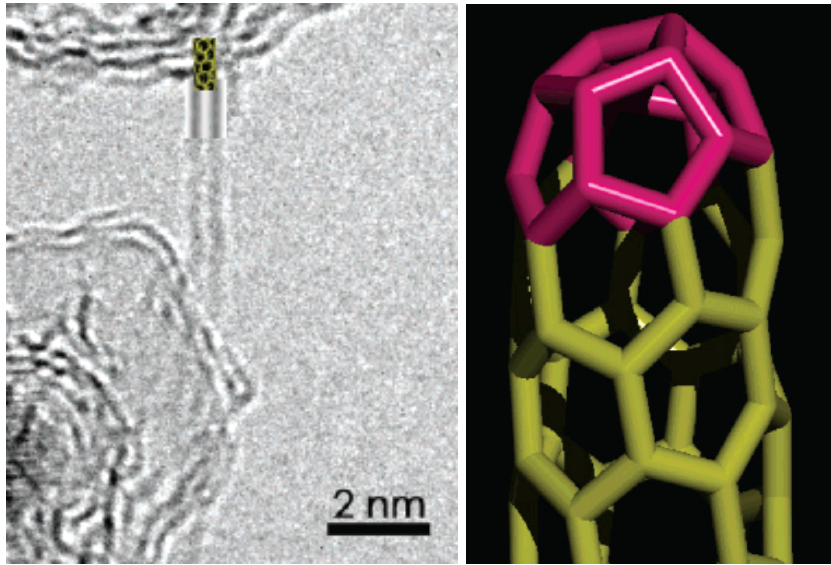


a_{C-C}	carbon-carbon distance		1.421 Å (graphite)
a	length of unit vector	$\sqrt{3} a_{C-C}$	2.461 Å
$\mathbf{a}_1, \mathbf{a}_2$	unit vectors	$\frac{a}{2}(\sqrt{3}, 1), \frac{a}{2}(\sqrt{3}, -1)$	in (x, y) coordinates
$\mathbf{b}_1, \mathbf{b}_2$	reciprocal unit vectors	$\frac{2\pi}{a}(\frac{1}{\sqrt{3}}, 1), \frac{2\pi}{a}(\frac{1}{\sqrt{3}}, -1)$	in (x, y) coordinates
\mathbf{C}_h	chiral vector	$n\mathbf{a}_1 + m\mathbf{a}_2$	n, m integer
L	circumference of tube	$L = \mathbf{C}_h = a\sqrt{n^2 + m^2 + nm}$	$0 \leq m \leq n$
d_t	diameter of tube	$d_t = L/\pi$	
θ	chiral angle	$\tan \theta = \frac{\sqrt{3}m}{2n+m}$	$0^\circ \leq \theta \leq 30^\circ$
d	highest common divisor of (n, m)		
d_R	highest common divisor of $(2n + m, 2m + n)$	$d_R = \begin{cases} d & \text{if } n - m \text{ is not a multiple of } 3d \\ 3d & \text{if } n - m \text{ is a multiple of } 3d \end{cases}$	
\mathbf{T}	translational vector of 1D unit cell	$\mathbf{T} = t_1\mathbf{a}_1 + t_2\mathbf{a}_2$ $t_1 = (2m + n)/d_R$ $t_2 = -(2n + m)/d_R$	t_1, t_2 integer
T	length of \mathbf{T}	$T = \sqrt{3}L/d_R$	
N	number of atoms per 1D unit cell	$N = 4(n^2 + m^2 + nm)/d_R$	$N/2 = \text{hexagons/unit cell}$

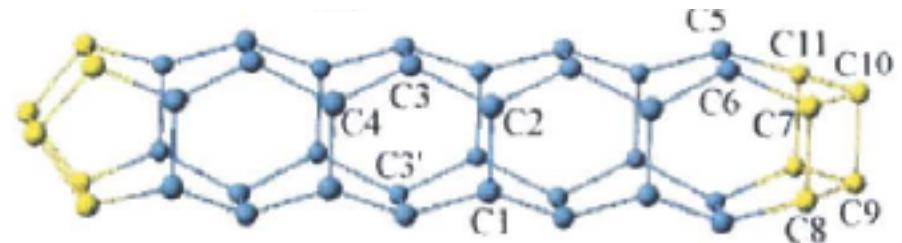
What is the smallest CNT?



4A



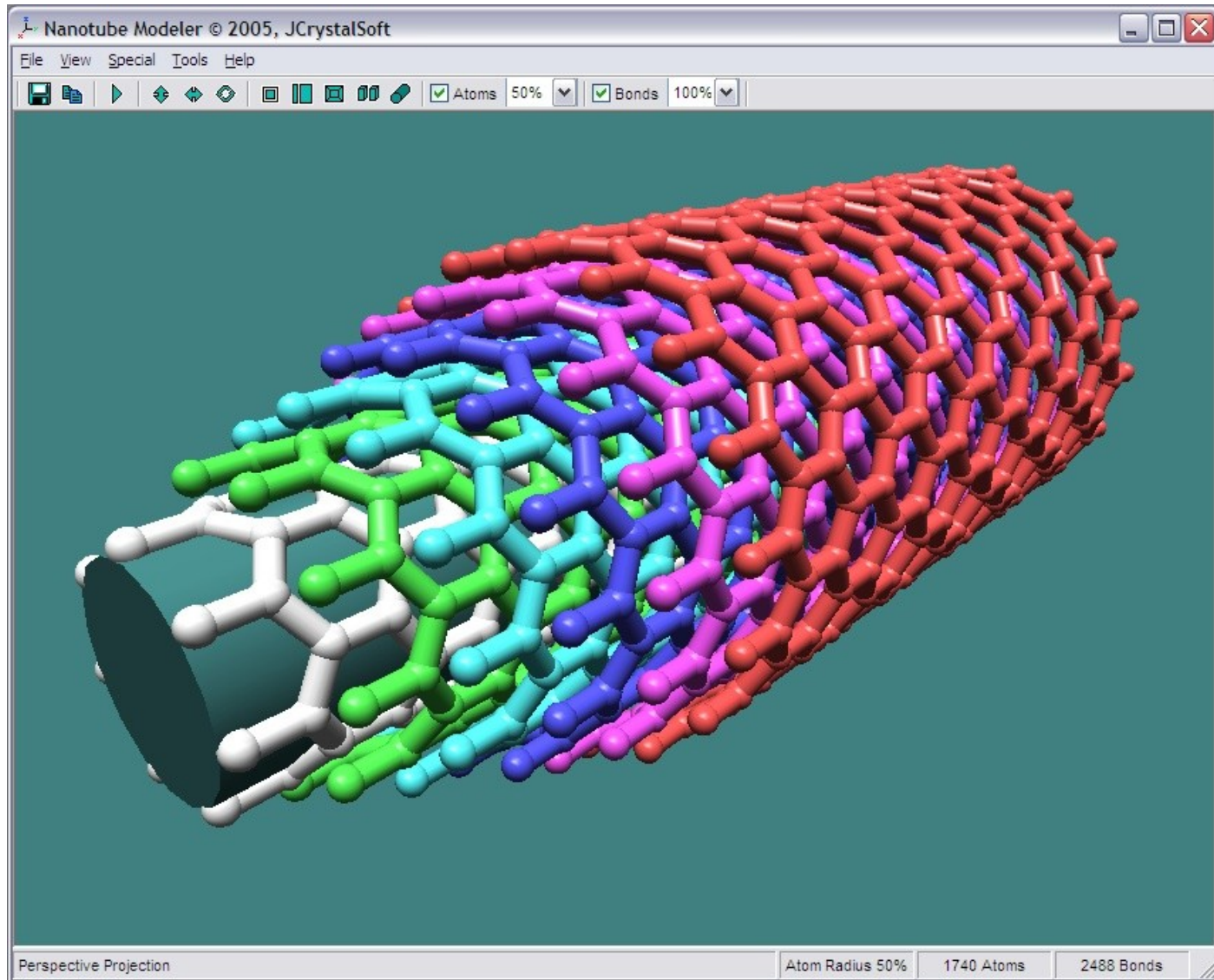
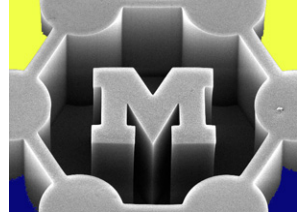
3A



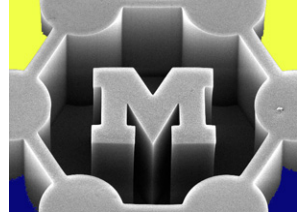
(d) 0.17 eV/atom

Nanotube modeler

<http://www.jcrystal.com/products/wincnt/>

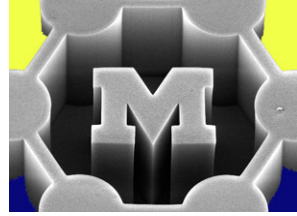


Today's agenda



- Microscopy: techniques and limits
 - Optical
 - Electron
 - Scanning probe (AFM/STM)
- Surface/structural analysis: electron and X-ray techniques
- Optical spectroscopy
 - Raman
 - UV/visible light
 - Infrared
- **This lecture could be an entire course (or more); our goal is to know the very basics of techniques we'll refer to in later topics.**
- **We'll overview how to measure properties in the coming lectures (mechanical, electrical, thermal, optical)**

Today's readings



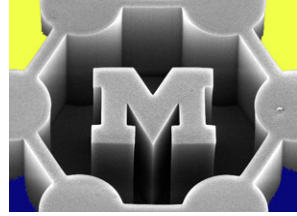
Nominal: (on ctools)

- Binning, Quate, and Gerber, **Atomic Force Microscope**
- Rao, **Characterization of Nanomaterials by Physical Methods**

Extras: (on ctools)

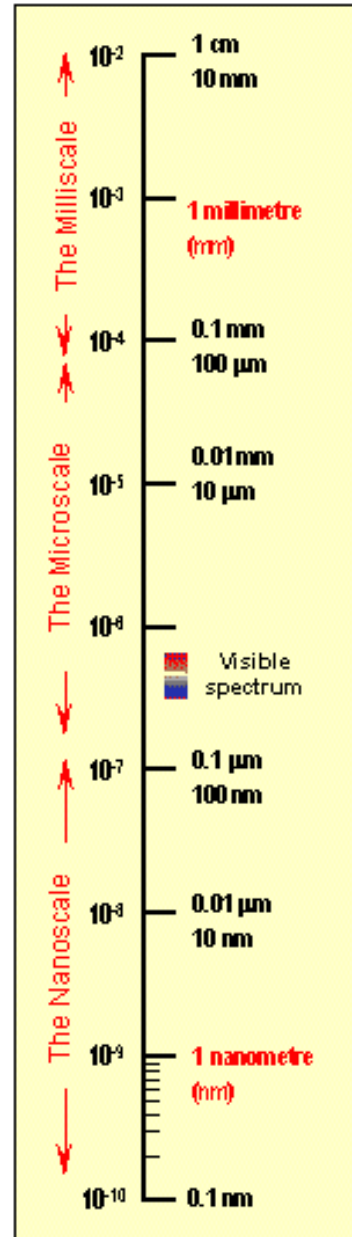
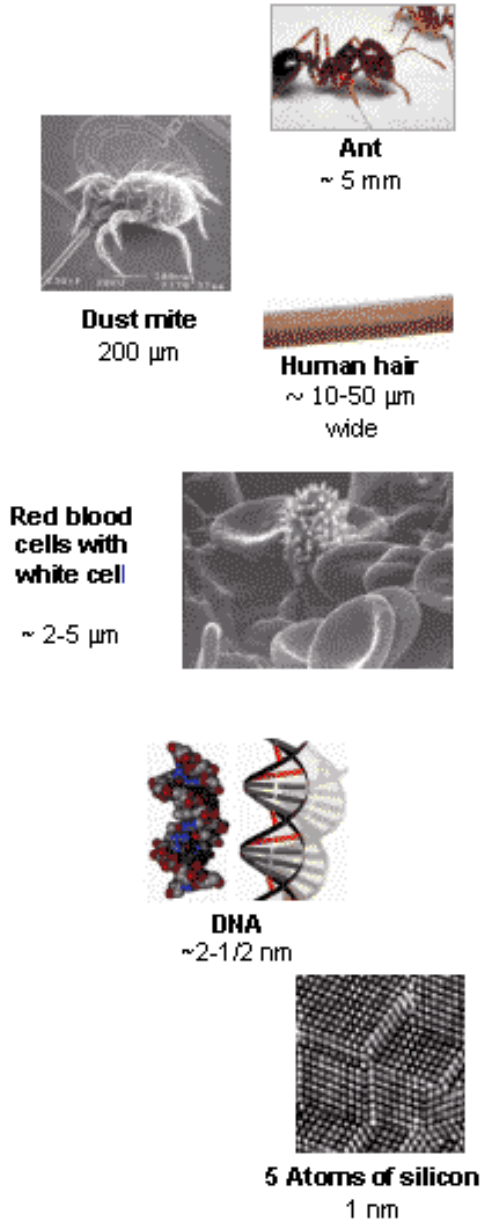
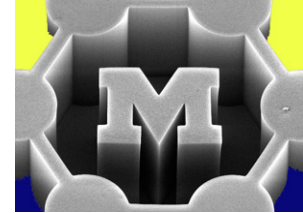
- Several papers on dynamic characterization, e.g., time-resolved electron microscopy

Additional resources



- References listed on these slides
- Internet search!
- Review papers (in journals)
- Many good books, e.g.,
 - Grasserbauer and Werner (eds.), *Analysis of Microelectronic Materials and Devices*, ISBN 0471950130
- Courses at UM:
 - Structural and chemical characterization of materials, Prof. Steve Yalisove (MSE465 W10)
 - Experimental methods in solids, Prof. Samantha Daly (ME599 was offered in W09)

Calibration



1 micrometer = 10^{-6} m

1 nanometer = 10^{-9} m

1 angstrom = 10^{-10} m

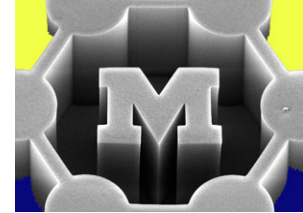
SO...

1 mm = 1,000,000 μm

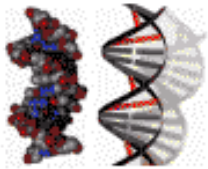
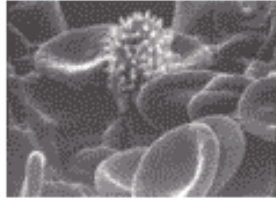
1 μm = 1000 nm

1 nm = 10 A

Resolution versus time



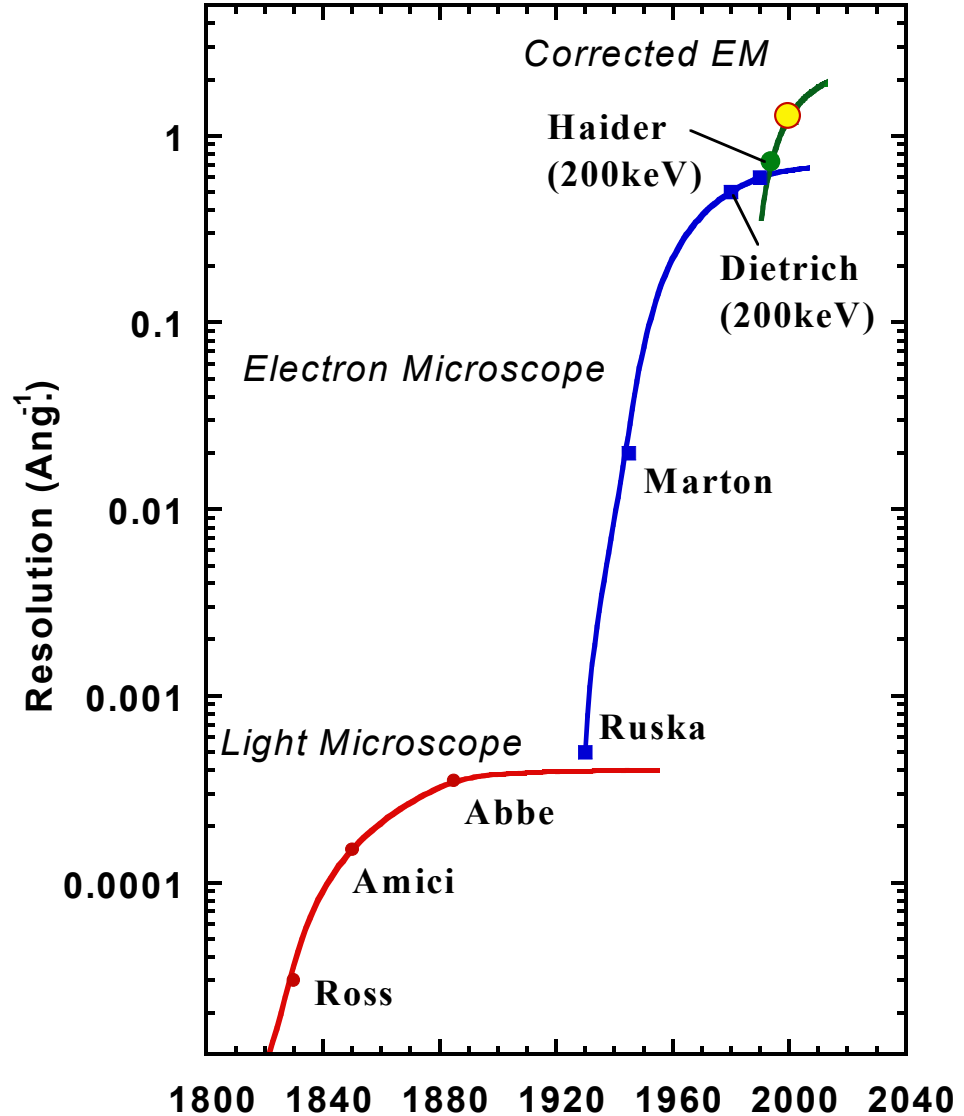
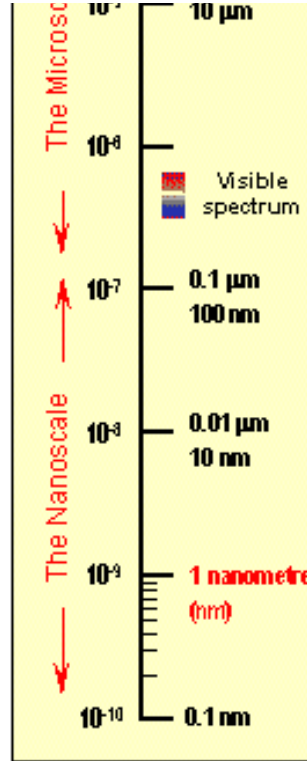
Red blood cells with white cell
~ 2-5 μm



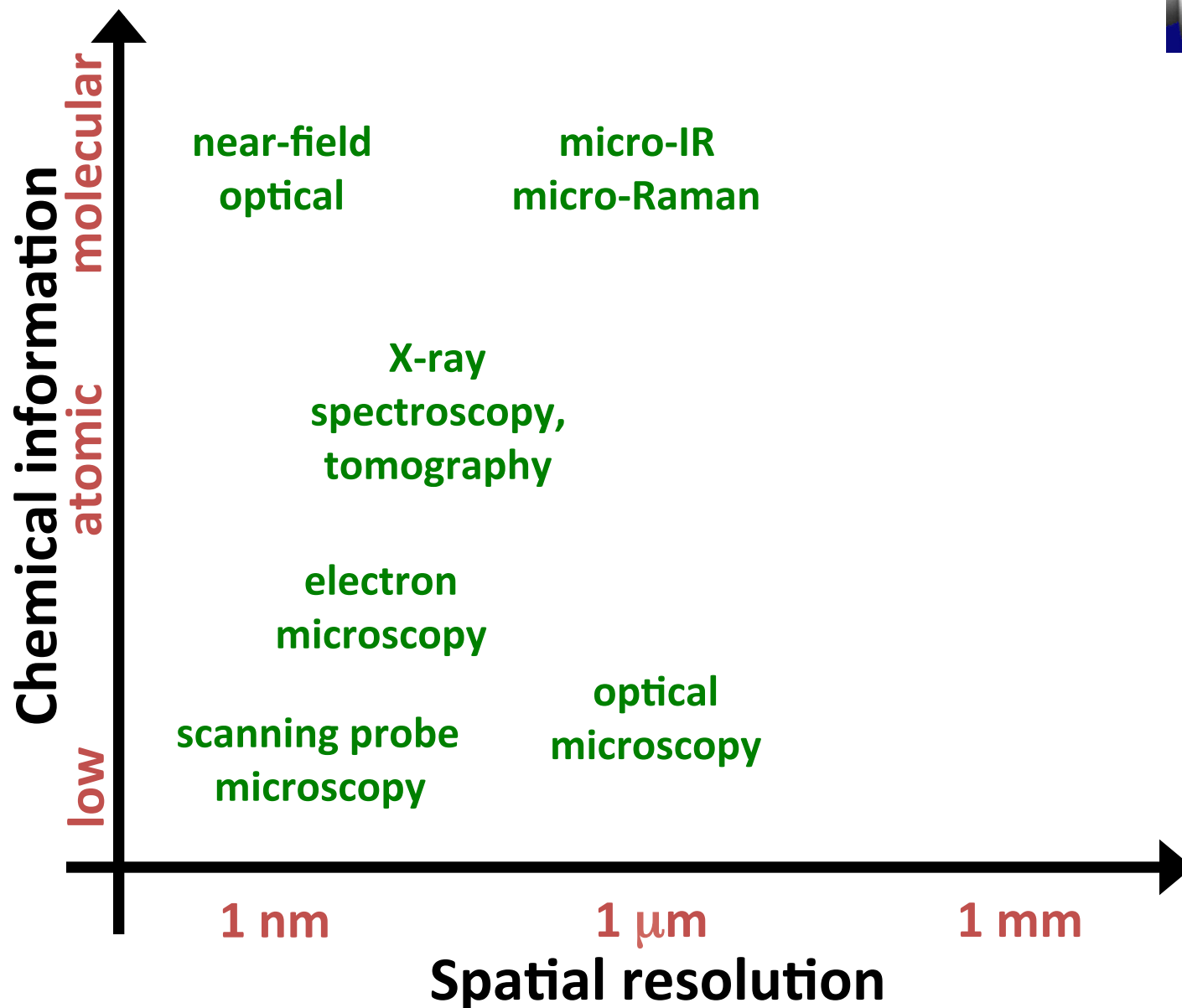
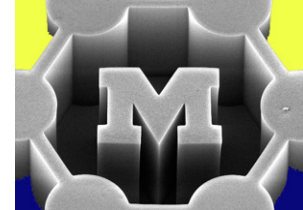
DNA
~2-1/2 nm



5 Atoms of silicon
1 nm



What types of information do we want?



Optical microscope

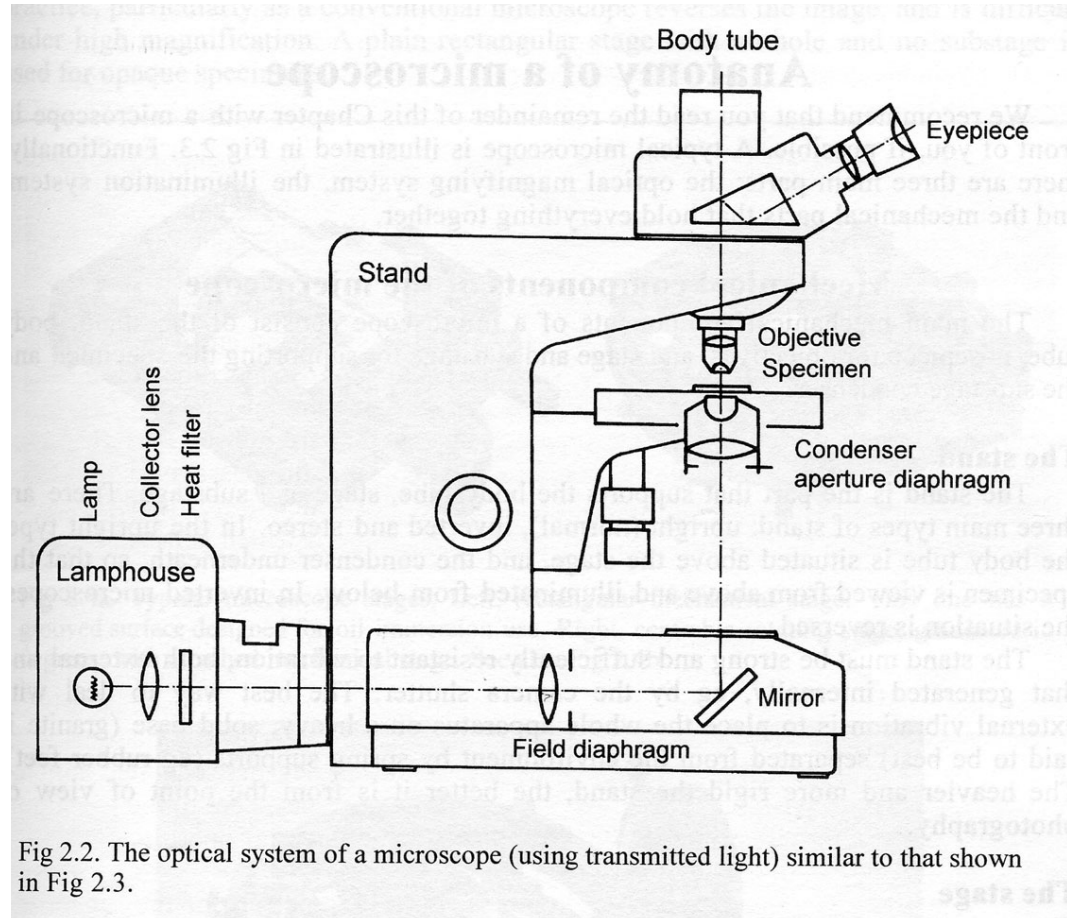
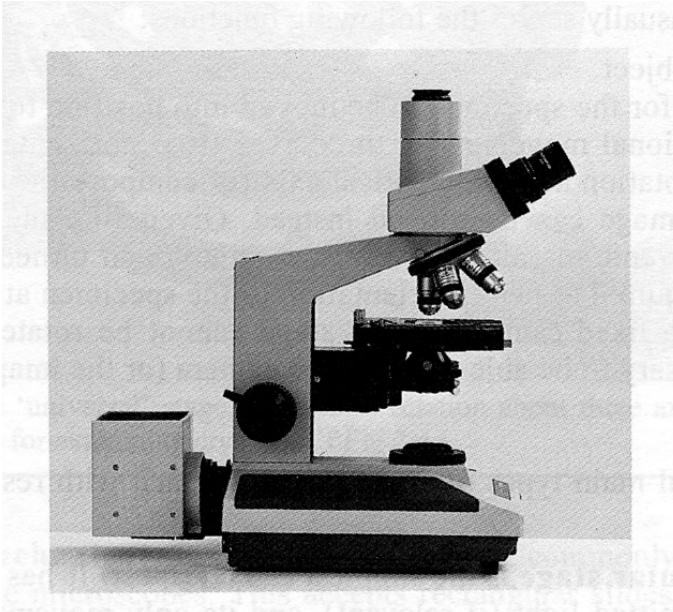
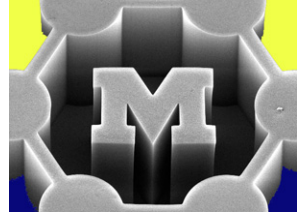
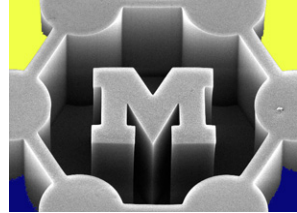
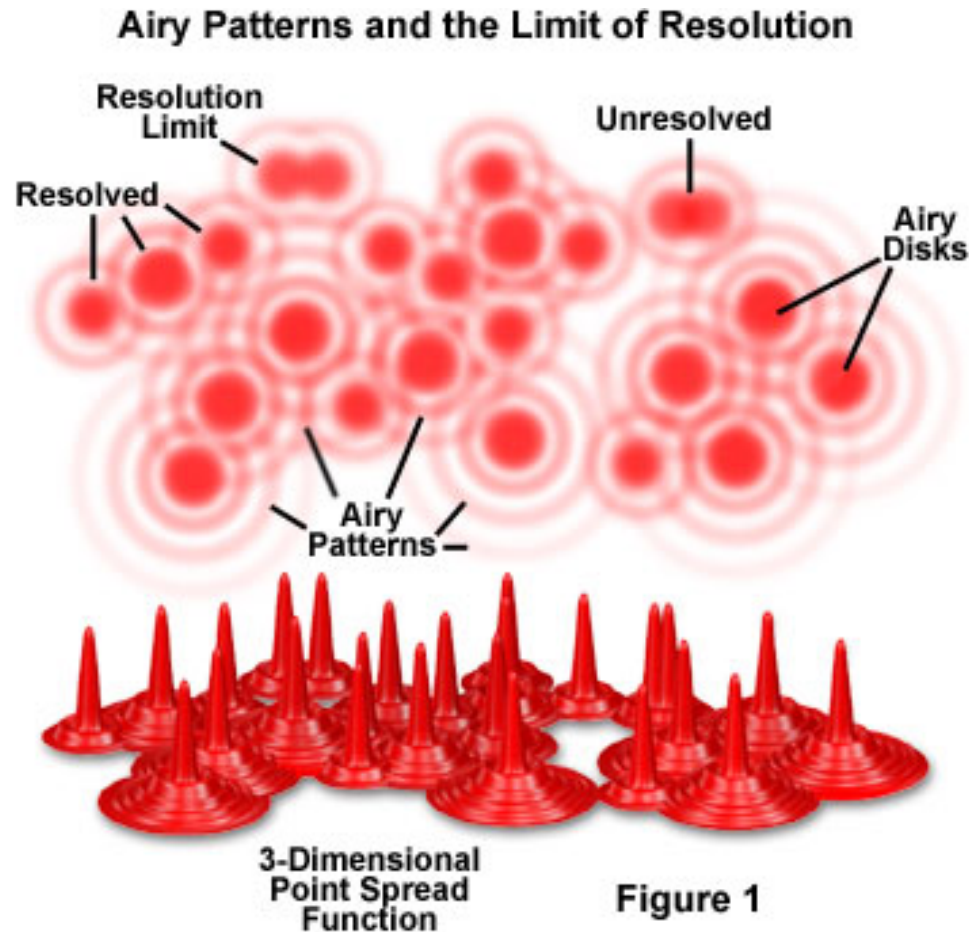


Fig 2.2. The optical system of a microscope (using transmitted light) similar to that shown in Fig 2.3.

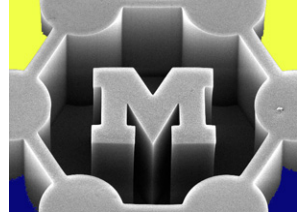
Limits of optical microscopy



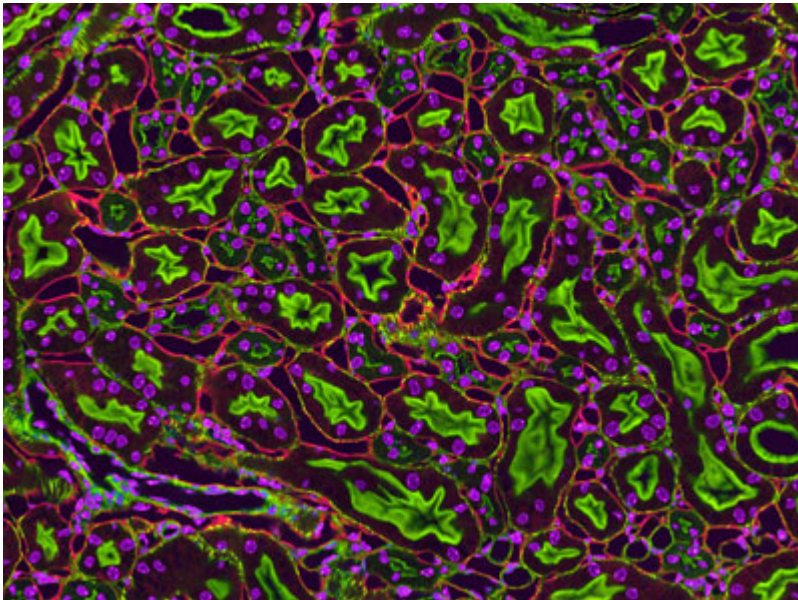
- Diffraction limit defines spatial resolution, $d = \lambda/NA$
- Ability to fit spread (airy) function determines point-to-point resolution of ideal emitters



Limits of optical microscopy

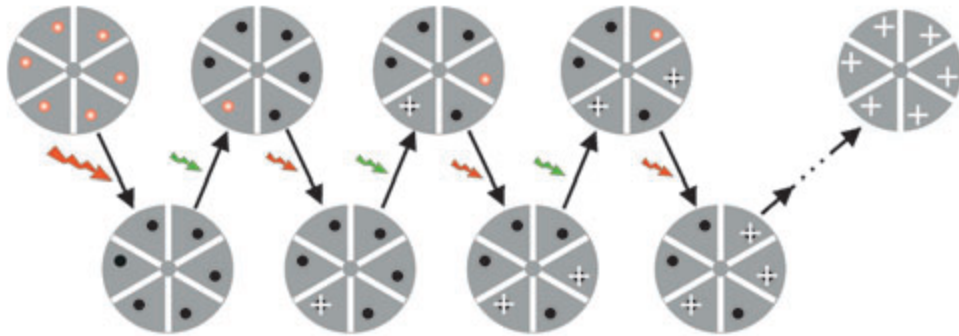
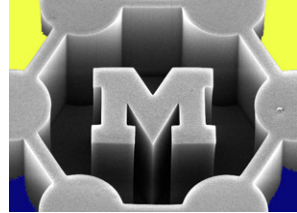


- Ways to beat the diffraction limit
 - Immersion optics (e.g., increase NA)
 - Prior knowledge of what should be in the image
 - Surface and tip-enhanced methods
 - Use fluorescent beacons (e.g., quantum dots) to tag specific locations

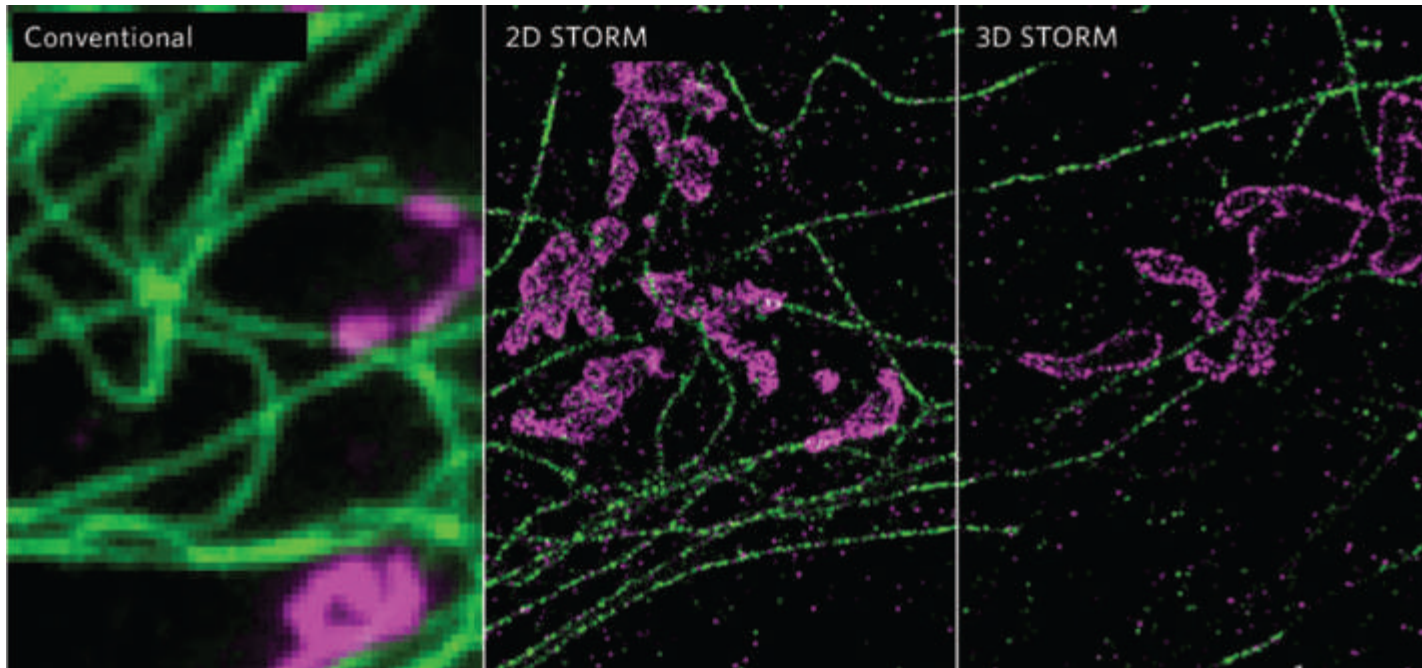


Thomas J. Deerinck
National Center for Microscopy & Imaging
Research
University of California - San Diego
La Jolla, California, USA
Quantum dot fluorescence image of mouse kidney
section (240x)

Stochastic optical reconstruction microscopy (STORM)



Switchable fluorophores



Scanning electron microscope (SEM)

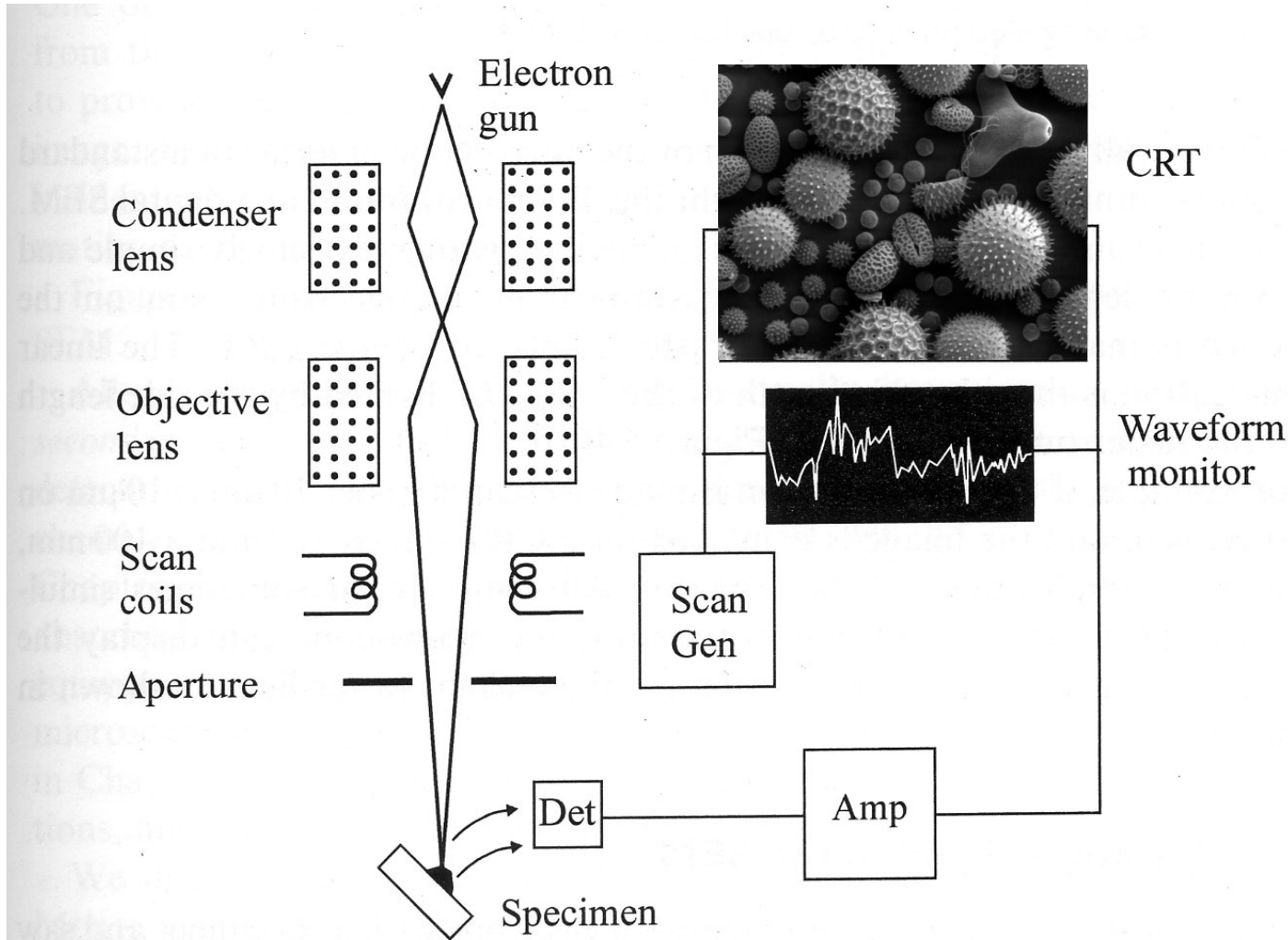
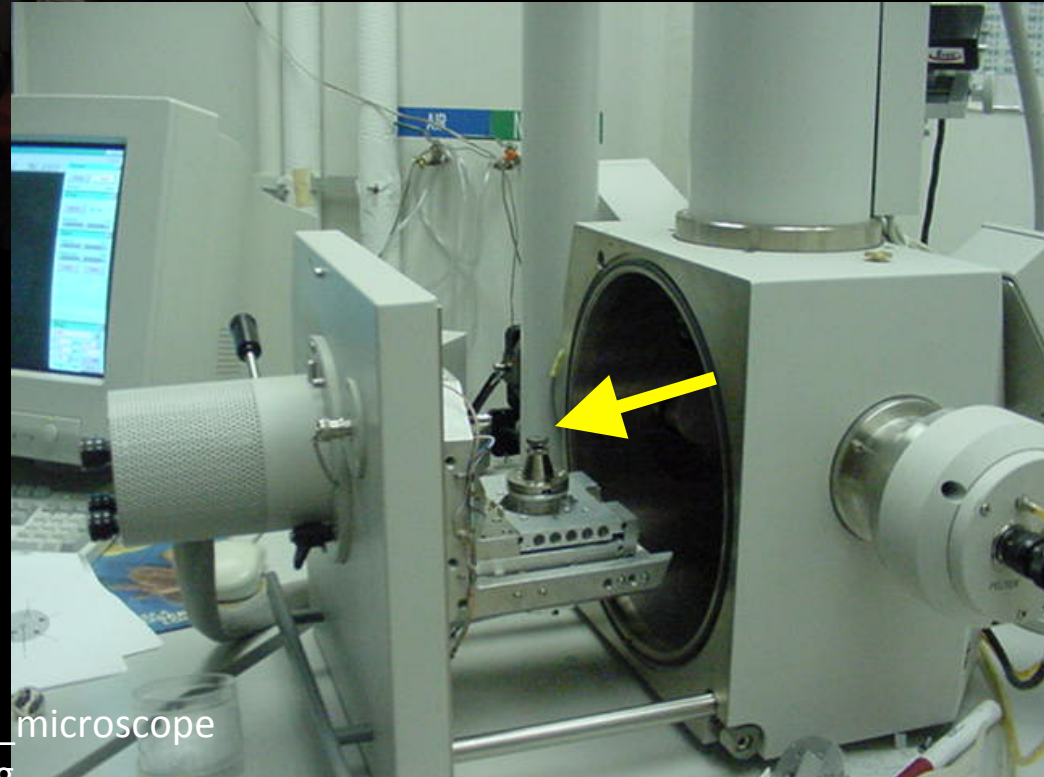
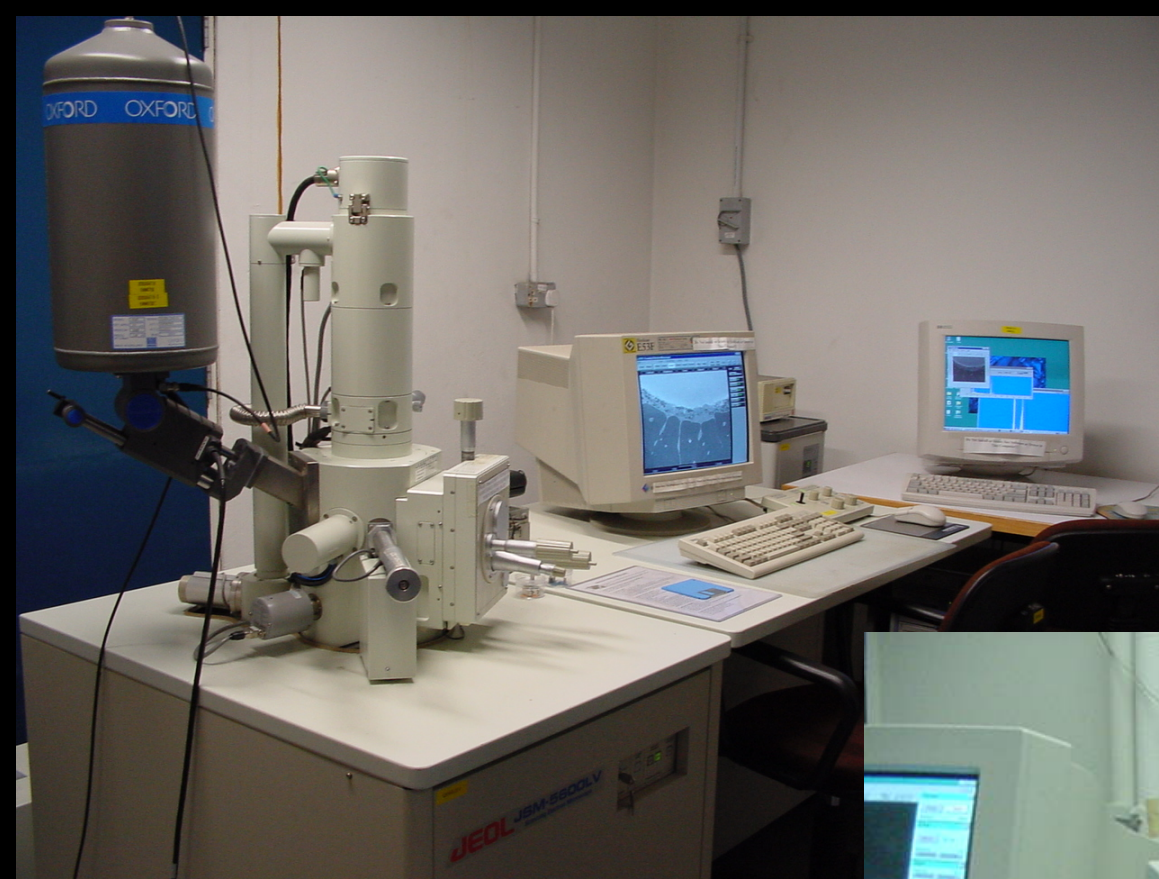
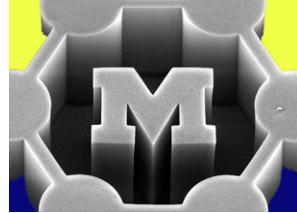


Figure 5.2 Schematic diagram showing the main components of a scanning electron microscope.



http://en.wikipedia.org/wiki/Scanning_electron_microscope
<http://serve.me.nus.edu.sg/mat/images/sem.jpg>

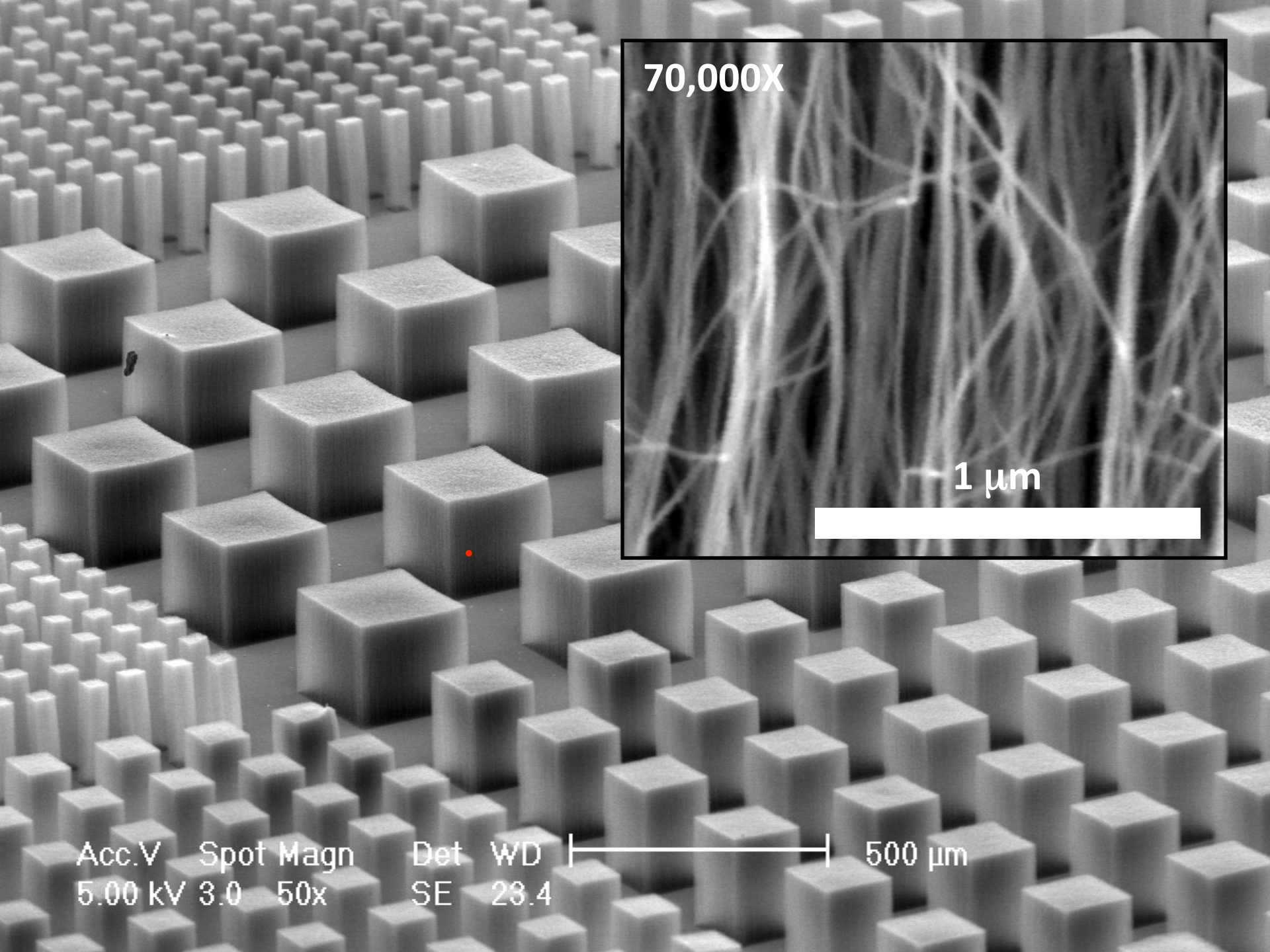


JEOL Conventional Tungsten High Vacuum SEMs

- Ideal for failure analysis, inspection, and characterization.

Available Models

	Resolution	Accelerating Voltage	Magnification	Stage
JSM-6390	3.0nm	0.5 to 30 kV	x5 to 300,000	X=125mm, Y=100mm
JSM-6390A				
JSM-6490	3.0nm	0.3 to 30 kV	x5 to 300,000	X=125mm, Y=100mm
JSM-6490A				



70,000X

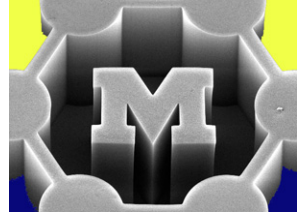
1 μm

Acc.V Spot Magn
5.00 kV 3.0 50x

Det WD
SE 28.4

500 μm

SEM sample preparation



- Electrically conductive sample surface required
- Affix to sample stage with conductive tape (e.g., carbon) or conductive epoxy (e.g., polymer and Ag particles)
- Coat non-conductive samples with a thin metal layer (typically 10-100 nm), OR use **environmental-SEM (E-SEM)**



It's cold outside!

NANO
LETTERS

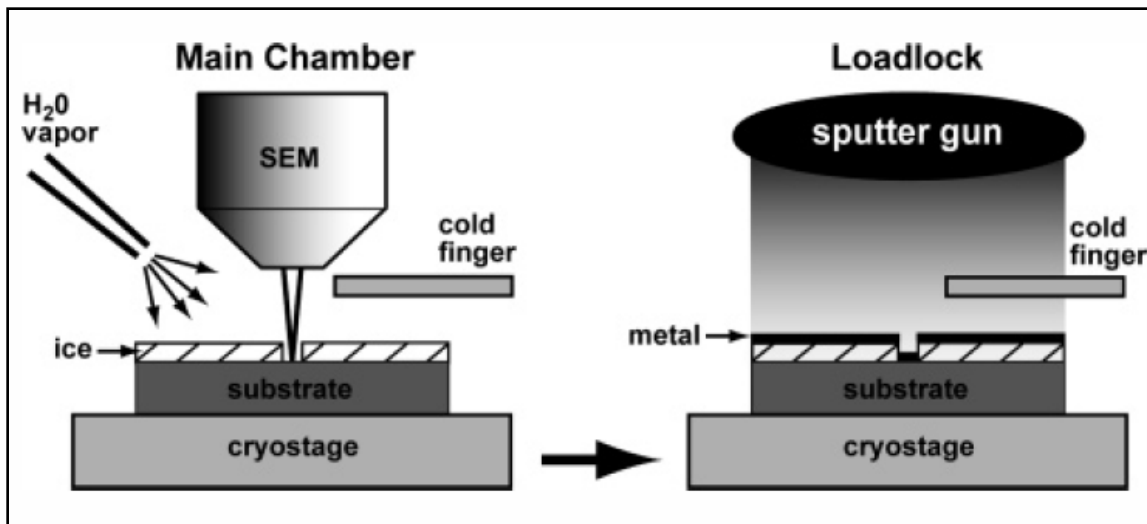
2005
Vol. 5, No. 6
1157–1160

Nanometer Patterning with Ice

Gavin M. King,^{*,†} Gregor Schürmann,[‡] Daniel Branton,[‡] and
Jene A. Golovchenko^{†,§}

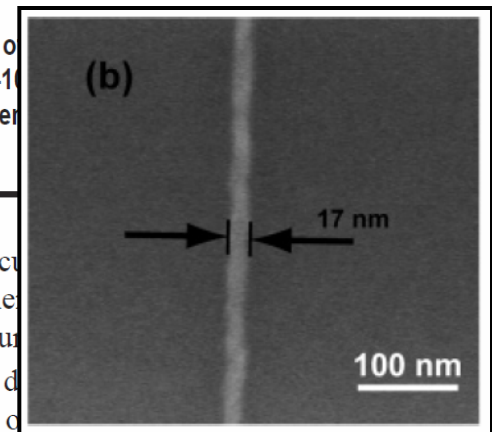
*Department of Physics, Department of Molecular and Cellular Biology,
and Division of Engineering & Applied Sciences, Harvard University,
Cambridge, Massachusetts 02138*

Received March 3, 2005; Revised Manuscript Received April 12, 2005



films of
sub-10
tion er

discu
dame
obscu
we d
por c
number of a combined scanning electron



device size, to enhance the role of quantum mechanical device characteristics, and to pattern increasingly complex substrates requires new lithographic approaches to define nanometer scale structures. Here we demonstrate a new approach to nanoscale e-beam patterning based on the condensation and beam stimulated sublimation of water ice.

microscope (SEM) and focused ion beam (FIB) apparatus (FEI Co., Hillsboro, Oregon). Subsequent exposure of the ice surface to focused energetic electron or gallium ion beams stimulates local removal of ice and ultimately exposes the underlying silicon substrate in whatever patterns the beams are programmed to produce. A forward-going laser beam

Transmission electron microscope (SEM)

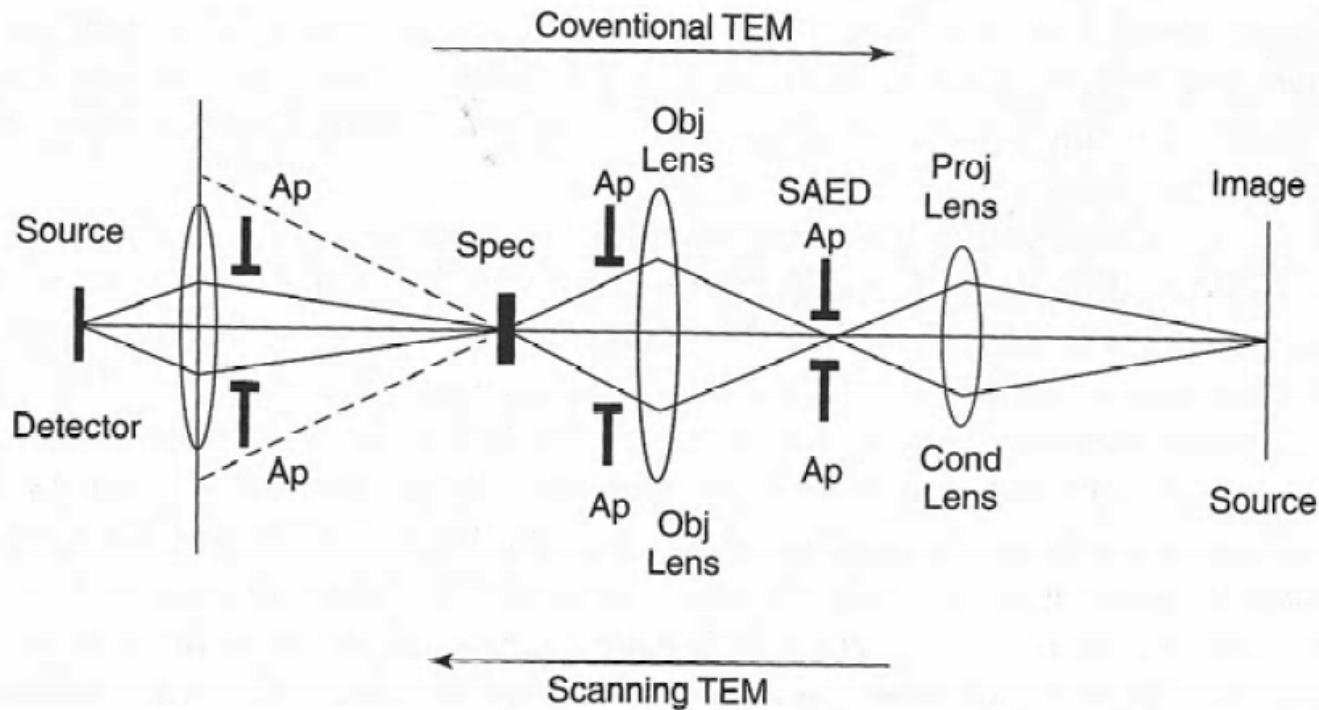
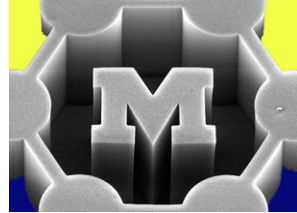
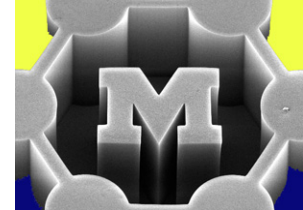


Figure 3.10. Ray diagram of a conventional transmission electron microscope (top path) and of a scanning transmission electron microscope (bottom path). The selected area electron diffraction (SAED) aperture (Ap) and the sample or specimen (Spec) are indicated, as well as the objective (Obj) and projector (Proj) or condenser (Cond) lenses. (Adapted from P. R. Buseck, J. M. Cowley, and L. Eyring, *High-Resolution Transmission Electron Microscopy*, Oxford Univ. Press, New York, 1988, p. 6.)

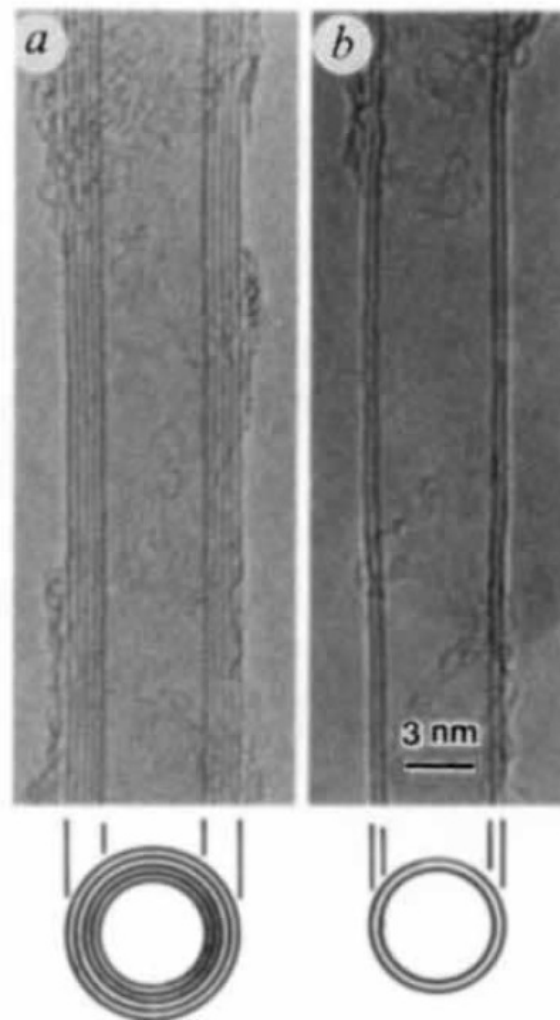
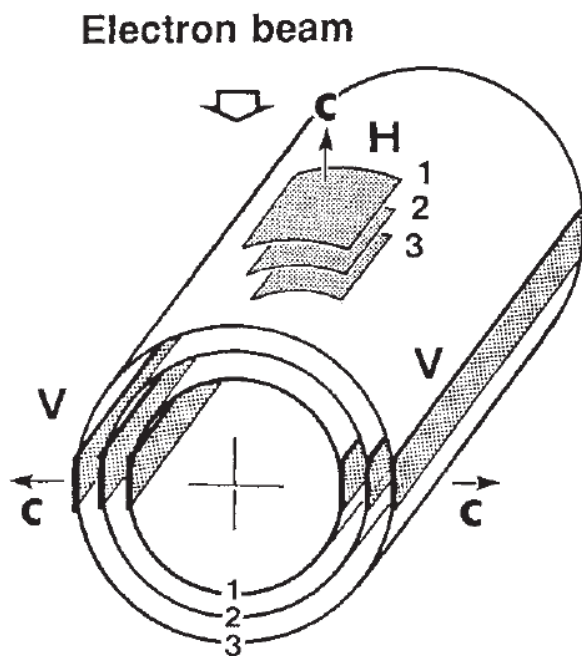


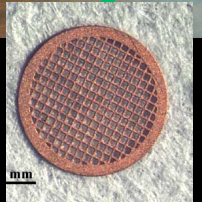
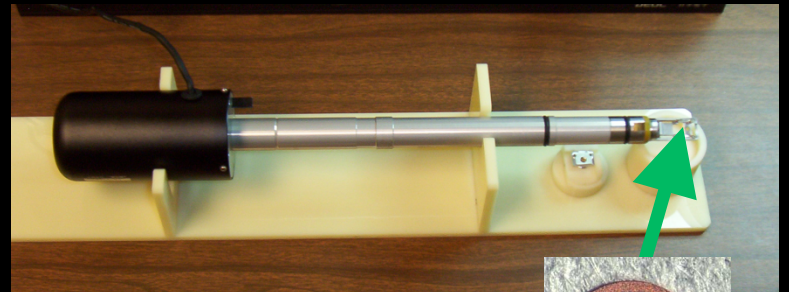
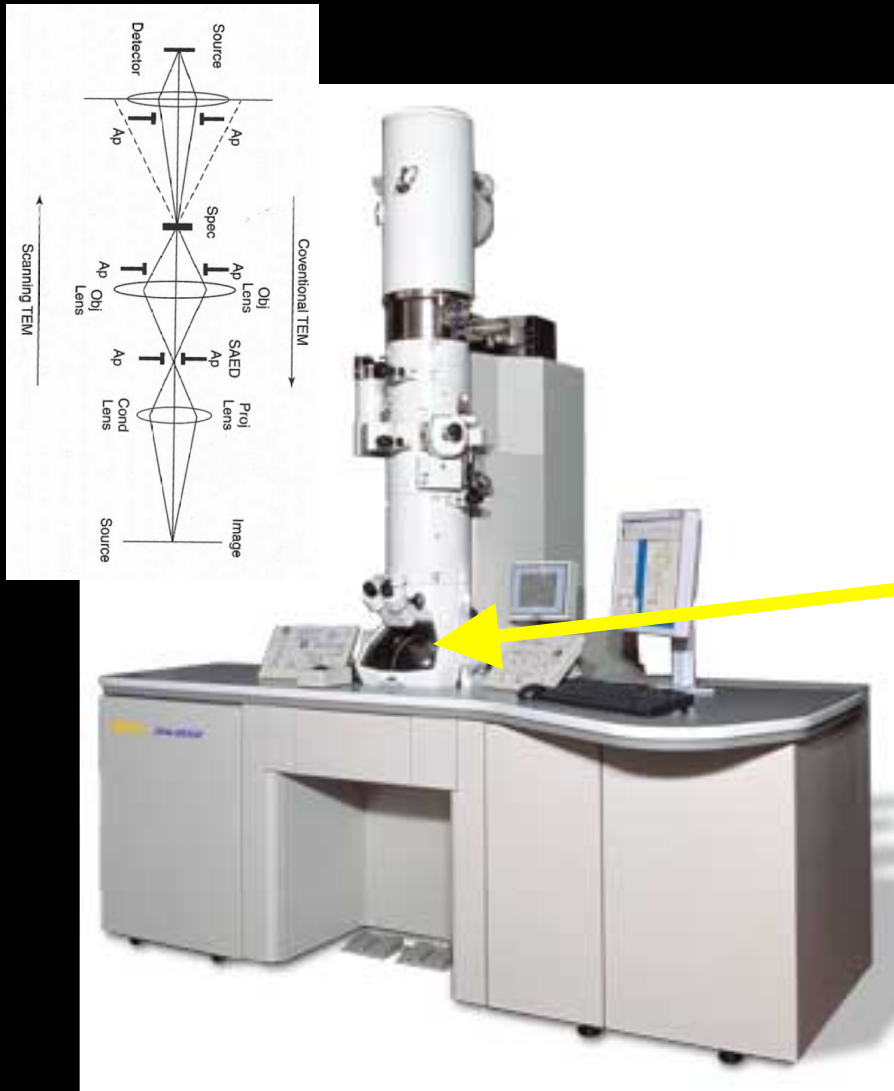
NATURE · VOL 354 · 7 NOVEMBER 1991

Helical microtubules of graphitic carbon

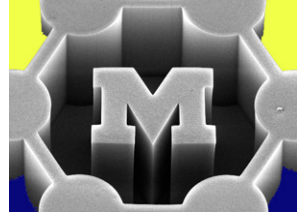
Sumio Iijima

NEC Corporation, Fundamental Research Laboratories.





<http://www.jeol.com>
<http://www.fei.com>



JEOL 200 kV Transmission Electron Microscopes

Available Models

	Resolution	Accelerating Voltage	Magnification
JEM-2100F	0.14nm Lattice	80 to 200 kV	x50 to 1,500,000
JEM-2100 LaB₆	0.10nm Lattice	80 to 200 kV	x50 to 1,500,000
JEM-2200FS	0.14nm Lattice	80 to 200 kV	x50 to 1,500,000
JEM-2500SE	STEM 0.2nm Lattice TEM 0.14nm Lattice	80 to 200 kV	x100 to 20,000,000

Electron beam can damage a structure

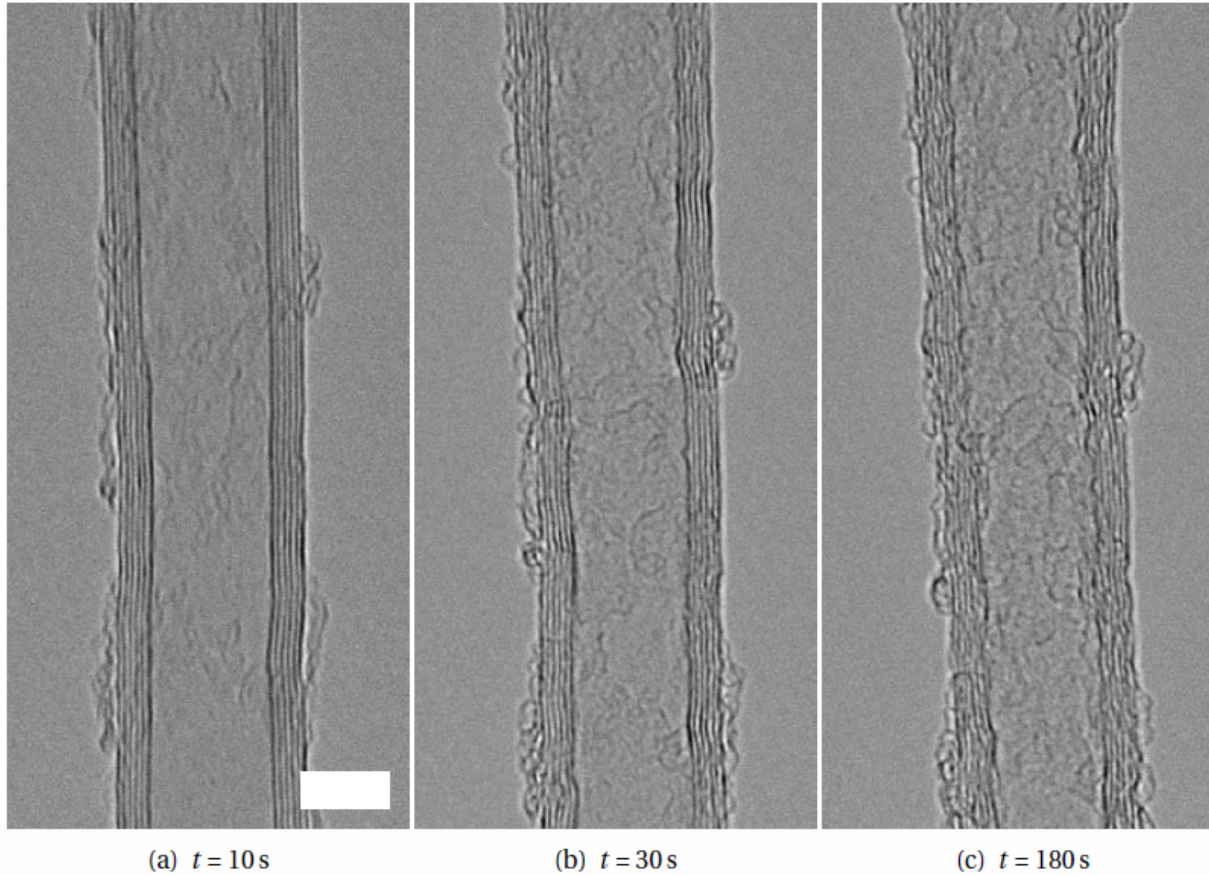
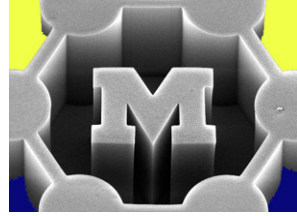
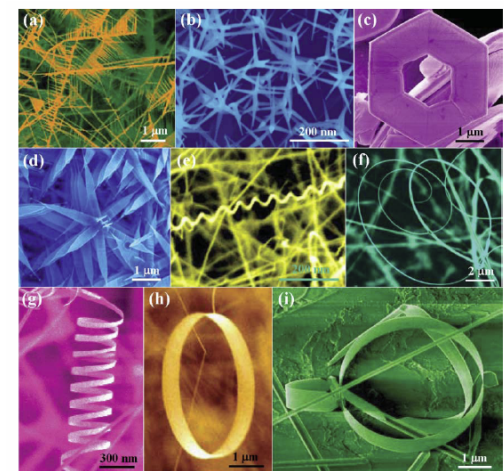
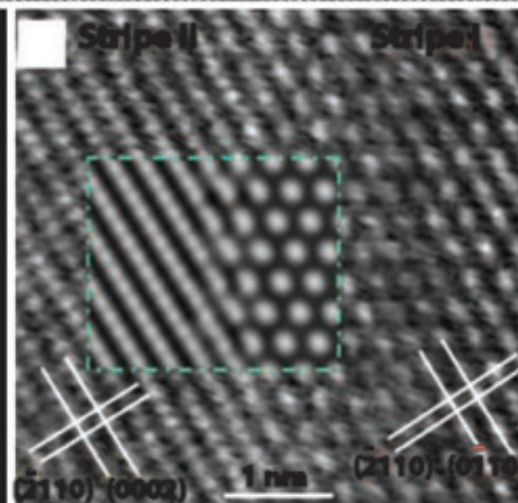
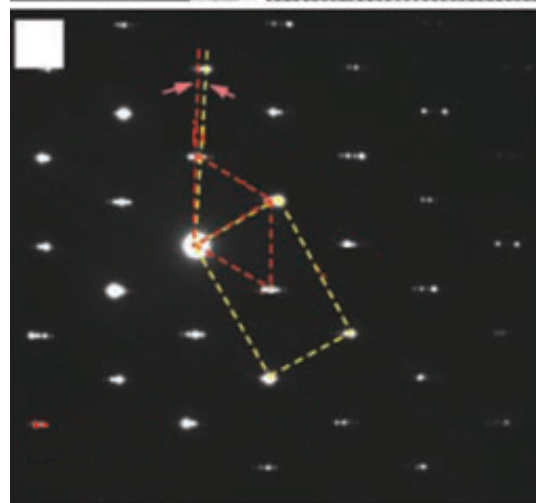
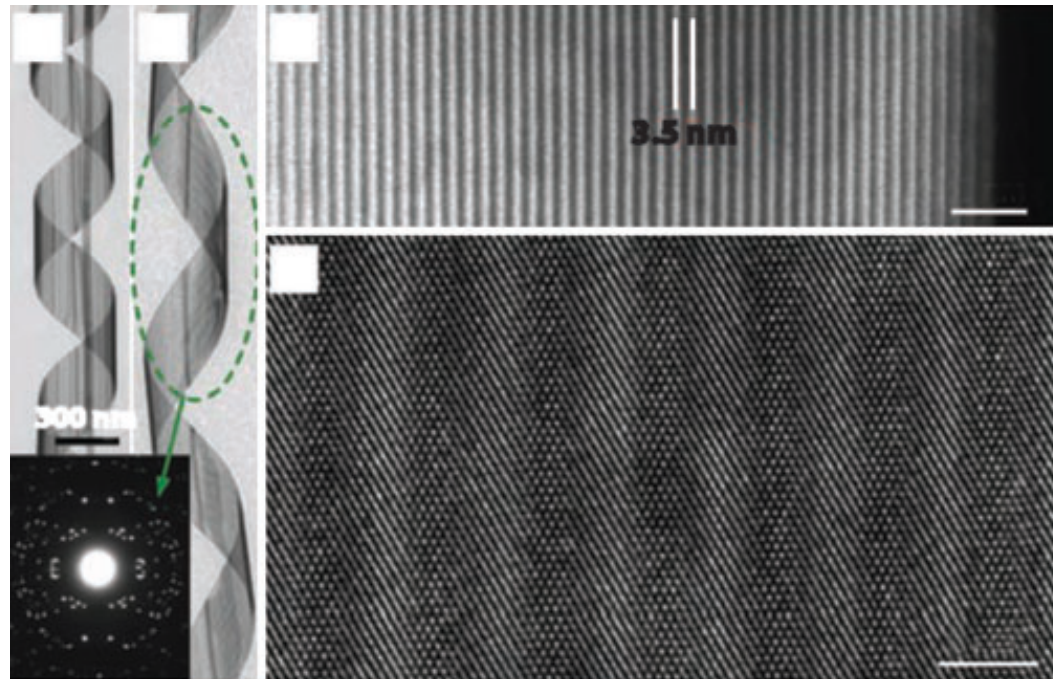
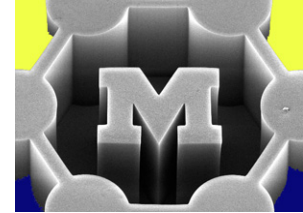


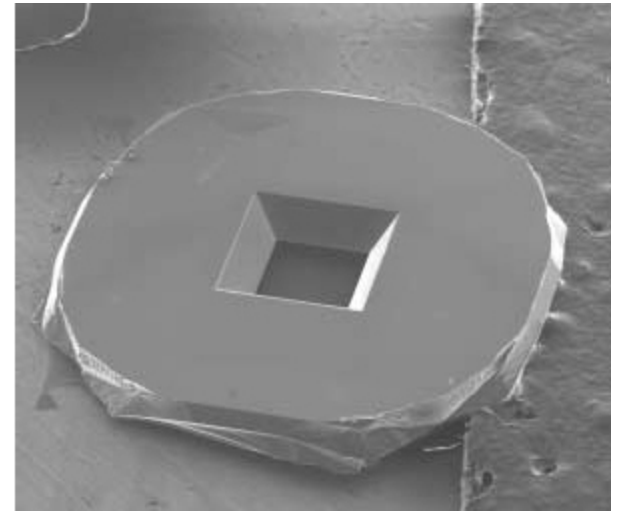
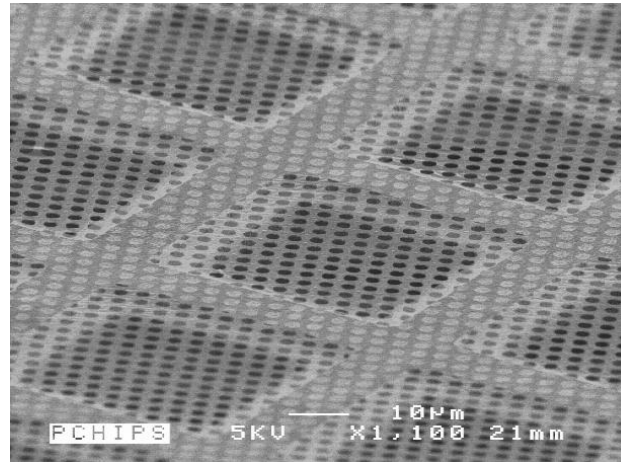
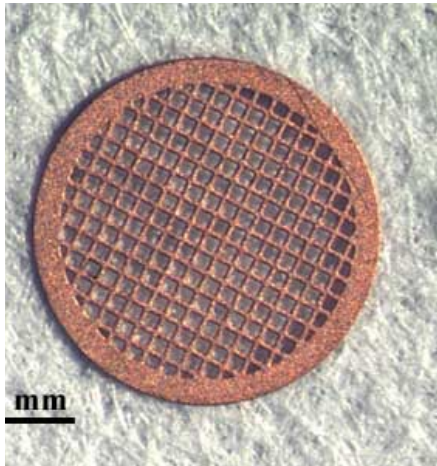
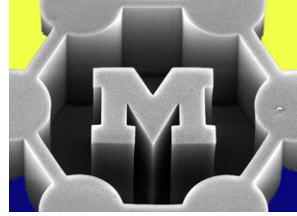
Figure 4-22. Damage to a MWNT by electron beam exposure during TEM imaging (JEOL-2011 at 200 keV). Scales 5 nm.

TEM characterization of ZnO helices



TEM sample preparation

- Grid, typically 3 mm diameter
- Membrane (< 10 nm thick) often suspended over grid
- Fabricate thin sections by ion milling or microtoming



Sample prep using a focused ion beam (FIB)

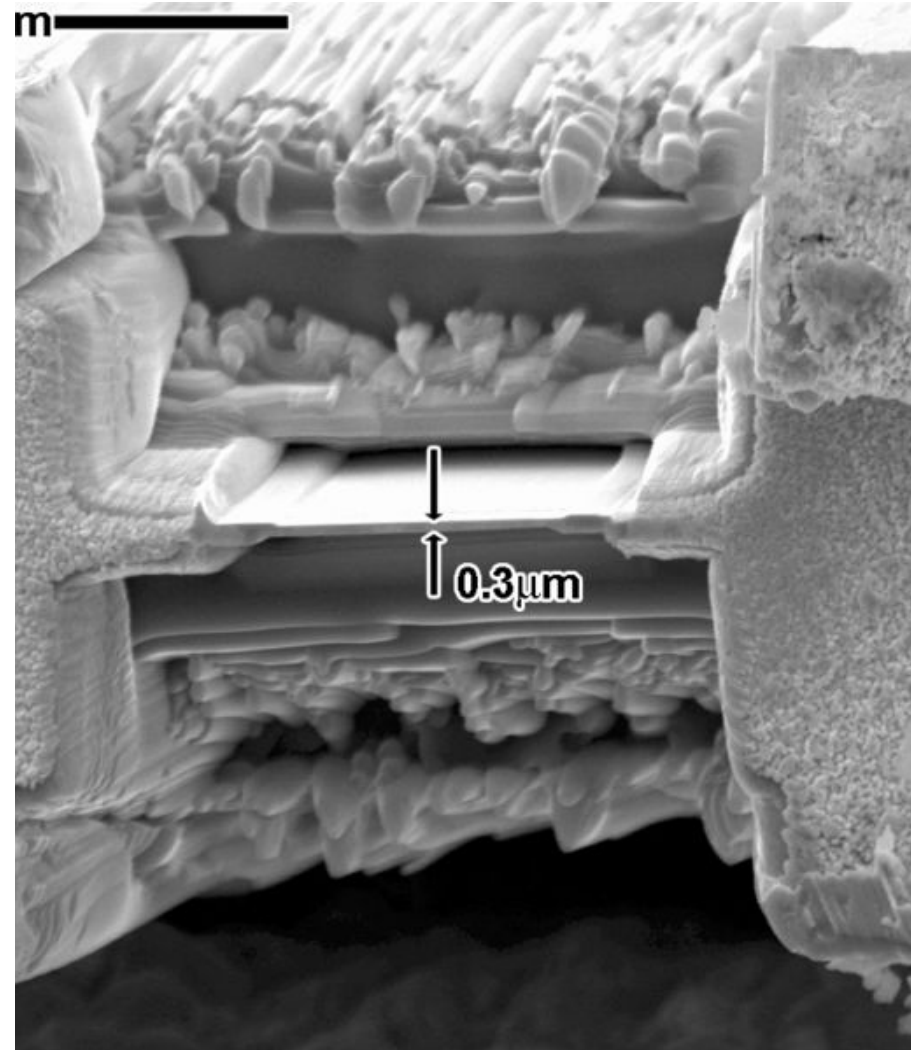
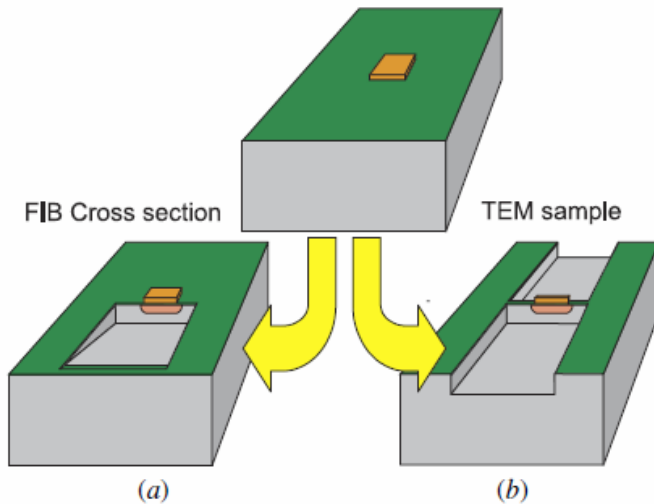
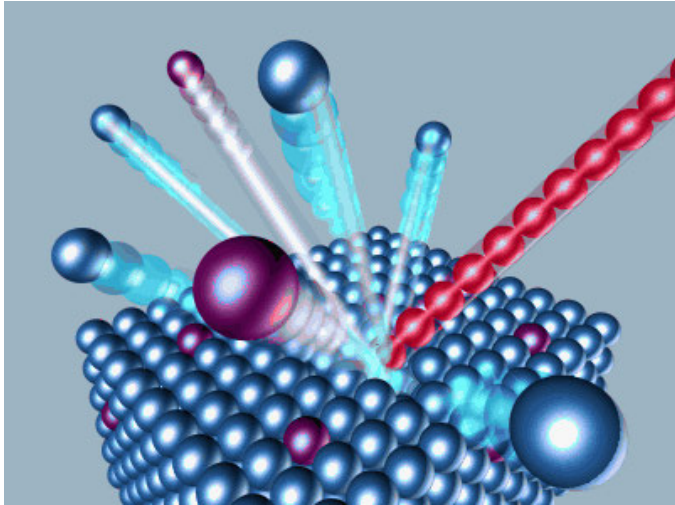
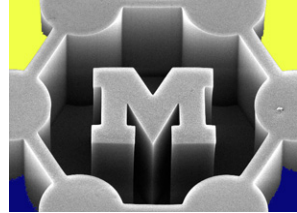
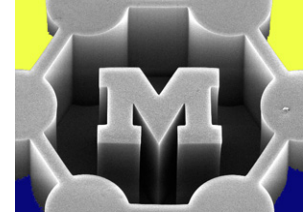


Figure 9. Sample with feature of interest can be (a) cross sectioned in the FIB. The section can be advanced until desired feature appears or (b) it can be prepared for inspection in a TEM.

Lens aberrations determine the practical resolution limit



- It's difficult to eliminate aberrations in metallic lenses

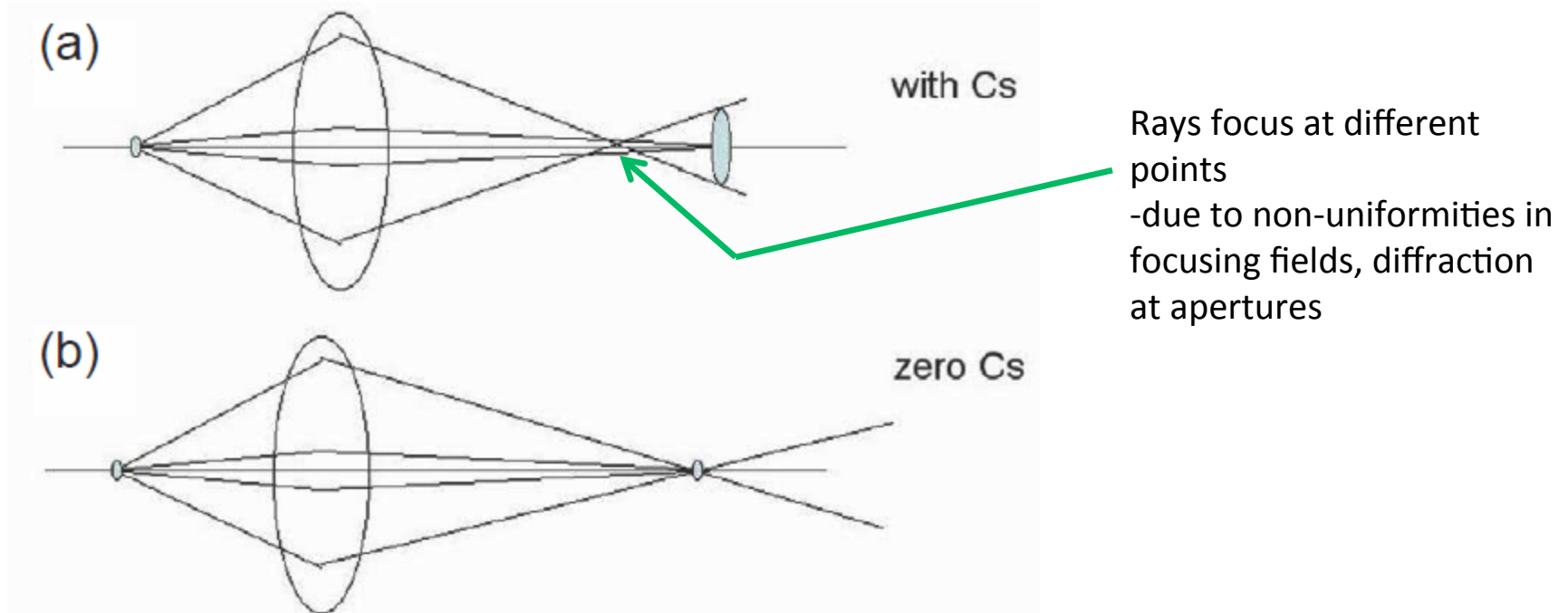


Fig. 1 (a) In a standard electron lens with spherical aberration, rays at different angles to the optic axis are brought to a focus at different points. (b) The effect of correcting the spherical aberration is to bring all rays into focus at the same point. The small blue area on the right of the lens represents the aberration disc.

Aberration-corrected TEM can show individual atoms (0.1 nm resolution)

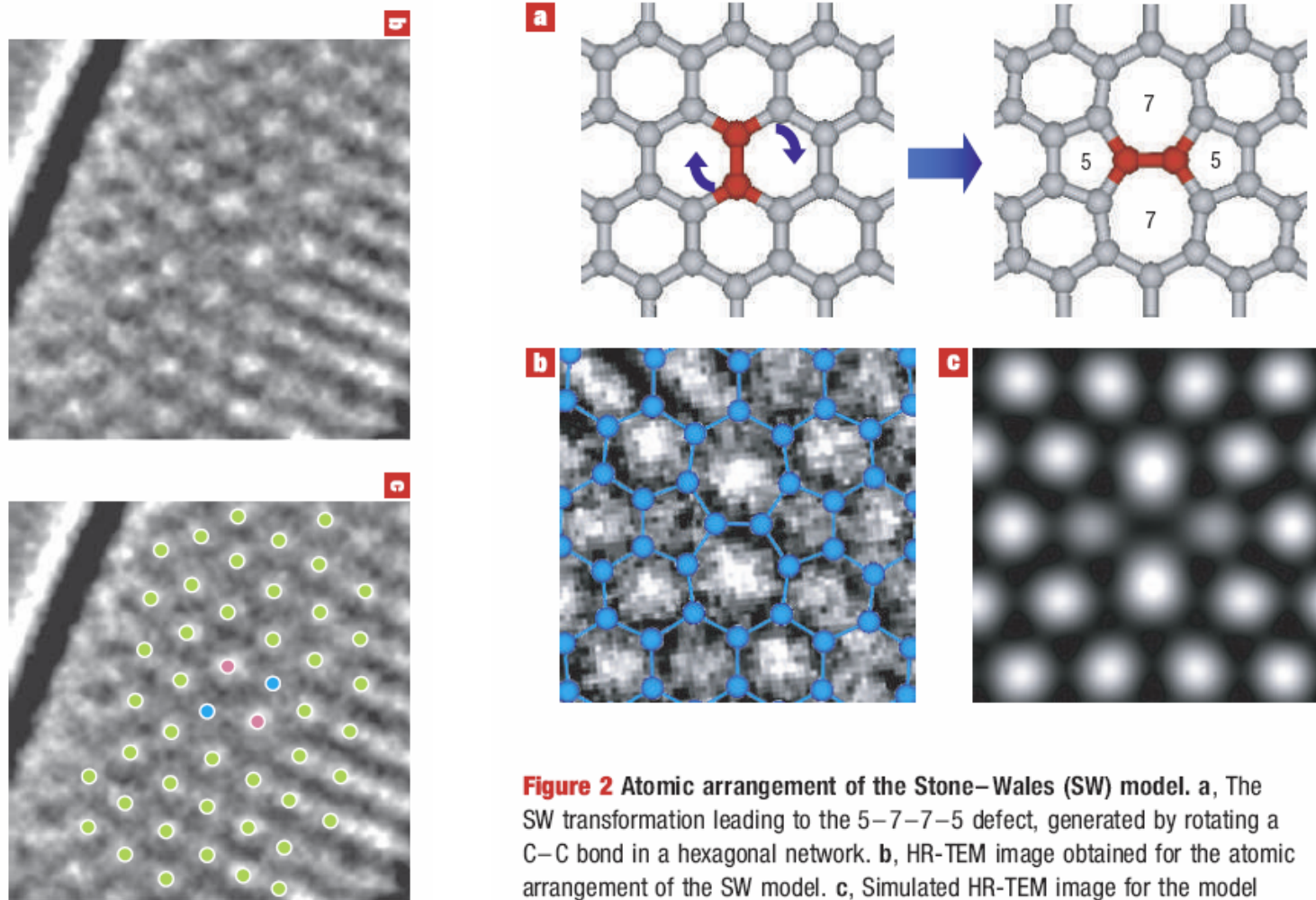
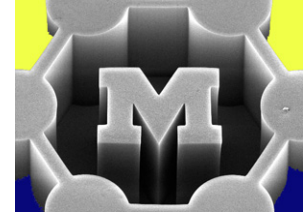
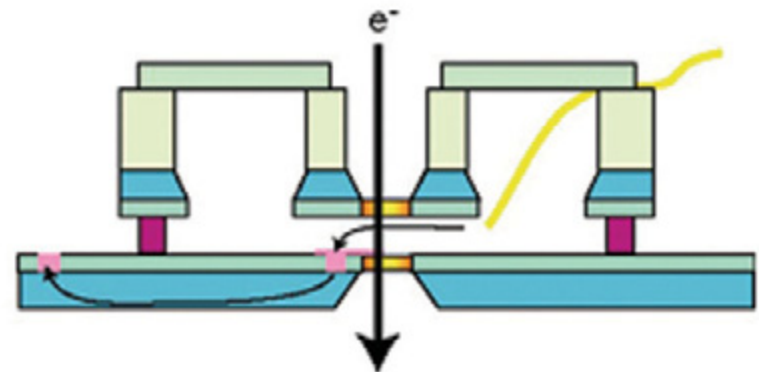
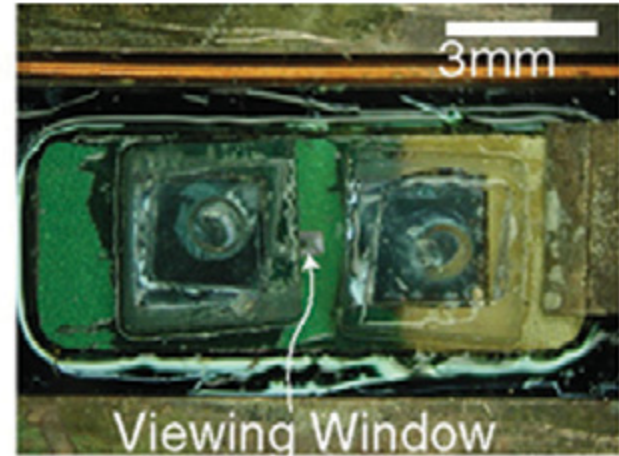
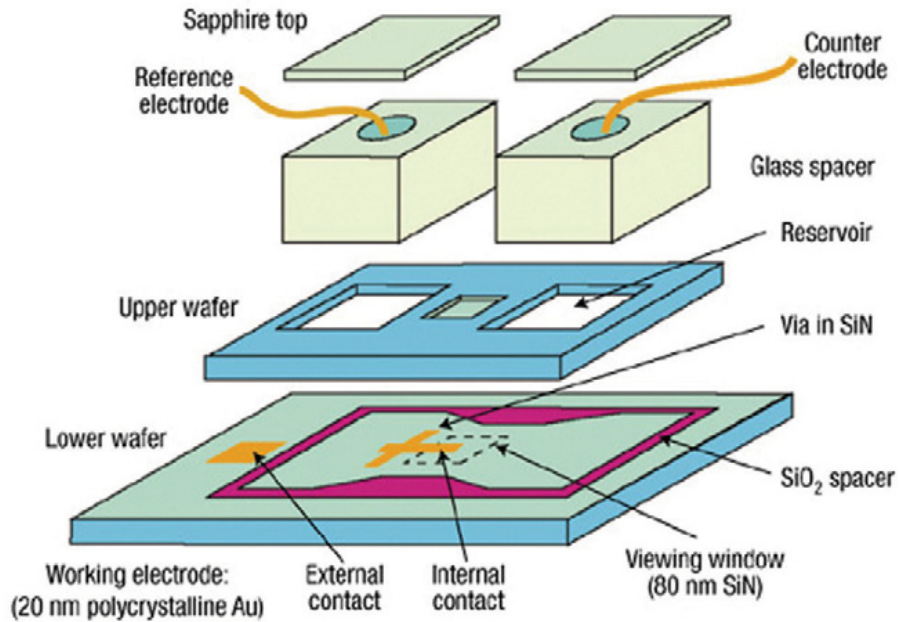
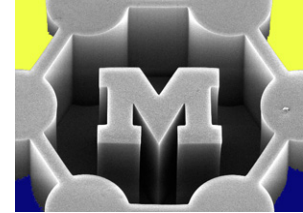
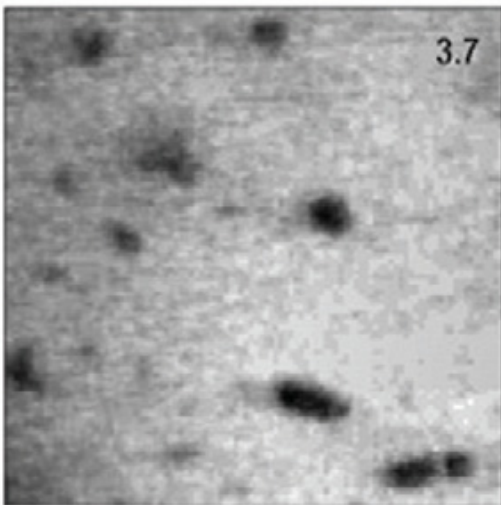
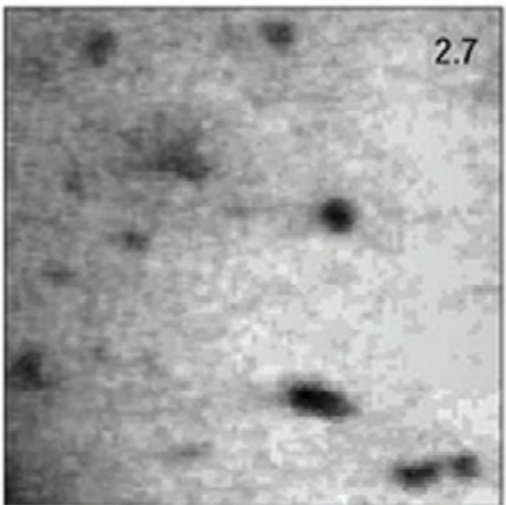
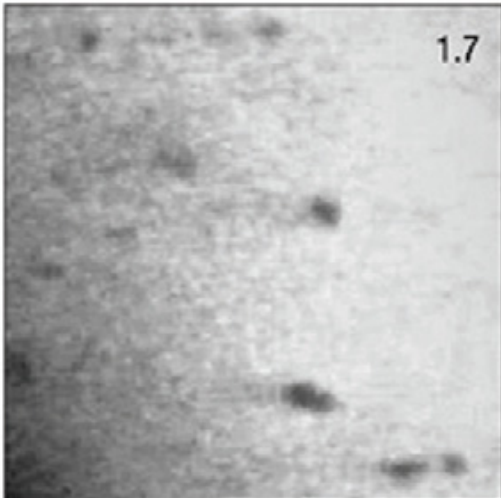
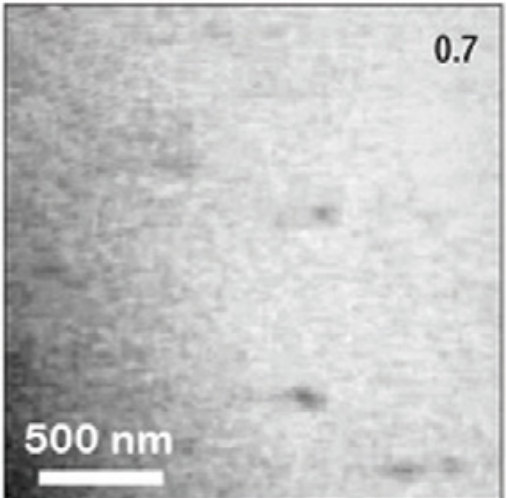
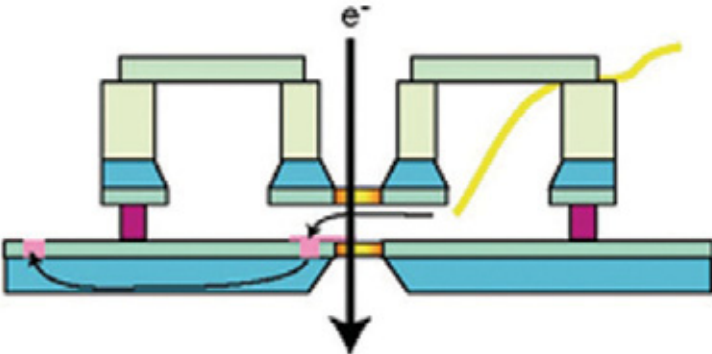
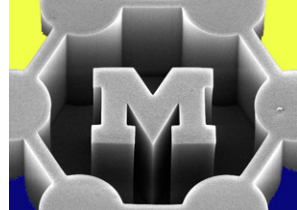


Figure 2 Atomic arrangement of the Stone–Wales (SW) model. **a**, The SW transformation leading to the 5–7–7–5 defect, generated by rotating a C–C bond in a hexagonal network. **b**, HR-TEM image obtained for the atomic arrangement of the SW model. **c**, Simulated HR-TEM image for the model shown in **b**.

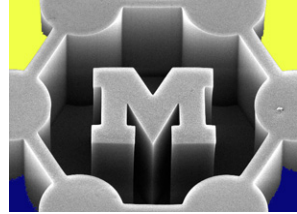
Environmental TEM (E-TEM) shows material dynamics



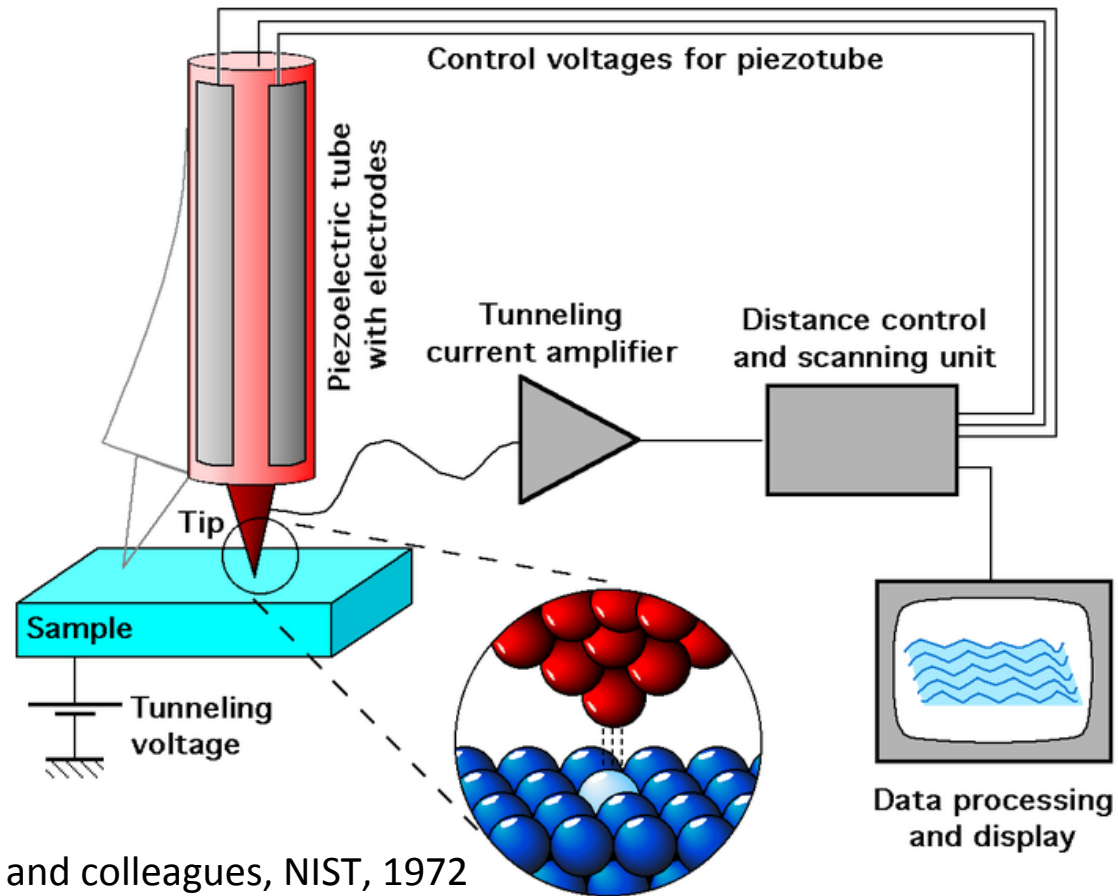


A sequence of images of the nucleation and subsequent growth of individual Cu crystallites during galvanic deposition at 5 mA/cm². The numbers in the upper right-hand corner indicate the number of seconds after the initiation of the current flow.

Scanning tunneling microscopy (STM)



- First to give real-space atomic resolution images
- $\sim 10\text{\AA}$ gap between conductive tip and conductive sample, using tunneling (exponential) current to measure displacement

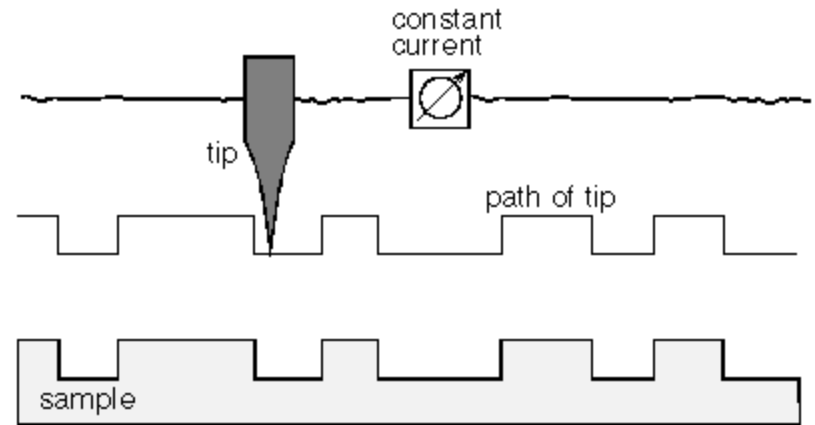
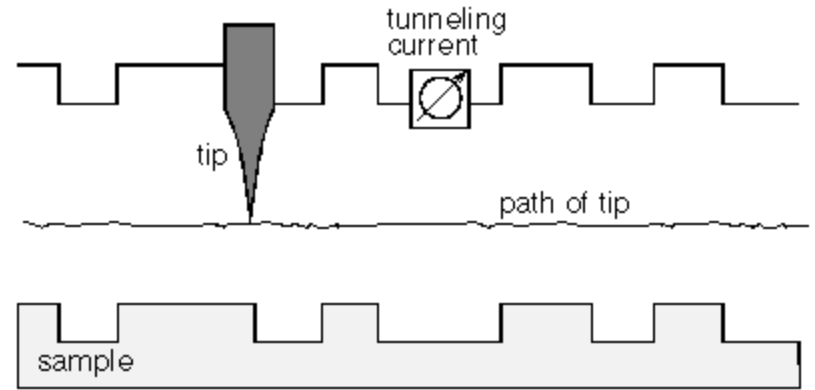
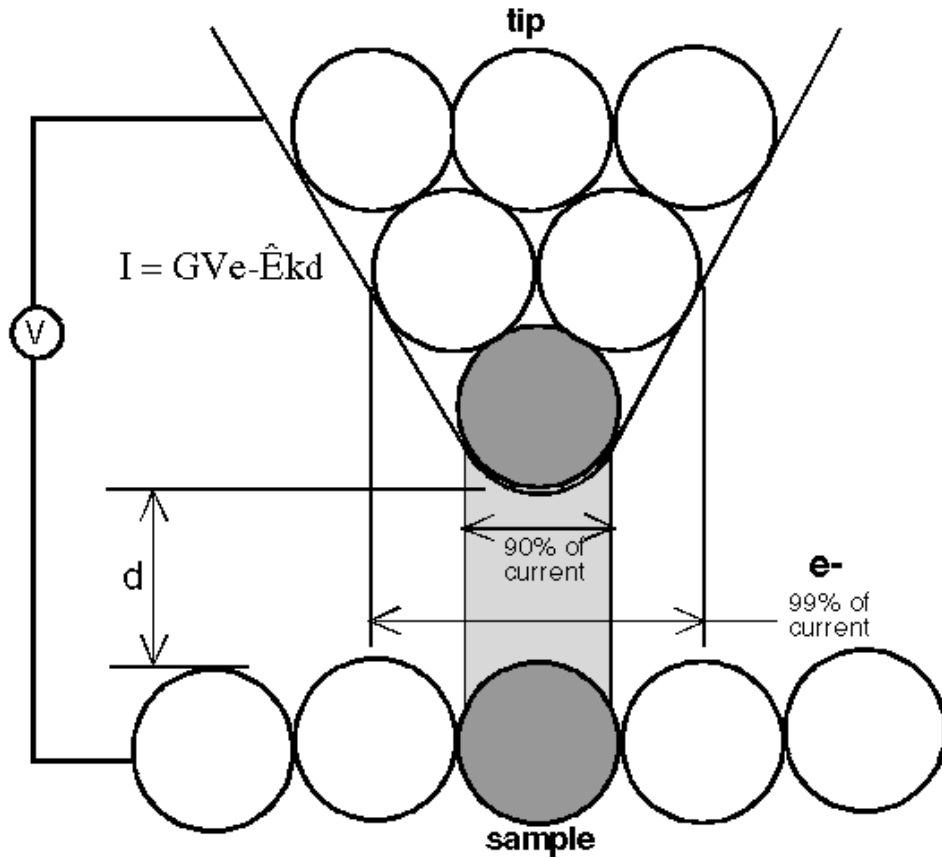
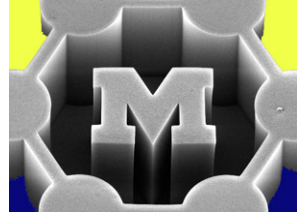


“topografiner” invented by Young and colleagues, NIST, 1972

<http://nvl.nist.gov/pub/nistpubs/sp958-lide/214-218.pdf>

Binnig and Rohrer (IBM), Nobel Prize, 1986

STM: scanning modes

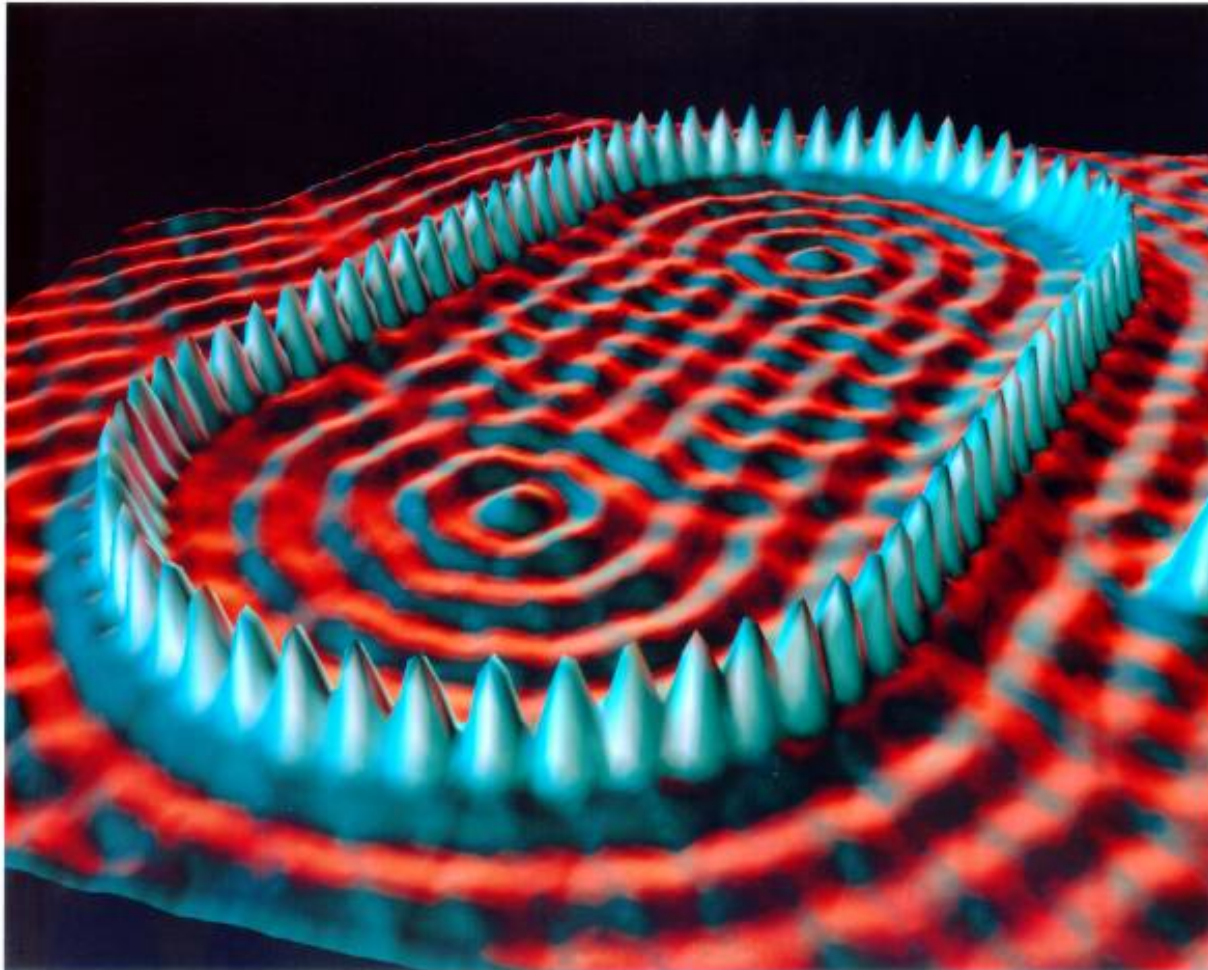
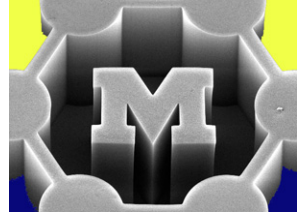


invented by Young and colleagues, NIST, 1972

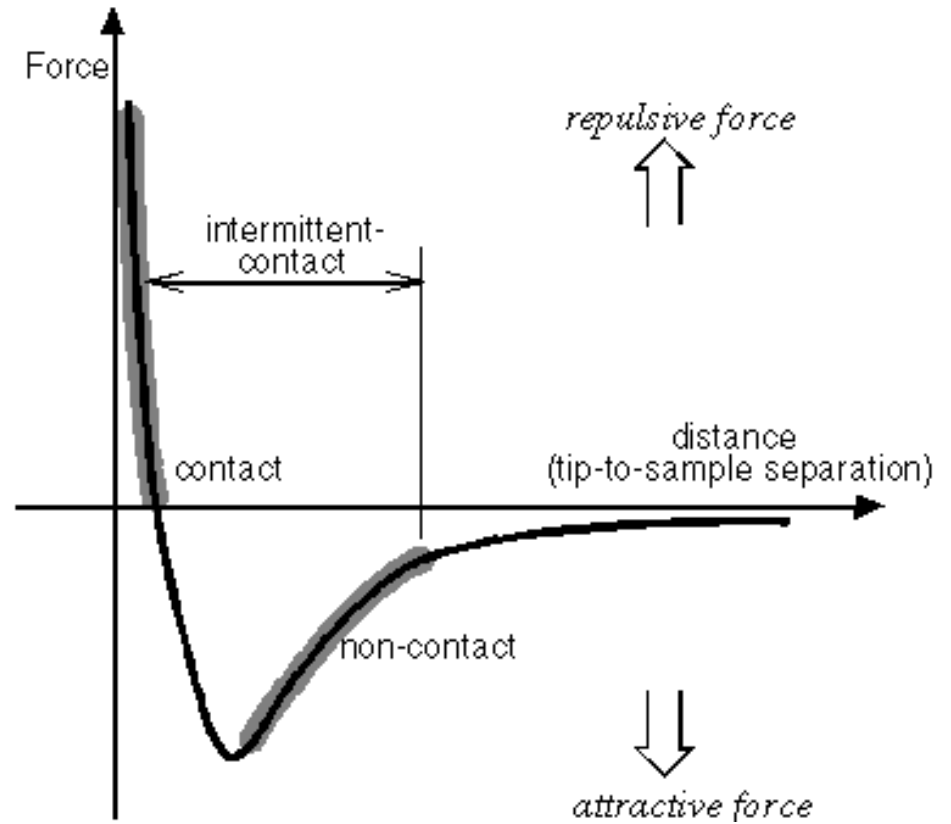
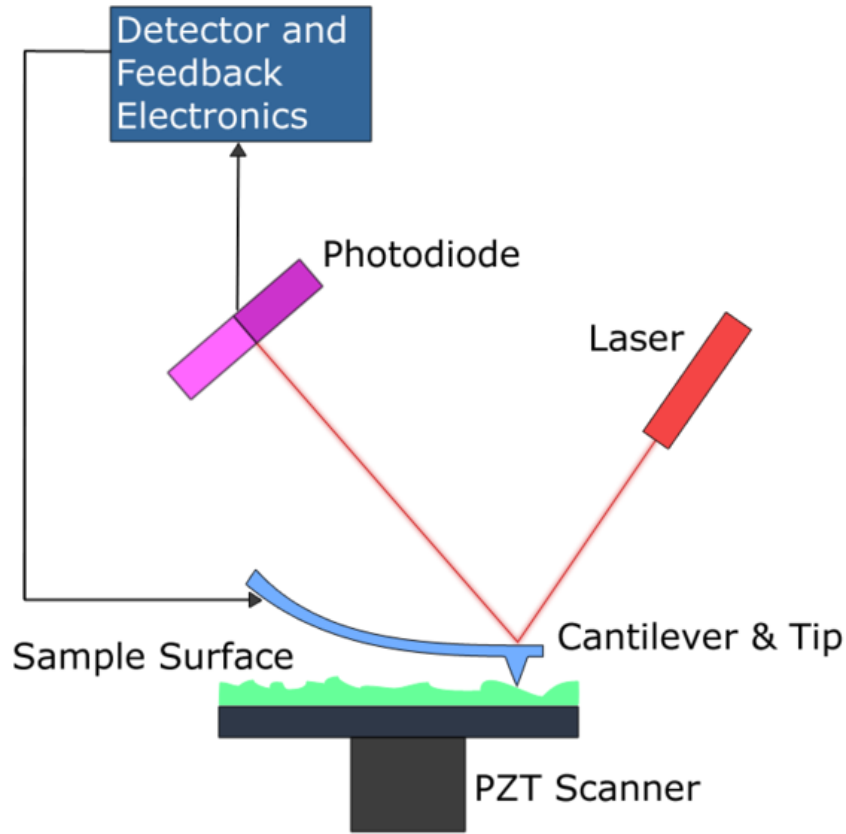
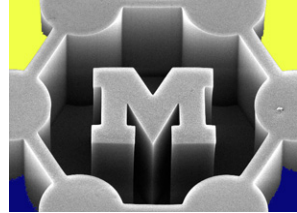
Binnig and Rohrer, Nobel Prize, 1986

Figure from park.com, A practical guide to scanning probe microscopy

Quantum corral



Atomic force microscopy

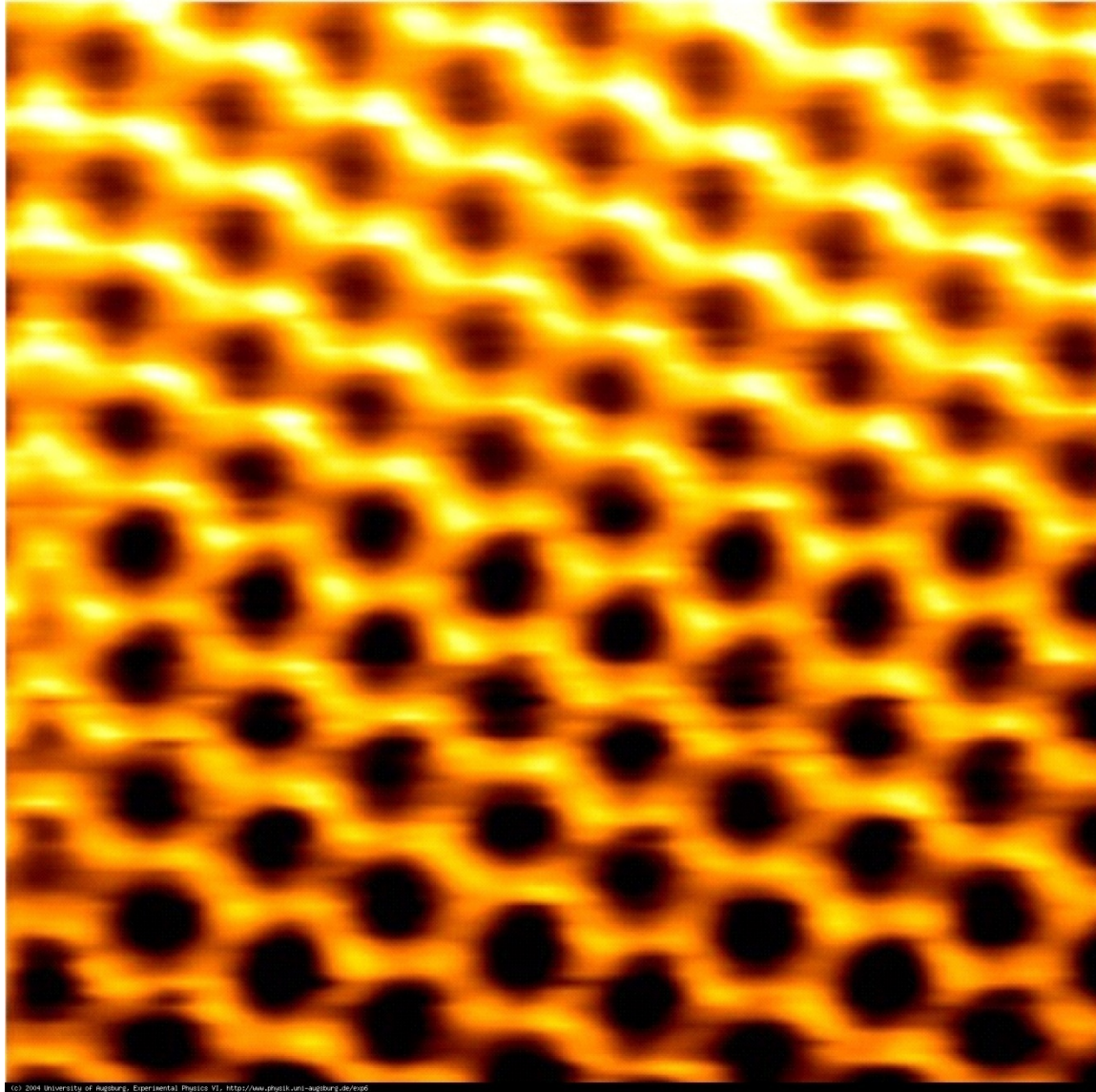
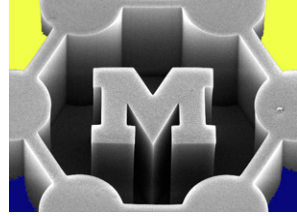


invented by Young and colleagues, NIST, 1972

Binnig and Rohrer, Nobel Prize, 1986

Park.com, A practical guide to scanning probe microscopy

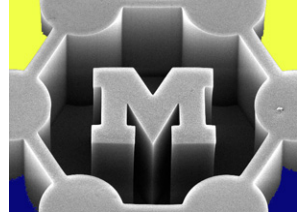
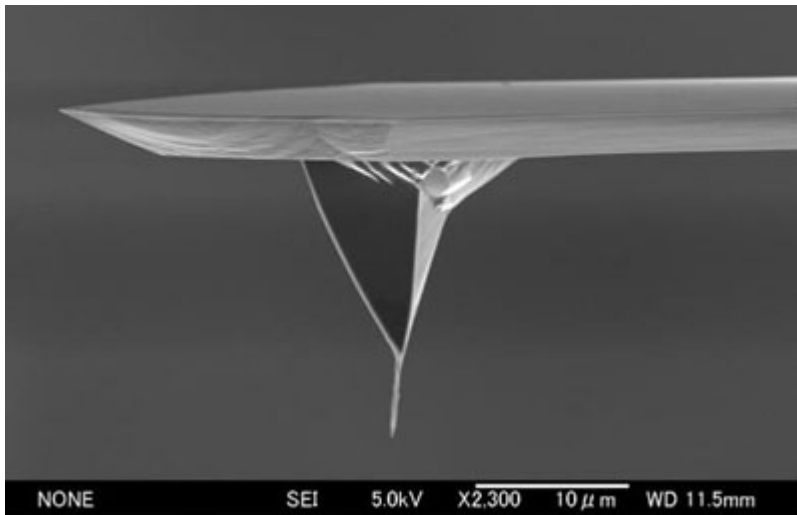
AFM image of graphite



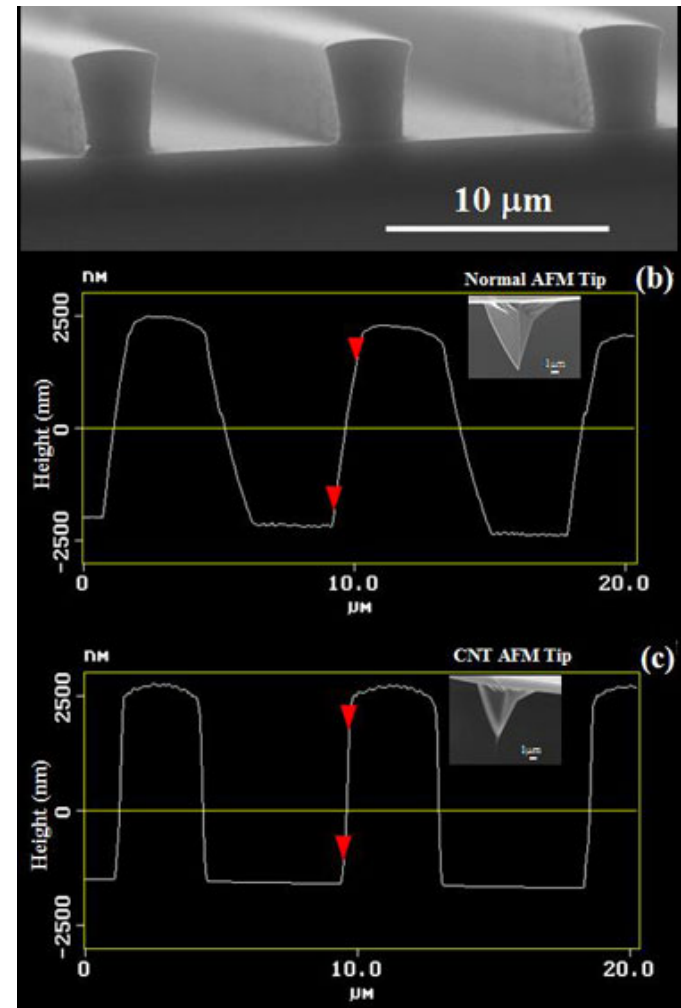
© 2004 University of Augsburg, Experimental Physics VI, <http://www.physik.uni-augsburg.de/exp6>

AFM cantilevers and tips

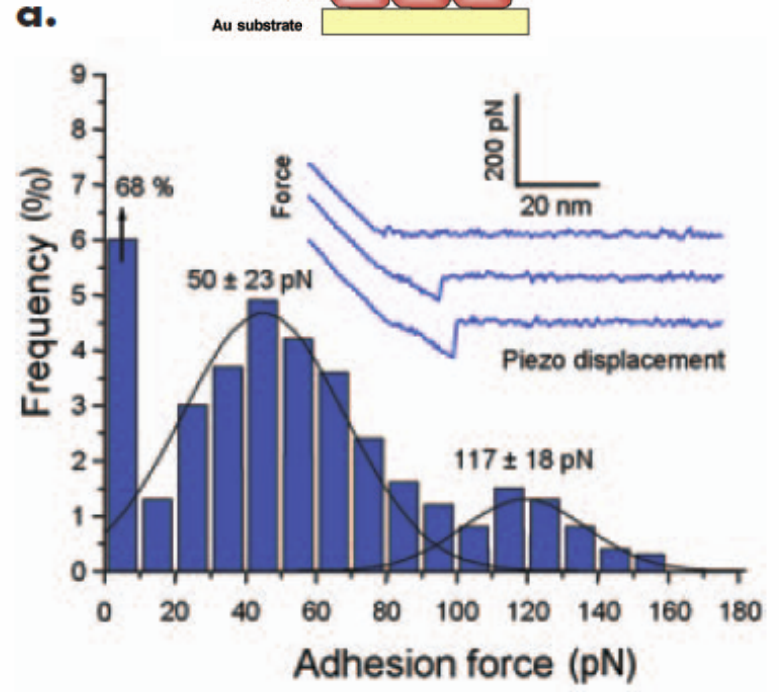
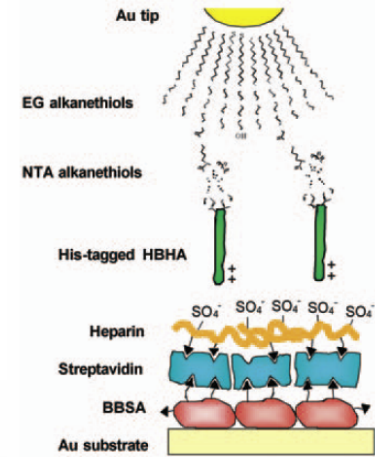
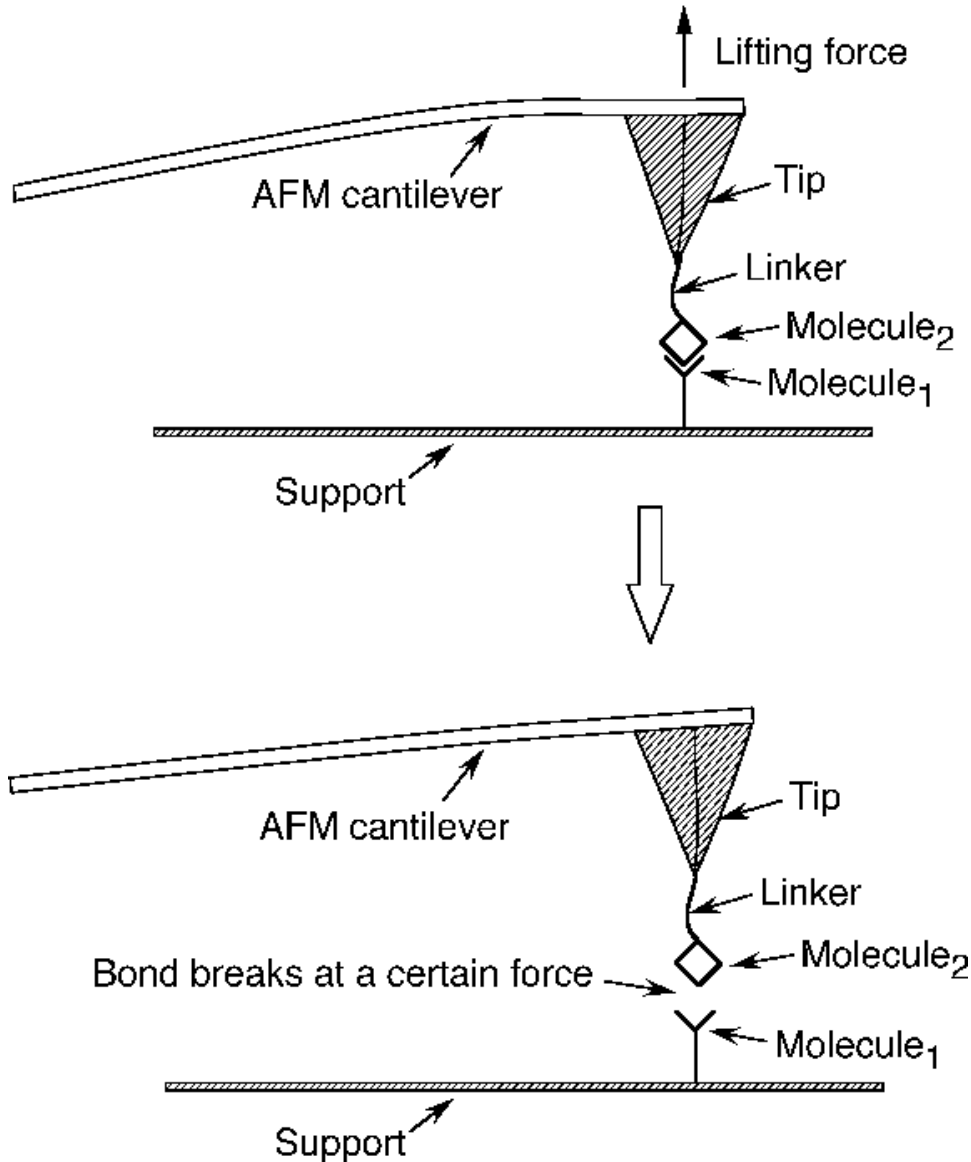
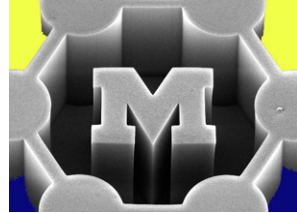
- Etched pyramids
- Oxide/etch sharpening
- Growth of nanostructured tips



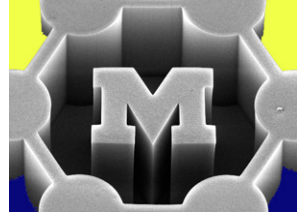
Tip/sample convolution



Actuating single molecules using AFM



High-speed (video-rate) AFM



- Key: resonant scanning in two axes

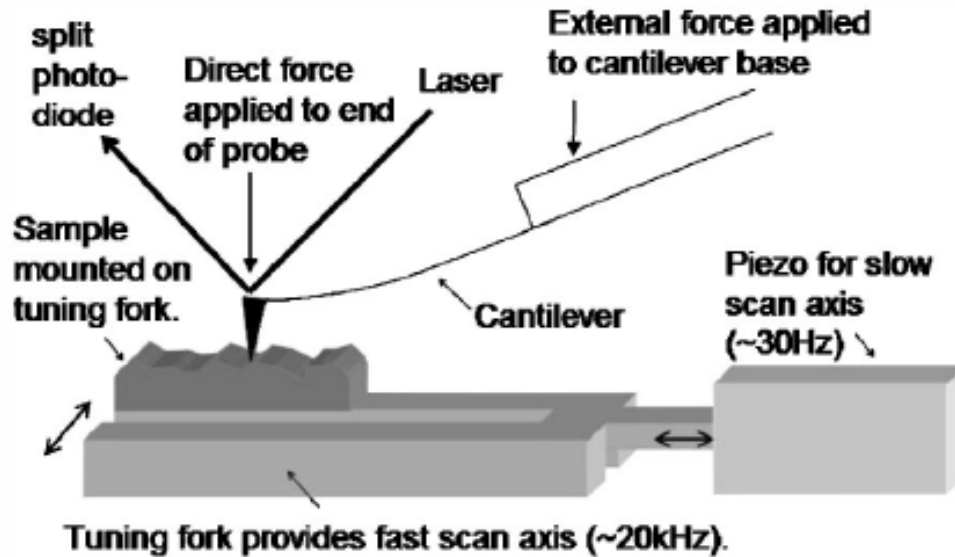


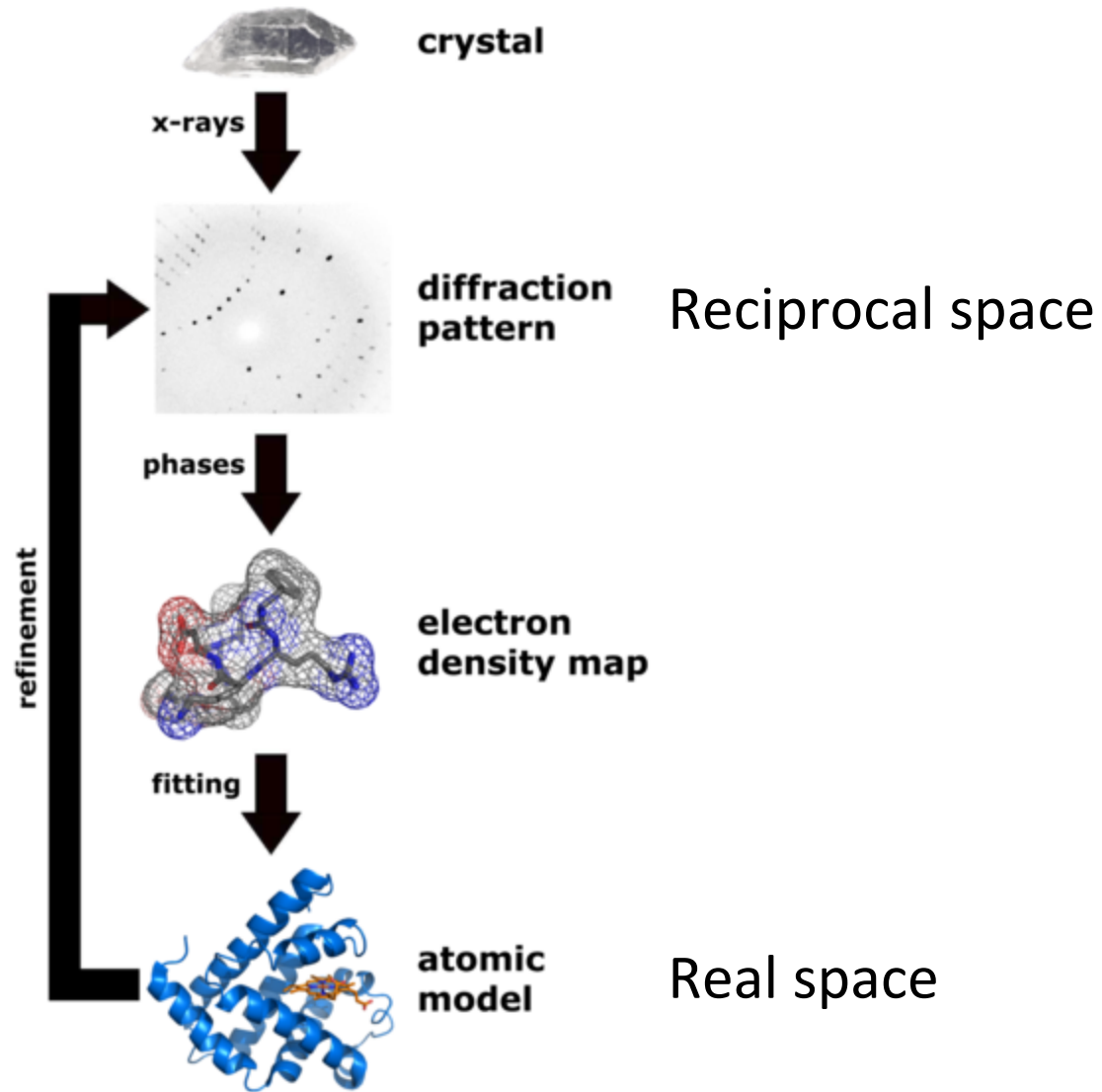
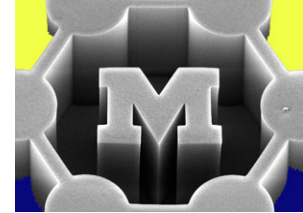
FIG. 1. A schematic of the HSAFM. The sample is mounted on a quartz crystal resonator that generates the fast scan axis and is driven in the orthogonal slow scan axis by a piezo actuator. An optical lever is used to measure the deflection of the microcantilever. An additional “direct force” is applied to the end of the cantilever, forcing the tip to maintain contact with the surface. By tuning the magnitude of the “direct force” and the degree of damping of the cantilever, a high bandwidth passive feedback loop is created.

VIDEOS

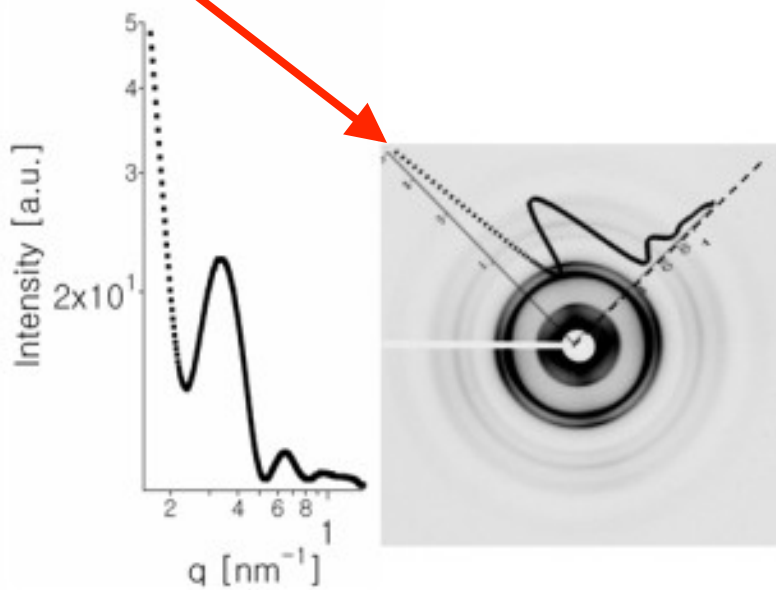
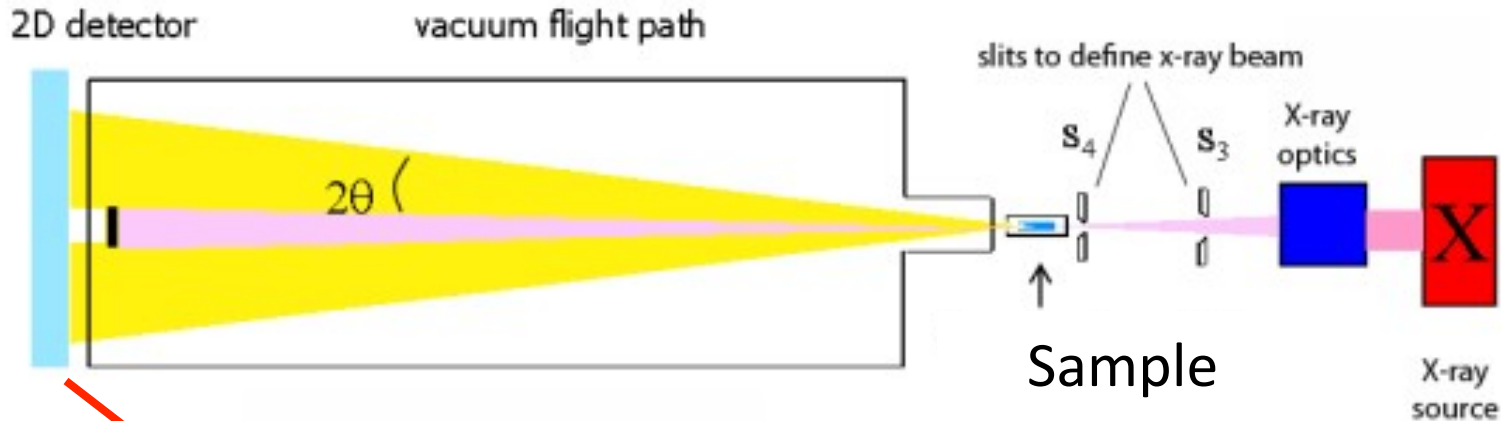
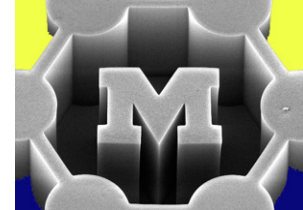
<http://www.infinitesima.com/VideoAFM-download.html>

<http://www.s.kanazawa-u.ac.jp/phys/biophys/roadmap.htm>

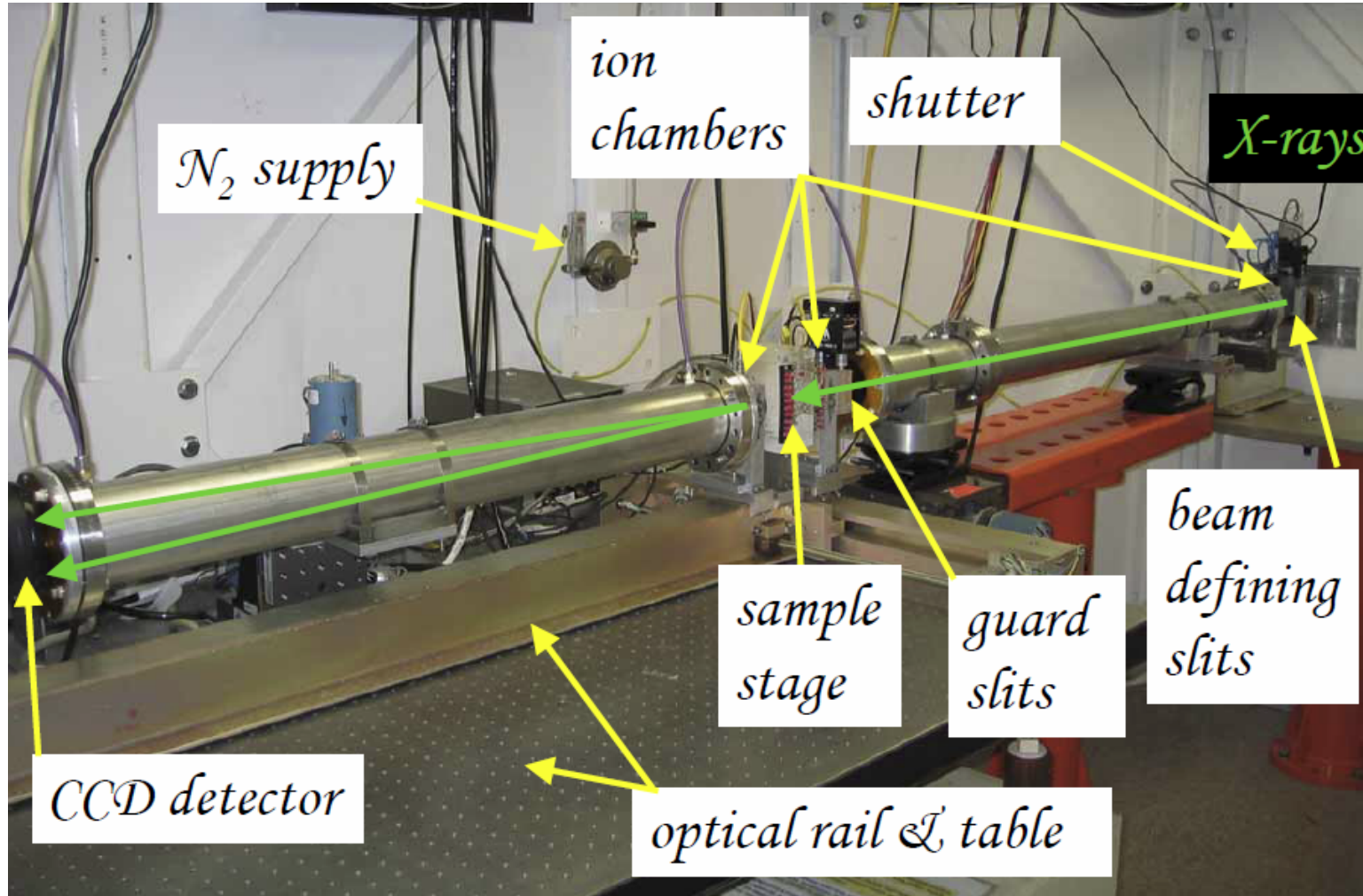
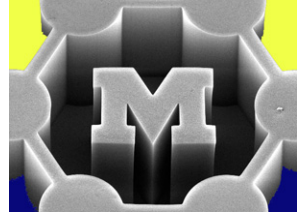
Structure determination using X-rays



X-ray scattering (diffraction)

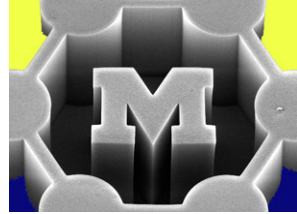


Typical SAXS beamline



http://www-ssrl.slac.stanford.edu/conferences/workshops/scatter2006/talks/pople_saxs_work_hop_060522.pdf

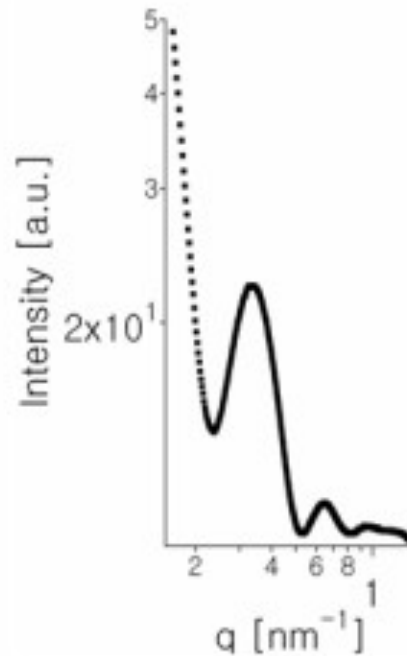
Scattering angles and feature sizes



Bragg's law:

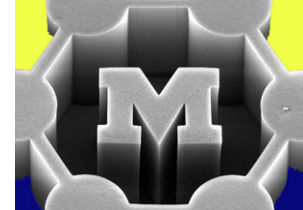
$$\lambda = 2d \sin \theta$$

$$q = \frac{2\pi}{d}$$

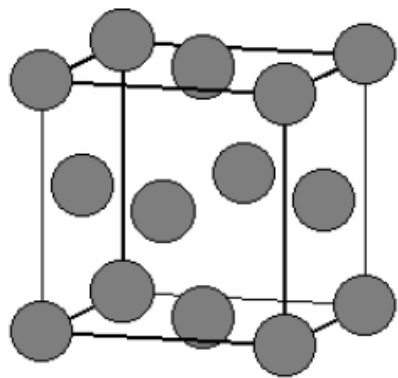


- Small-angle (SAXS): ~5-50 nm
- Wide-angle (WAXS): smaller features than SAXS, to lattice spacing and below
- Ultra small-angle (USAXS): larger features than SAXS, e.g., structure-structure interactions

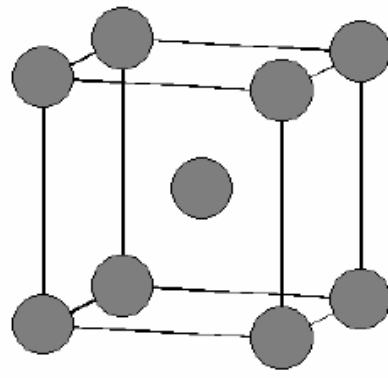
Diffraction rings \rightarrow atomic spacings



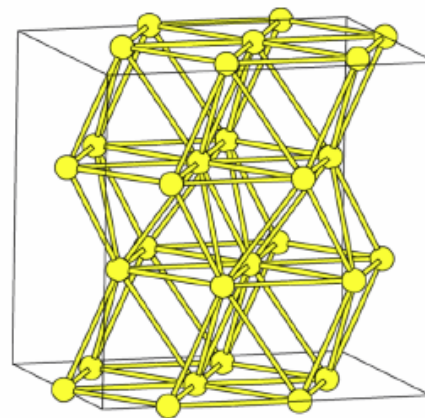
Real space packing



Face centered cubic



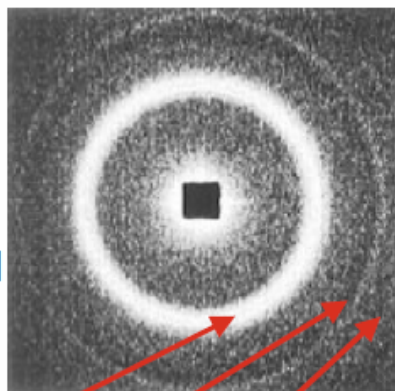
Body centered cubic



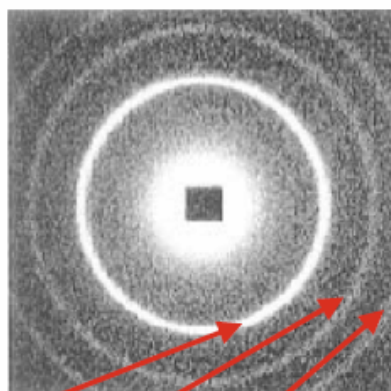
Hexagonal

Reciprocal space image

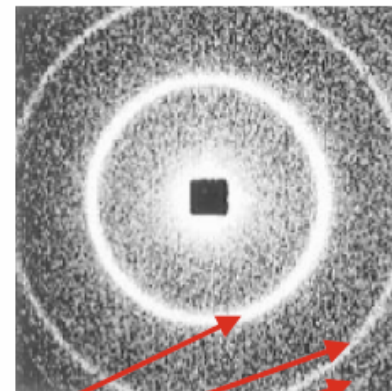
(unoriented domains)



Normalized peak positions $\equiv 1; =\sqrt{4/3}; =\sqrt{8/3}$

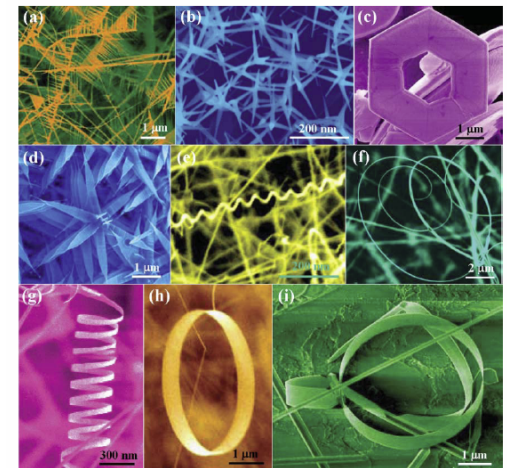
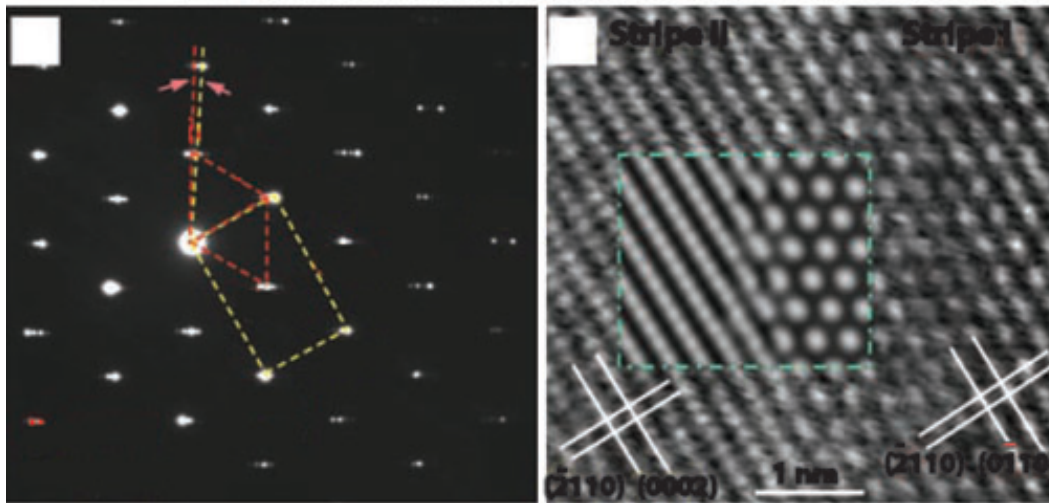
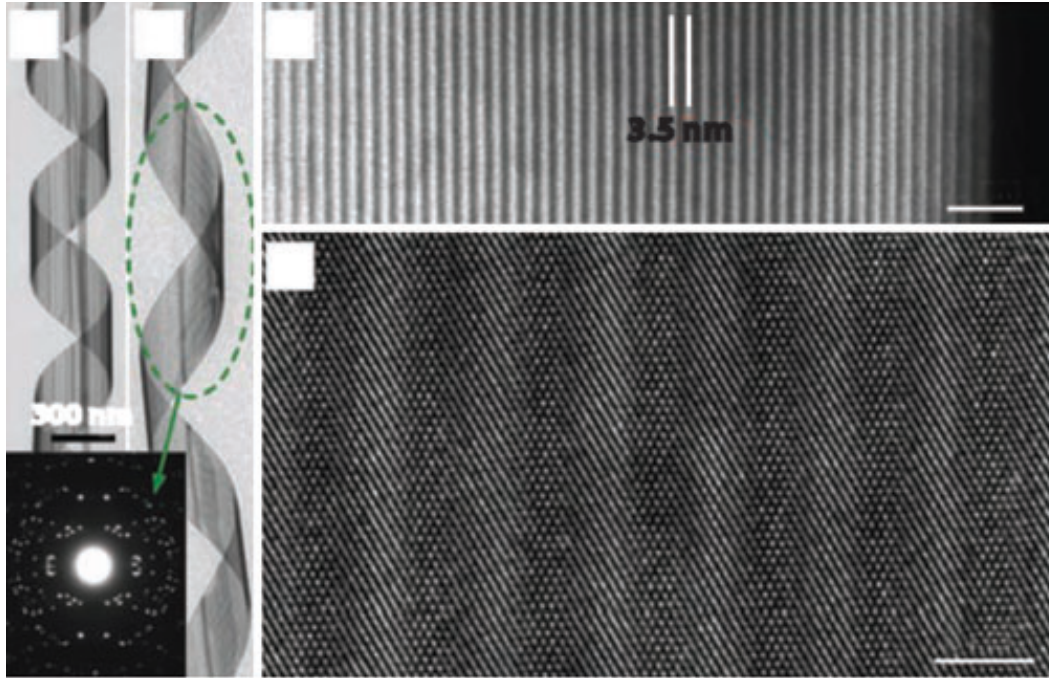
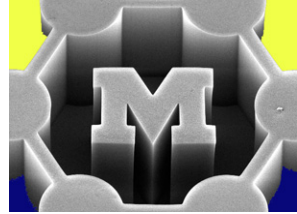


$\equiv 1; =\sqrt{2}; =\sqrt{3}$



$\equiv 1; =\sqrt{3}; =\sqrt{4}$

Electron diffraction in TEM





ICDD

The International Centre for Diffraction Data

[汉语/漢語](#) [Español](#) [Français](#) [Italiano](#) [Português](#) [русский язык](#)

[Home](#) [About](#) [Contact](#) [Sitemap](#)

Common features and applications

Use of embedded editorial and quality analyses

Embedded application software in the PDF

Hints and shortcuts

[HOME](#) [About ICDD](#) [Products](#) [Membership](#) [Education](#) [GiA](#) [Resources](#) [Developers](#) [DXC](#) [Search](#)

► [Home](#)

Frequently Visited Pages:

[Events Calendar](#)

[ICDD Events and Conference Schedule](#)

[Advances in X-ray Analysis](#)

[2007 Public Report \(PDF\)](#)

[Powder Diffraction Journal](#)

[Grant-in-Aid Program](#)

[ICDD Awards](#)

[ICDD Product Tutorials](#)

The International Centre for Diffraction Data

ICDD

Our Mission and Vision



The International Centre for Diffraction Data® (ICDD®)

is a non-profit scientific organization dedicated to collecting, editing, publishing, and distributing powder diffraction data for the identification of crystalline materials. The membership of the ICDD consists of worldwide representation from academe, government, and industry.

PPXRD-7

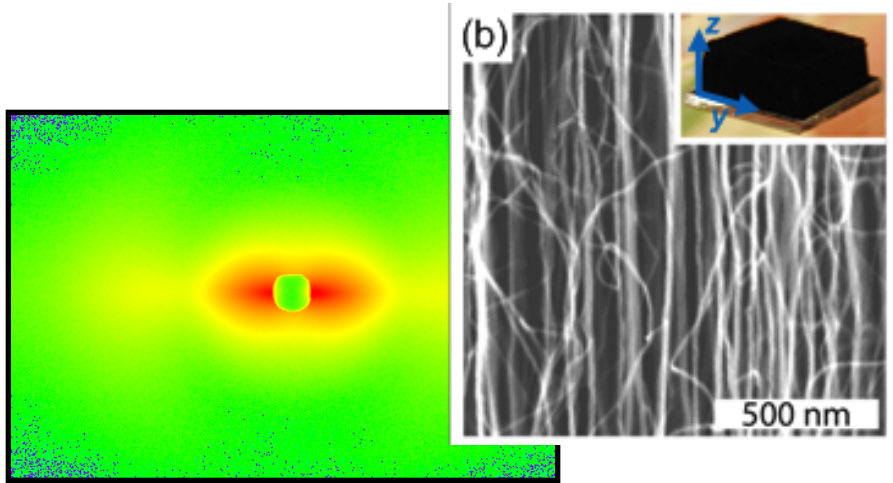
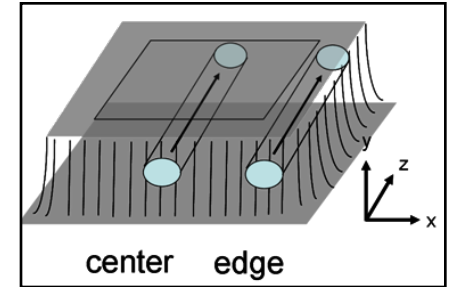
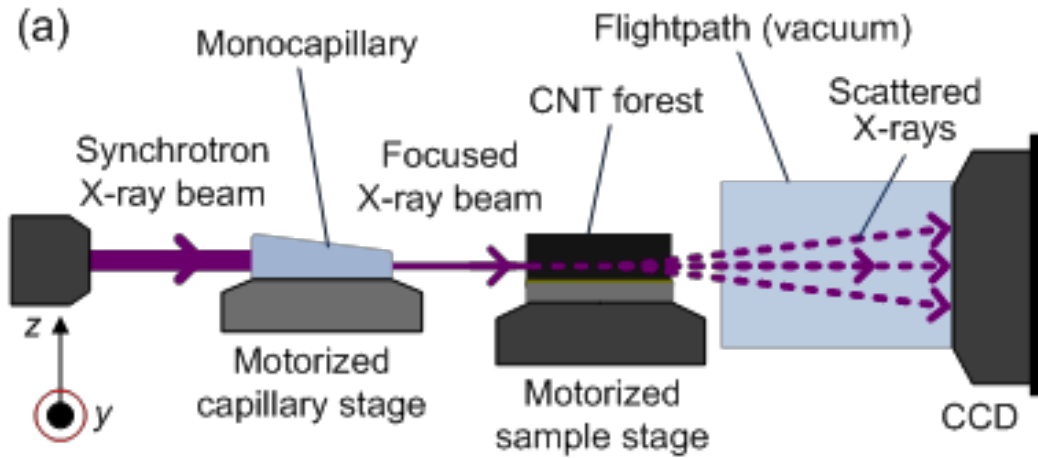
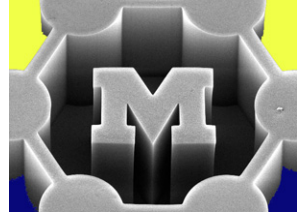
The 7th Pharmaceutical Powder X-ray Diffraction Symposium will be held in Orlando, FL, U.S.A.

Learn more @ www.icdd.com/ppxrd

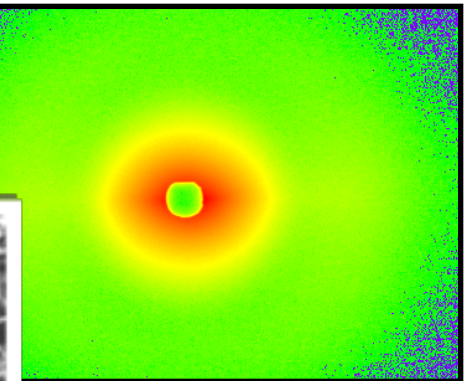
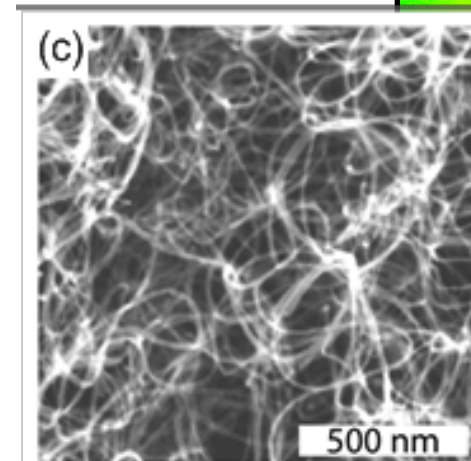
Upcoming Events:

ICDD Clinics on X-ray Powder Diffraction - Session I - Fundamentals of X-ray Powder Diffraction:
2-6 June 2008

Characterizing CNT forests by SAXS

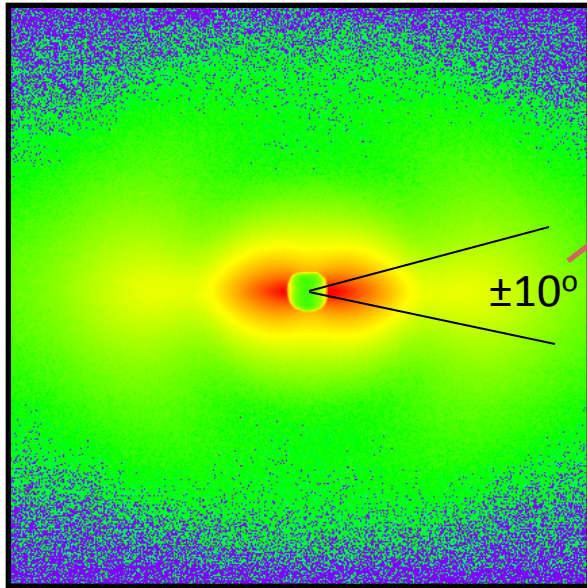
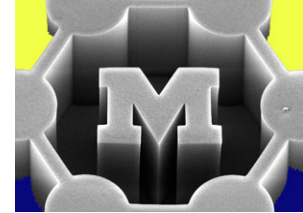


Aligned



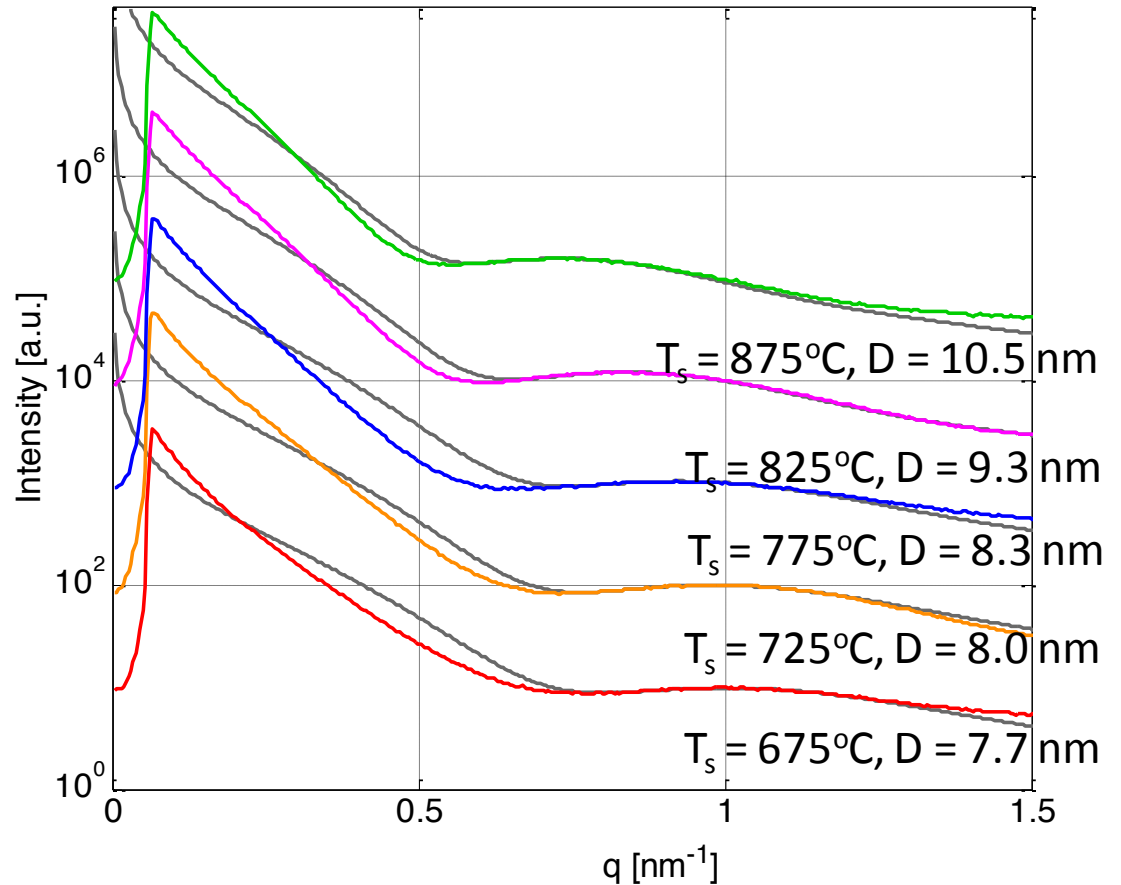
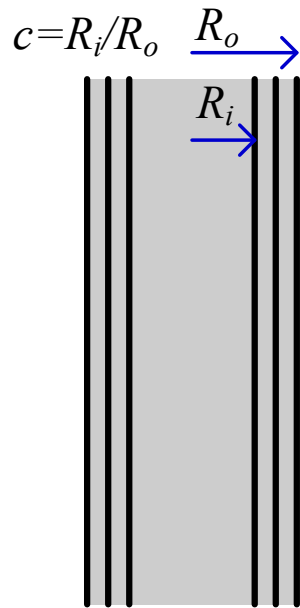
Unaligned

Measuring CNT diameter using SAXS



$$\int_{-\pi/18}^{\pi/18} I(q, \theta) d\theta$$

$$f(q, R_o) = \Delta\rho R_o \frac{2\{J_1(R_o q) - cJ_1(cR_o q)\}}{qR_o(1-c^2)}$$



Grazing incidence SAXS (GI-SAXS)

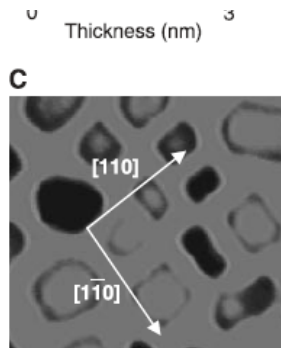
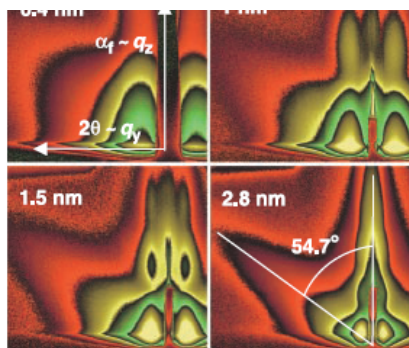
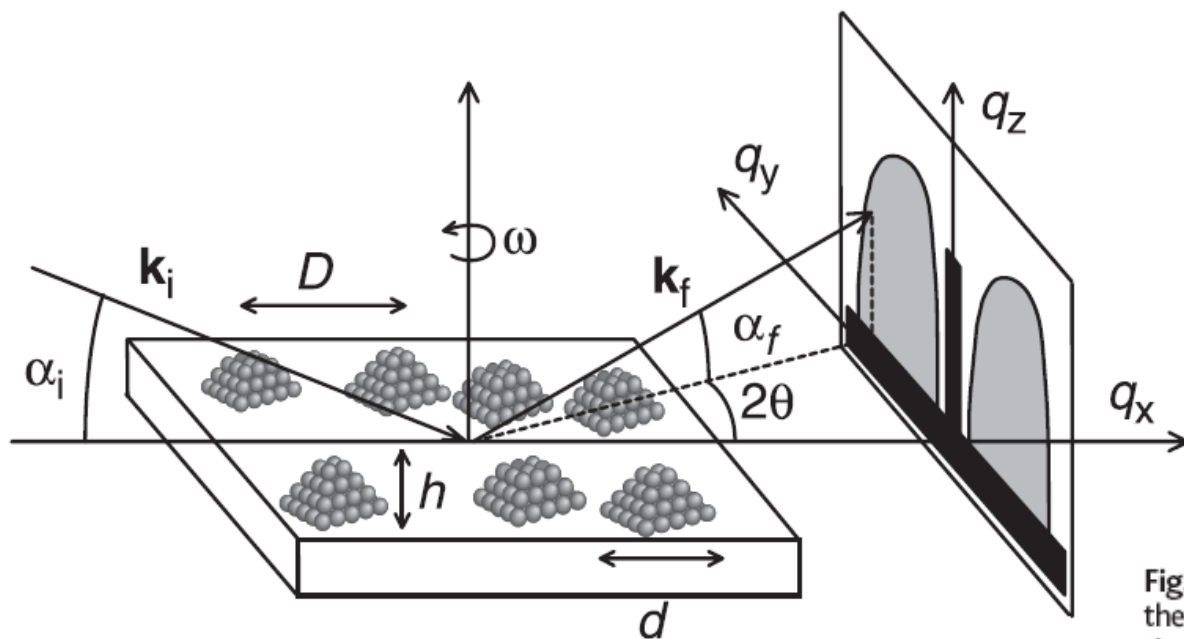
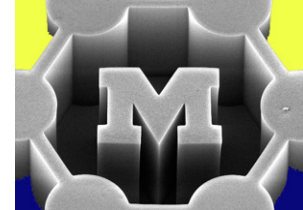
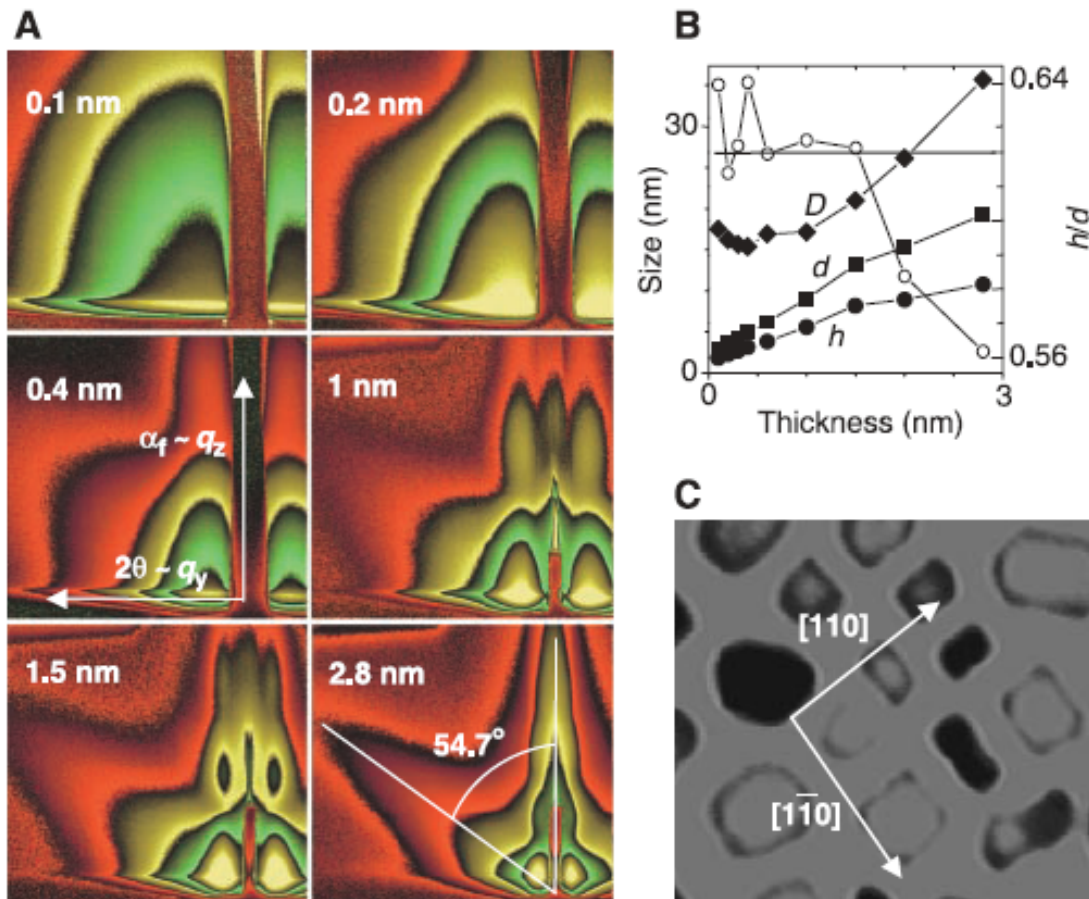
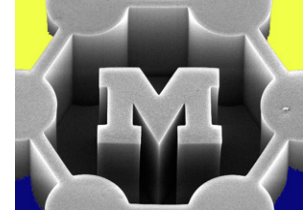
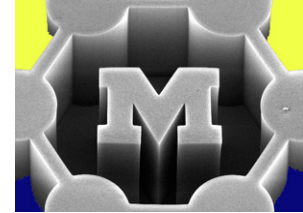


Fig. 1. The principles behind GISAXS. k_i and k_f are the incident and scattered wave vectors, respectively, yielding the momentum transfer (i.e., the reciprocal space vector) $q = k_f - k_i$. The angles α_i , α_f , and 2θ are related to the components of the momentum transfer, either parallel (q_x and q_y) or perpendicular (q_z) to the sample surface, by the equations $q_x = |k_i|[\cos 2\theta \cos \alpha_f - \cos \alpha_i]$, $q_y = |k_i|[\sin 2\theta \cos \alpha_f]$, and $q_z = |k_i|[\sin \alpha_f + \sin \alpha_i]$. Close to the origin in reciprocal space because they are small, the in-plane and out-of-plane scattering angles, 2θ and α_f scale with the components q_y and q_z of q . The sample can be rotated around its surface normal by an ω rotation, which defines the orientation of the incident x-ray beam with respect to the in-plane crystallographic directions. A beam stop protects the bidimensional detector from the direct and reflected beams.

Grazing incidence SAXS (GI-SAXS)

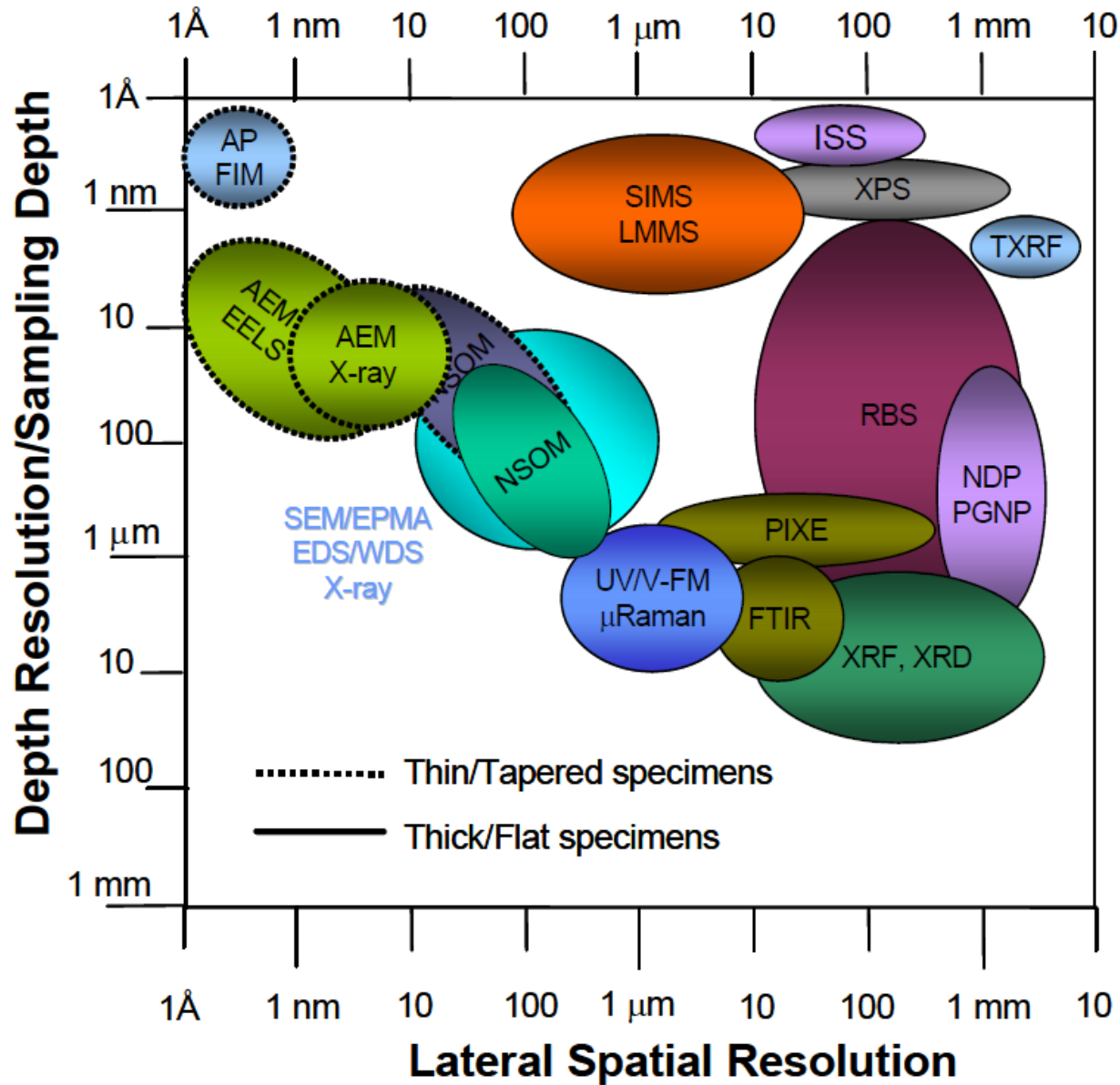
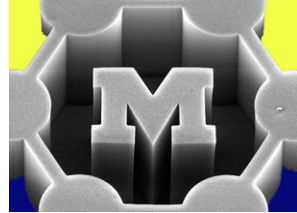


Chemical analysis

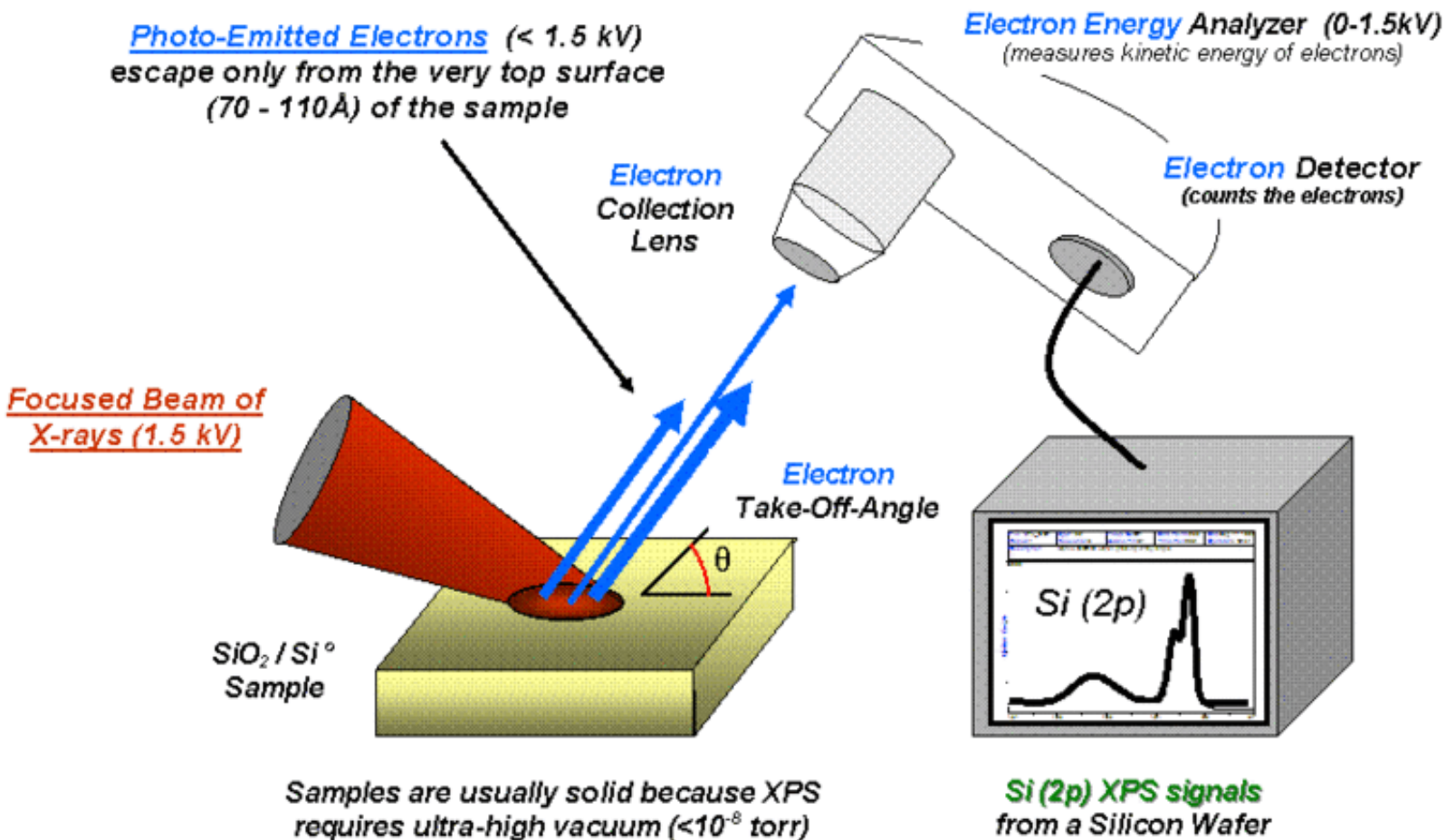
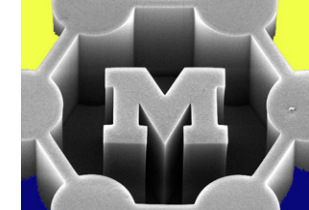


- **X-ray photoelectron spectroscopy (XPS)** → compounds
 - X-rays in, electrons out
- **Energy-dispersive X-ray spectroscopy** → elements
 - electrons in, X-rays out
- Auger electron spectroscopy → elements
 - Electrons in, electrons out
- **Optical spectroscopy: peak** → **vibrational mode**
 - Resonant Raman spectrometry
 - IR spectroscopy
- Mobility-based measurements of gases and liquids, e.g., mass spectrometry
- **Electron and X-ray techniques = VACUUM**
- **Optical techniques = AMBIENT**

Lateral resolution vs. depth resolution



X-ray photoelectron spectroscopy (XPS)



Output used to determine material → $E_{binding} = E_{photon} - E_{kinetic} - \phi$ ← Work function of spectrometer (calibrated)

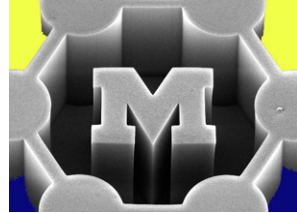
X-rays in → E_{photon}

Measured → $E_{kinetic}$

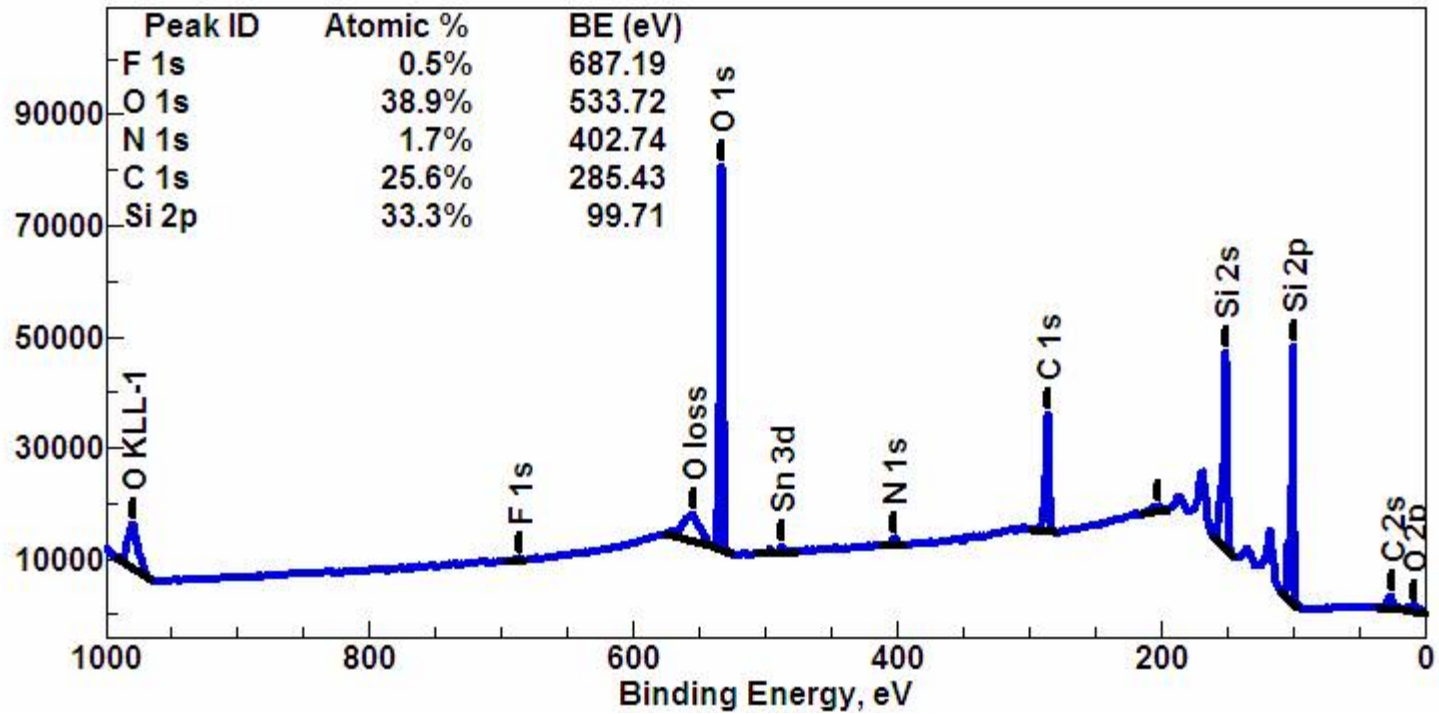
http://en.wikipedia.org/wiki/X-ray_photoelectron_spectroscopy

Work function of the spectrometer: <http://www.rikenkeiki.com/pages/AC2.htm>

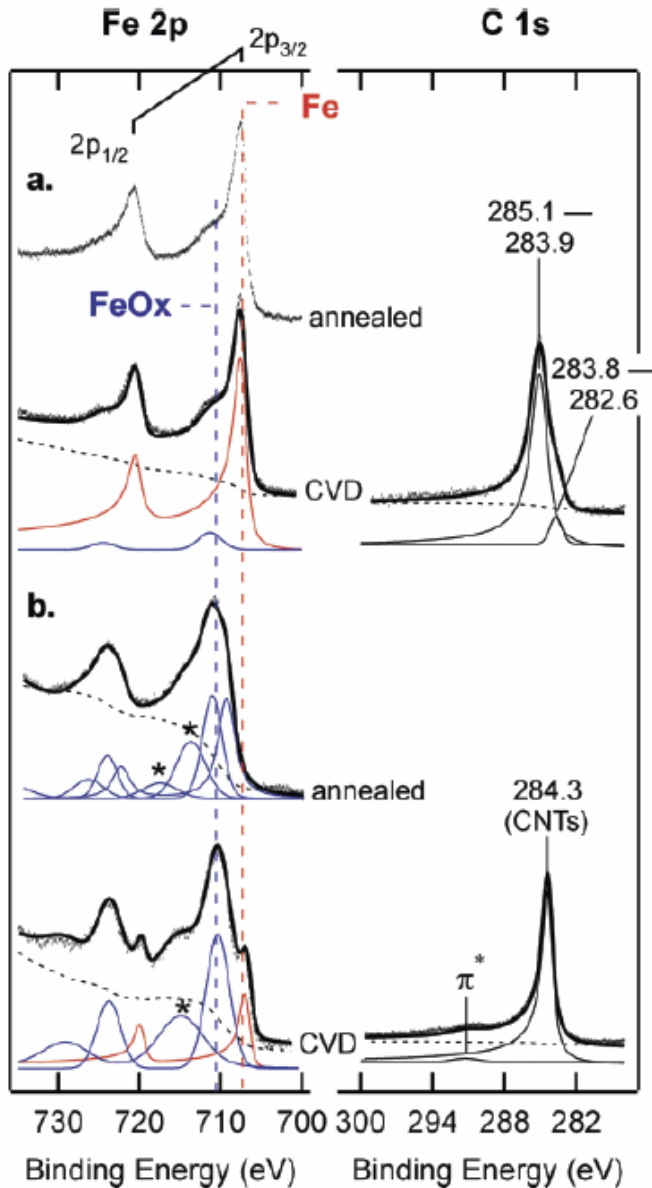
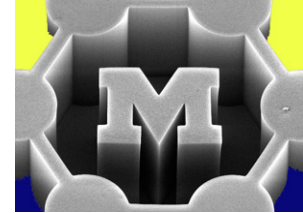
XPS



Counts



Is the CNT growth catalyst metal or oxide?



**metallic Fe
on Al_2O_3**

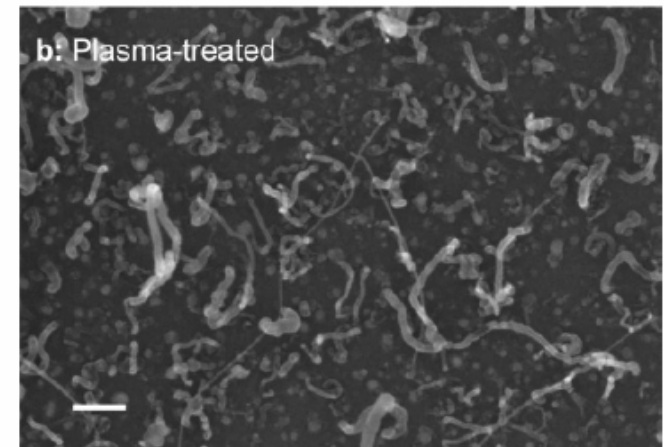
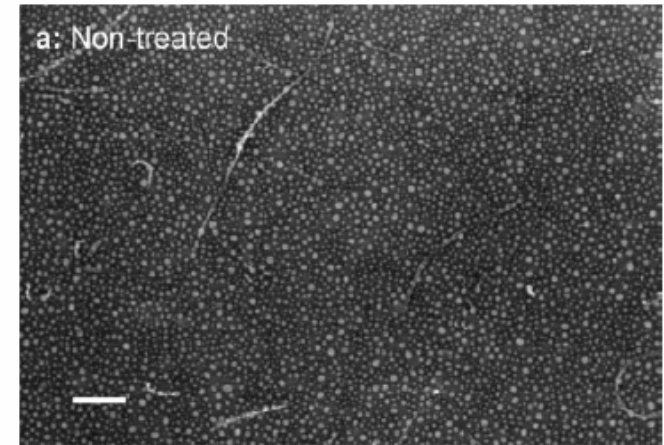
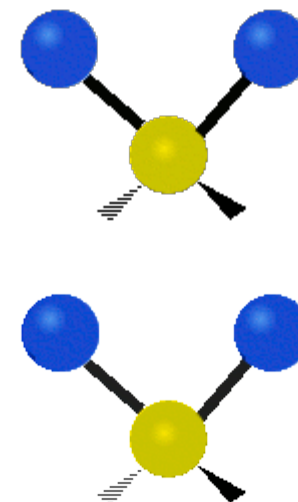
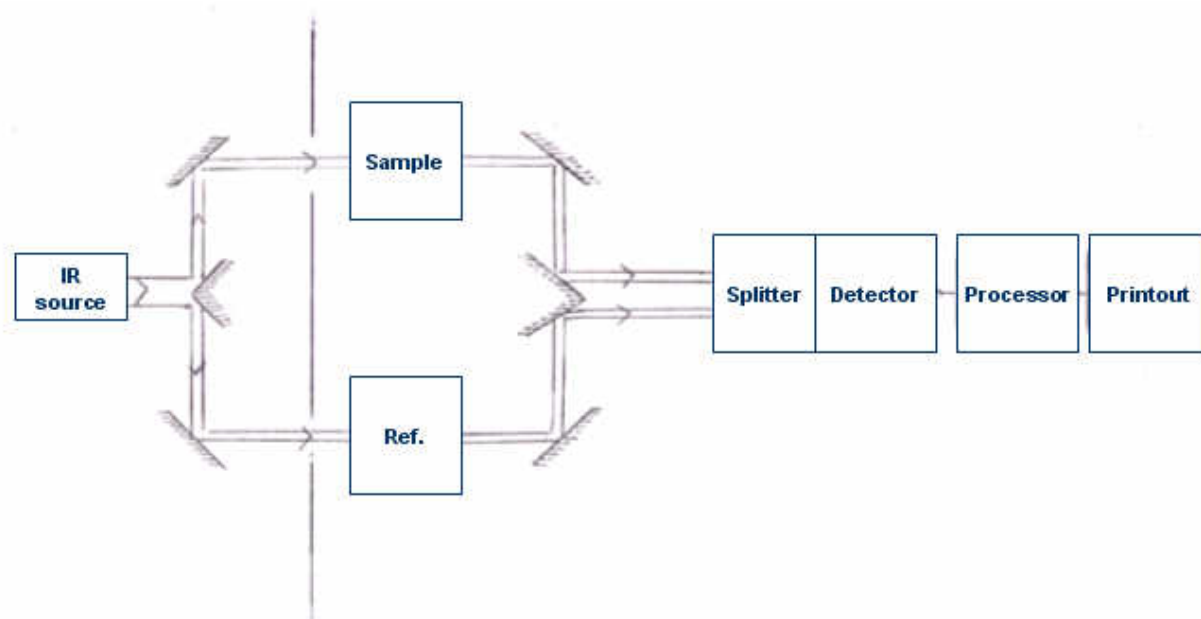
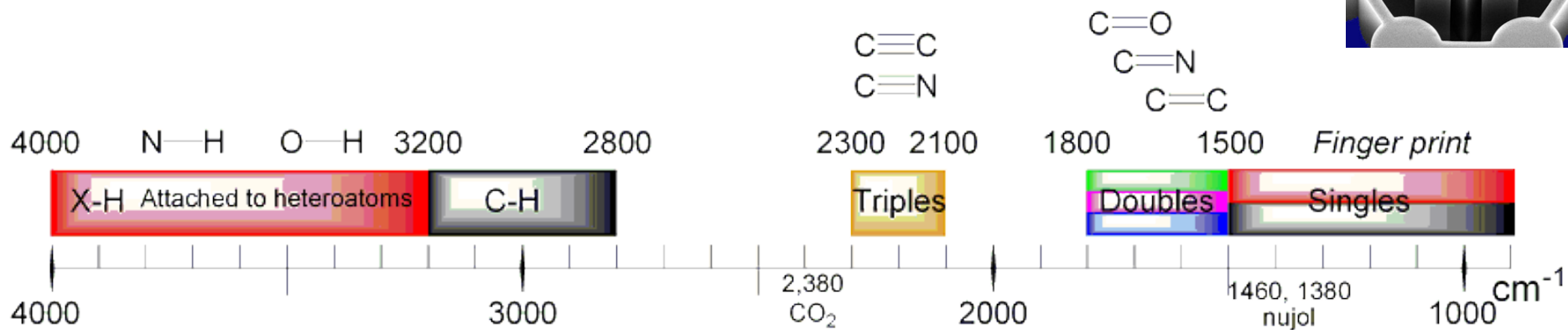
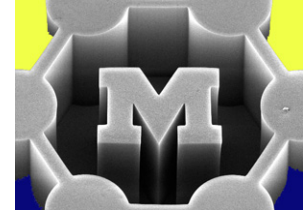
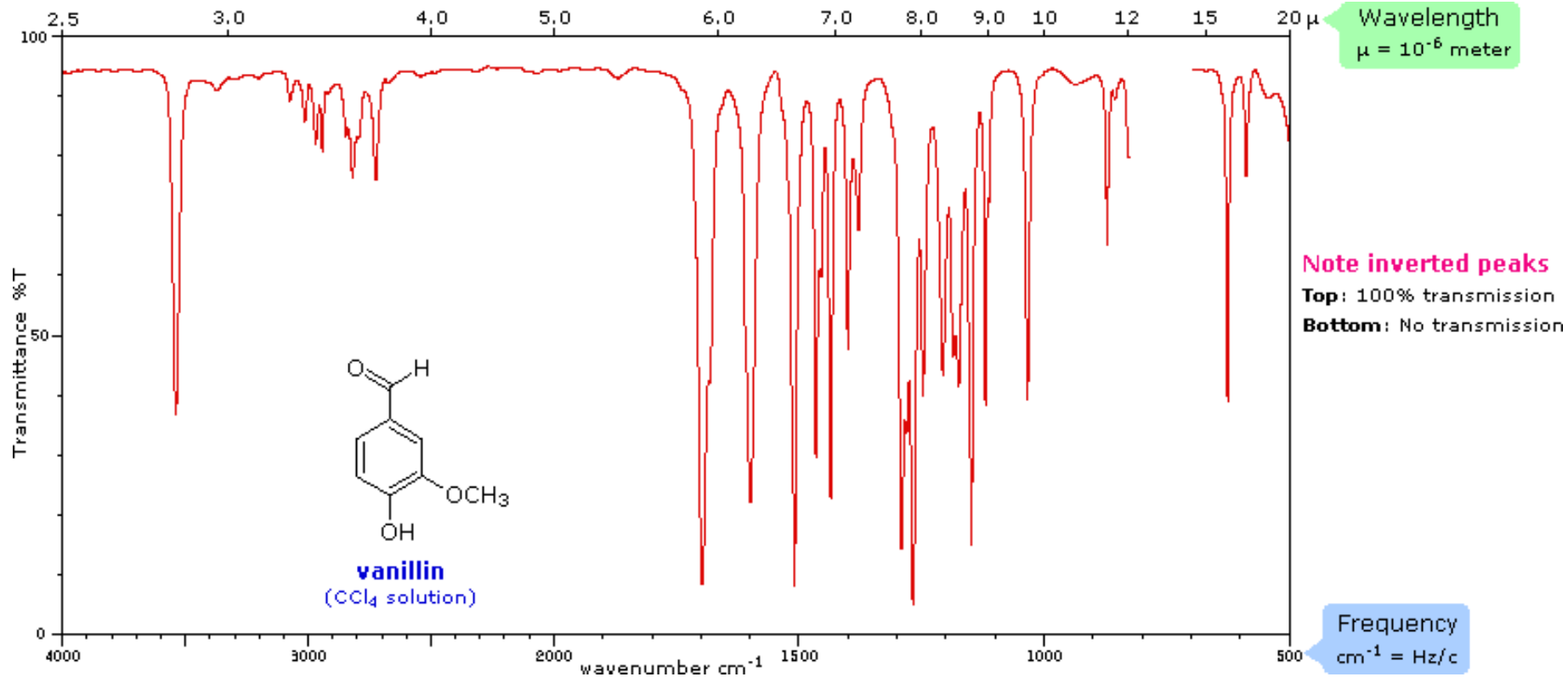
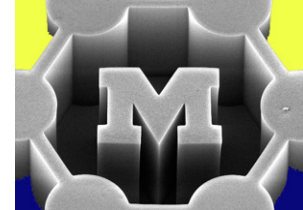


Figure 3. SEM images after CVD onto substrates with Al_2O_3 buffer layers. (a) CVD performed without previous O_2 plasma treatment; (b) CVD performed after O_2 plasma treatment. Scale bars are 100 nm.

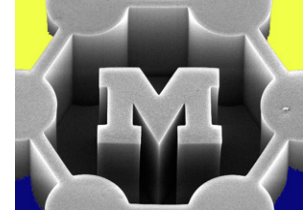
Infrared (IR) spectrometry



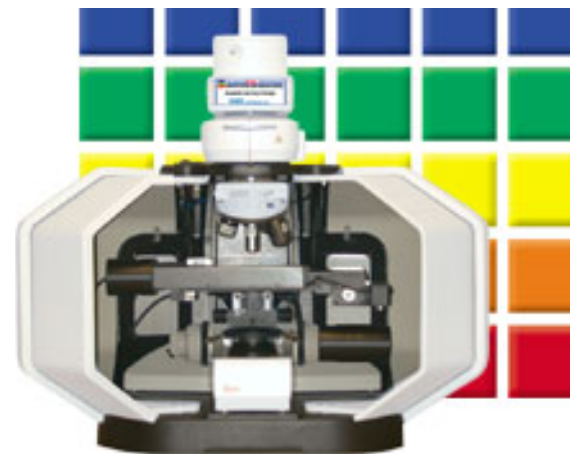
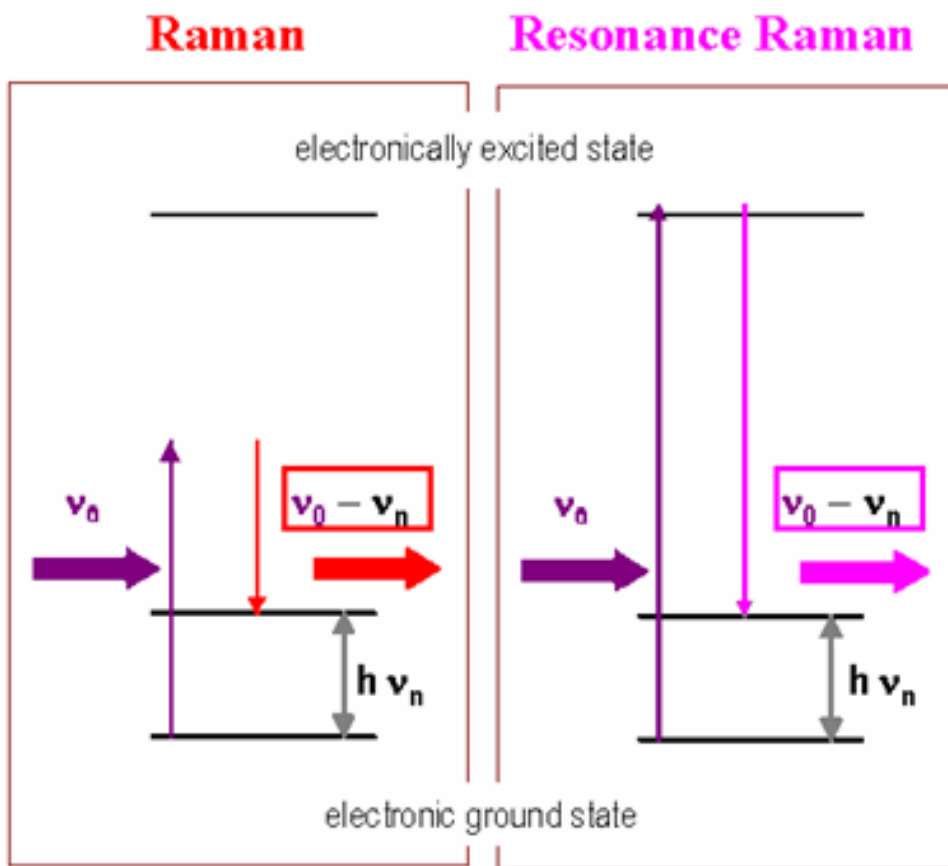
Infrared (IR) spectrometry



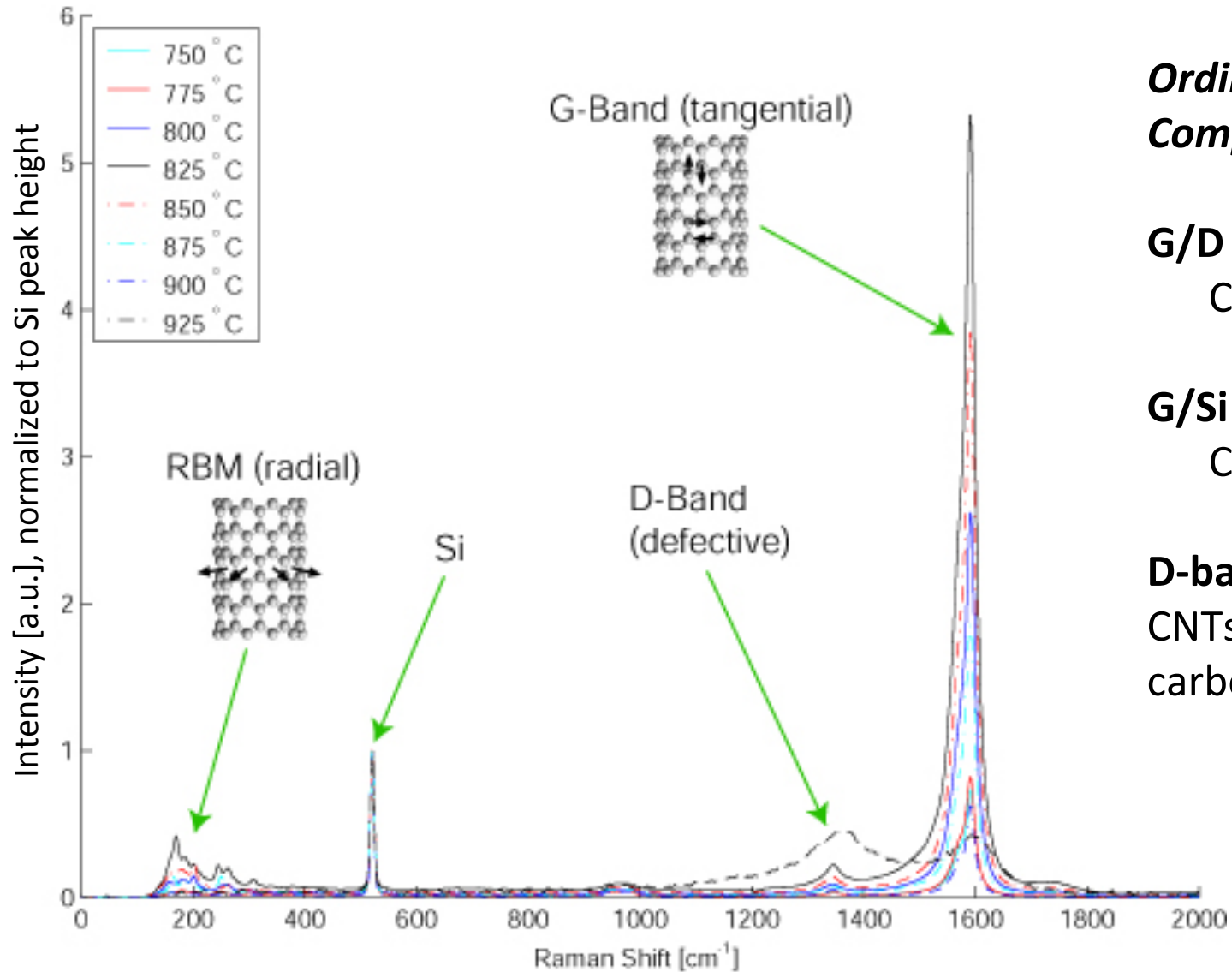
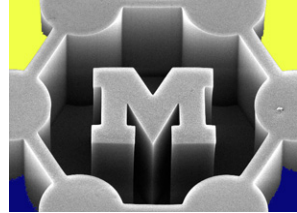
Raman spectroscopy



- Raman shift: scattered light shifts in frequency when it excites a molecular vibration; tuning this excitation to an electronic transition in the sample gives a huge enhancement



Raman spectroscopy of CNTs



Ordinal Comparisons:

G/D Ratio =
CNT quality

G/Si Ratio =
CNT yield

D-band = Defects in CNTs and defective carbon on substrate

Raman peak of a SWCNT shifts with strain ...like a guitar string

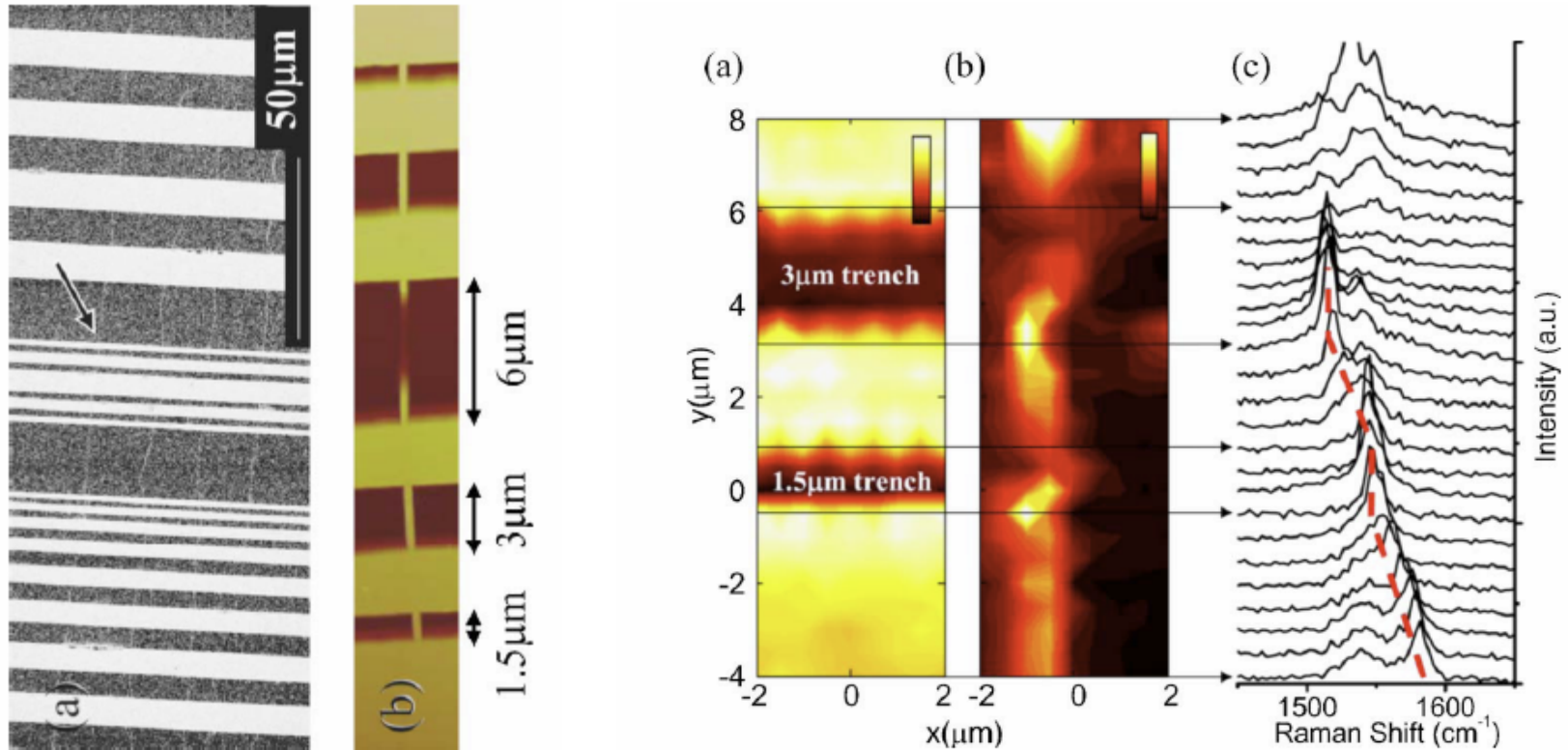
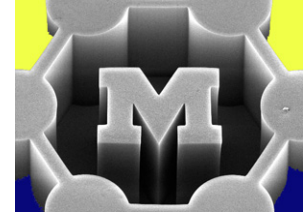
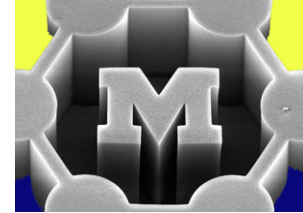
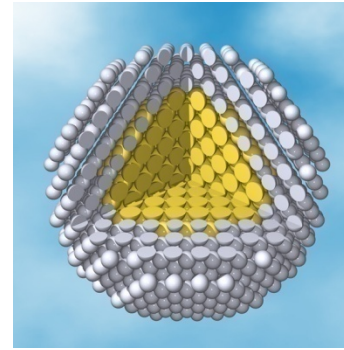
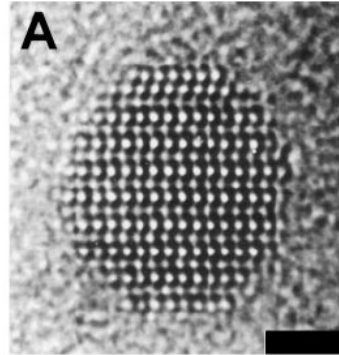
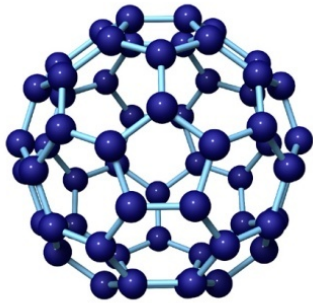


FIG. 3. (Color online) (a) 2D integrated intensity map of the silicon peak at 520 cm^{-1} . The dark regions correspond to the trench regions. (b) 2D integrated intensity map of the G band between 1500 and 1600 cm^{-1} taken from a SWCNT in the same region as in (a). (c) Actual G -band spectra along the length of the SWCNT shown in (b). The peak frequency of the most intense peak is observed to shift linearly with respect to the position on the substrate and remains constant across the trenches.

How were these pictures taken?



0-D



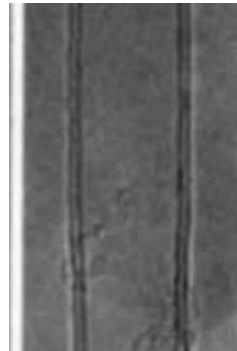
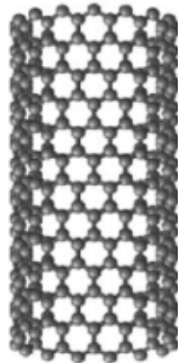
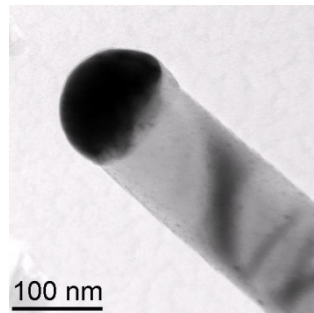
Nanoclusters

Magic #'s of atoms
≤1 nm size

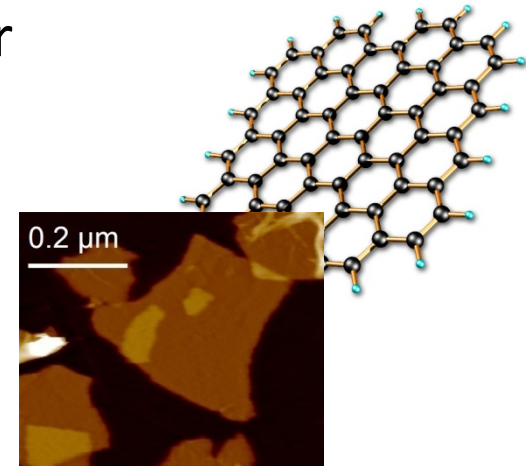
Nanoparticles

100's-1000's of atoms
~1-100 nm diameter

1-D



2-D



Nanowires

Filled

~1-100 nm dia, up to mm long and beyond!

Nanotubes

Hollow

Nanosheets

~1 atom thick

Characterization facilities at UM



Electron Microbeam Analysis Laboratory (EMAL)

<http://www.emal.engin.umich.edu/>

Facilities: Scanning Electron Microscope (SEM), Transmission Electron Microscope (TEM), X-ray Photo-electron Spectroscopy (XPS), Focused Ion Beam (FIB), and others.

X-Ray MicroAnalysis Laboratory (XMAL)

<http://www.mse.engin.umich.edu/research/xmal>

Facilities: X-ray Diffraction and X-ray Scattering

Michigan Ion Beam Laboratory (MIBL)

<http://www-ners.engin.umich.edu/research/Mibl/index.html>

Facilities: Rutherford Backscattering Spectroscopy, Ion Implantation